Master Thesis, Department of Geosciences

Geology and geochronology of the Hardangerjøkulen Klippe and its basement

Erik Jensen

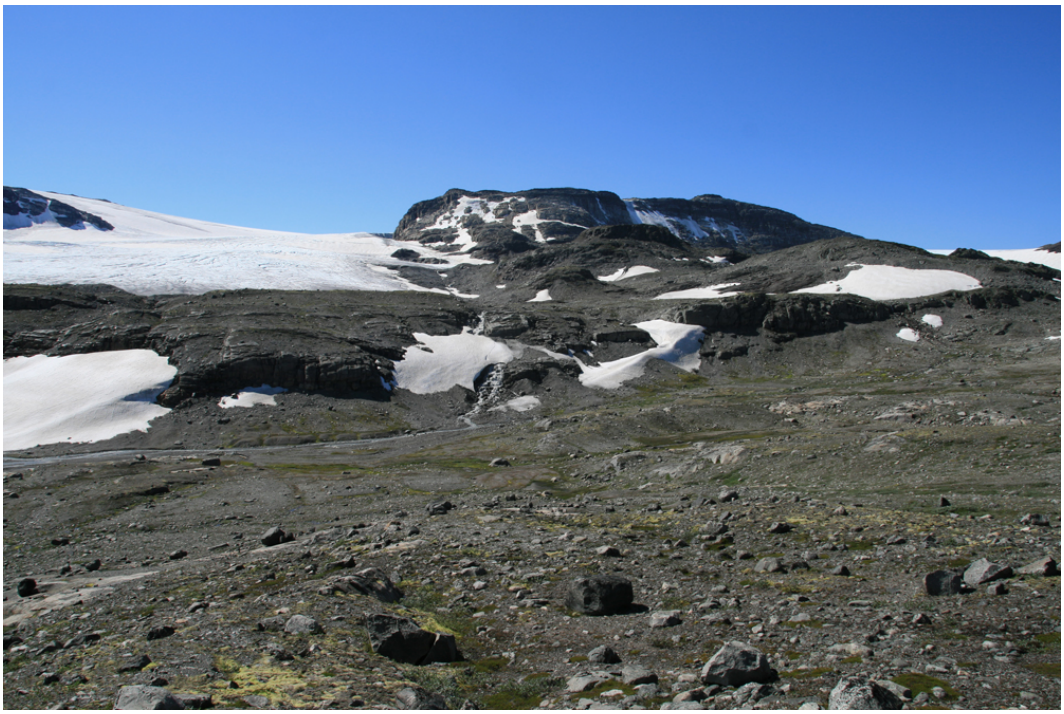

UNIVERSITY OF OSLO
FACULTY OF MATHEMATICS AND NATURAL SCIENCES

Geology and geochronology of the Hardangerjøkulen Klippe and its basement

Erik Jensen

Master Thesis in Geosciences

Discipline: Geology

Department of Geosciences

Faculty of Mathematics and Natural Sciences

University of Oslo

December 2012

Tutor: Prof. Fernando Corfu

This work is published digitally through DUO – Digitale Utgivelser ved UiO

http://www.duo.uio.no

It is also catalogued in BIBSYS (***http://www.bibsys.no/english***)

Acknowledgments

I would first of all like to thank my supervisor Professor Fernando Corfu for providing me with an interesting thesis, and I'm also grateful for all the valuable support and guidance he has given me to understand this complex geology better.

Special thanks to Geir, Stian and Magnus for helpful discussions and support.

Thanks to Erika for the accommodation and hospitality at Finse Alpine Research Center.

I also want to thank my family for their great support throughout the whole time preparing the thesis.

And thanks to my beloved Katrine, for constantly support and considerations.

Abstract

The study area, which is located north-east of Hardangerjøkulen, south central Norway, is characterized by autochthonous basement overlain by allochthonous nappes formed in response to 420 Ma Caledonian orogeny. Lithological the basement in the study area is dominated by three main types: fine and coarse grained granodiorite, amphibolite/gabbro and coarse grained granite with large feldspar phenocrysts. Granite is the main bedrock type at Finse, but the exposed basement in the study area is primarily granodiorite. The study area located at north side of Hardangerjøkulen also comprises gabbro. All three lithologies, granite, granodiorite and gabbro display 988.1 ±3.1 Ma zircon age. And the titanite ages for the granite are 957.0 ±2.4 Ma and 964.8 ±2.5 Ma, gabbro: 955.5 ±2.3 Ma and 963.8±2.5 Ma, and granodiorite 937.7 ±2.2 Ma and 916.9 ±5.8 Ma. While felsic and mafic lithologies tend to be dominant in isolated areas, the coarse and fine grained granodiorite shows intermixing with amphibolite. Several dikes usually as pegmatite cut the mafic and the felsic units with a preferred orientation, during 939.0±8.7 Ma. Some of these dike have responded either in brittle or ductile manner to a superimposed constrictional strain, with compressional axis trending north-south and extensional axis east-west. The top of the basement is characterized by a weathered surface, regolith. The surface is topographically fluctuating at most 100 meter from lowest to highest level. Where the basement is relatively topographically high, it is highly folded and schistose with fold axis trending NE-SW and kinematic movement towards NW.

The overlying phyllitic layer has various thicknesses between one to tens of meter, and is highly schistose with a dark red to black color and distinct sheen. Foliation plane measurements display a rather inhomogeneous plane without any preferred orientation, and also due to the fact that the fold-axes are rotating from NW-SE to NE-SW.

Phyllite has weakly responded during folding of the overlaying thrust sheet, Lower nappe, which is an informal unit part of lower middle allochthon, since Phyllite is often in-folded in Lower nappe fold structures. This unit is comprised of several different rock types with more or less different lithologies, such as fine-banded gneiss and schist, carbonate, volcanic tuff and also lithologies very similar to Phyllite. The Lower nappe is highly folded with mylonitic fabric, and displays the same fold-axis rotation as seen in Phyllite. Folds in this unit have a magnitude at several to tens of meters with nearly 0 degree plunge of the axis surface and between 0° – 30° degrees plunge of the fold hinge, and would be either a g*ently inclined* or *recumbent* fold geometry. The majority fold-axes orientations in the Lower nappe are NW-SE with vergence towards NE, while the secondary fold-axis orientation is NE-SW with vergence towards NW. These two fold-axis orientations are separated by a kinematic contact zone which displays rotation towards NE-SW. Foliation measurements for the Lower nappe confirm that there are areas where the planes changes, but overall this unit has far more homogenous plane orientations compare to Phyllite. The highest unit is the "*Upper nappe*", another informal name, but this is the crystalline basement part of upper Middle Allochthon. Mylonitic fabric and highly sheared and folded rocks with coarser grain sizes relative to the Lower nappe, characterize this unit as banded gneiss. Fold axis are trending NW-SE with vergence towards NE.

Table of contents

1 Introduction ____ *1*

2 Methodology ____ *10*

2.1 Introduction ____ **10**

2.2 Field method ____ **11**

2.3 Mapping ____ **11**

2.4 Cross section and stereonet ____ **12**

2.5 Approximate orientations ____ **12**

2.6 Geochronology -TIMS ____ **12**

2.6.1 Theoretical background ____ 12

2.6.1.1 Uranium ____ 12

2.6.1.2 Zircon ____ 14

2.6.1.3 Titanite ____ 16

2.6.2 Analytical Preparation ____ 17

2.6.3 Analytical work ____ 18

2.6.4 Calculations ____ 20

2.7 Thin Section ____ **22**

2.8 Terminology ____ **23**

3 Description ____ *28*

3.1 Introduction ____ **28**

3.2 Rock description ____ **29**

3.2.1 Basement ____ 29

3.2.1.1 Granodiorite ____ 30

3.2.1.2 Granite ____ 31

3.2.1.3 Amphibolite and gabbro ____ 32

3.2.1.4 Pegmatite ____ 33

3.2.1.5 Dikes and intermixing ____ 34

3.2.1.6 Top of the basement ____ 38

3.2.1.7 Faults and folds ____ 40

3.2.2 Phyllite ____ 45

3.2.2.1 Measurements ____ 47

3.2.3 Lower nappe Unit ____ 49

3.2.3.1 Lithostratigraphic log ____ 49

3.2.3.2 Measurements ____ 54

3.2.4 Upper nappe ____ 56

3.3 Lower nappe and Phyllite structures ____ **60**

3.3.1 The general structure of the East and the West side at Middalen glacier ____ 61

3.3.2 Structural description ____ 62

3.3.3 Fold structures ____ 68

4 Geochronology ____ *70*

4.1 Introduction ____ **70**

4.2 Granodiorite ____ **70**

4.3 Granite ____ **73**

4.4 Pegmatite 74
4.5 Gabbro 76
4.6 Datasheet Mass spectrometer 79
5 Discussion ***80***
5.1 Development of the Basement 80
5.2 Development of the allochthonous nappes and infolded Phyllite 85
5.2.1 Proto Upper nappe 85
5.2.2 Proto Lower nappe 85
5.2.3 Proto-Upper nappe collision 86
5.2.4 Sveconorwegian Extensional phase 86
5.2.5 Lithological mirror image 90
5.2.6 Multiple kinematic directions 91
5.2.7 Caledonian orogeny 94
5.3 Younger faults 95
5.4 Map and Cross section 96
5.5 Graphical model 97
6 Conclusion ***98***
7 References ***99***

Appendix 1: Fold-axes data

Appendix 2: Information map: Localities, samples, cross-section and section with close up-view

Appendix 3: Tectonostratigraphic map

Appendix 4: Cross-section B-B'

Appendix 5: Cross-section C-C'

Appendix 6: Cross-section D-D'

1 Introduction

Regional geology

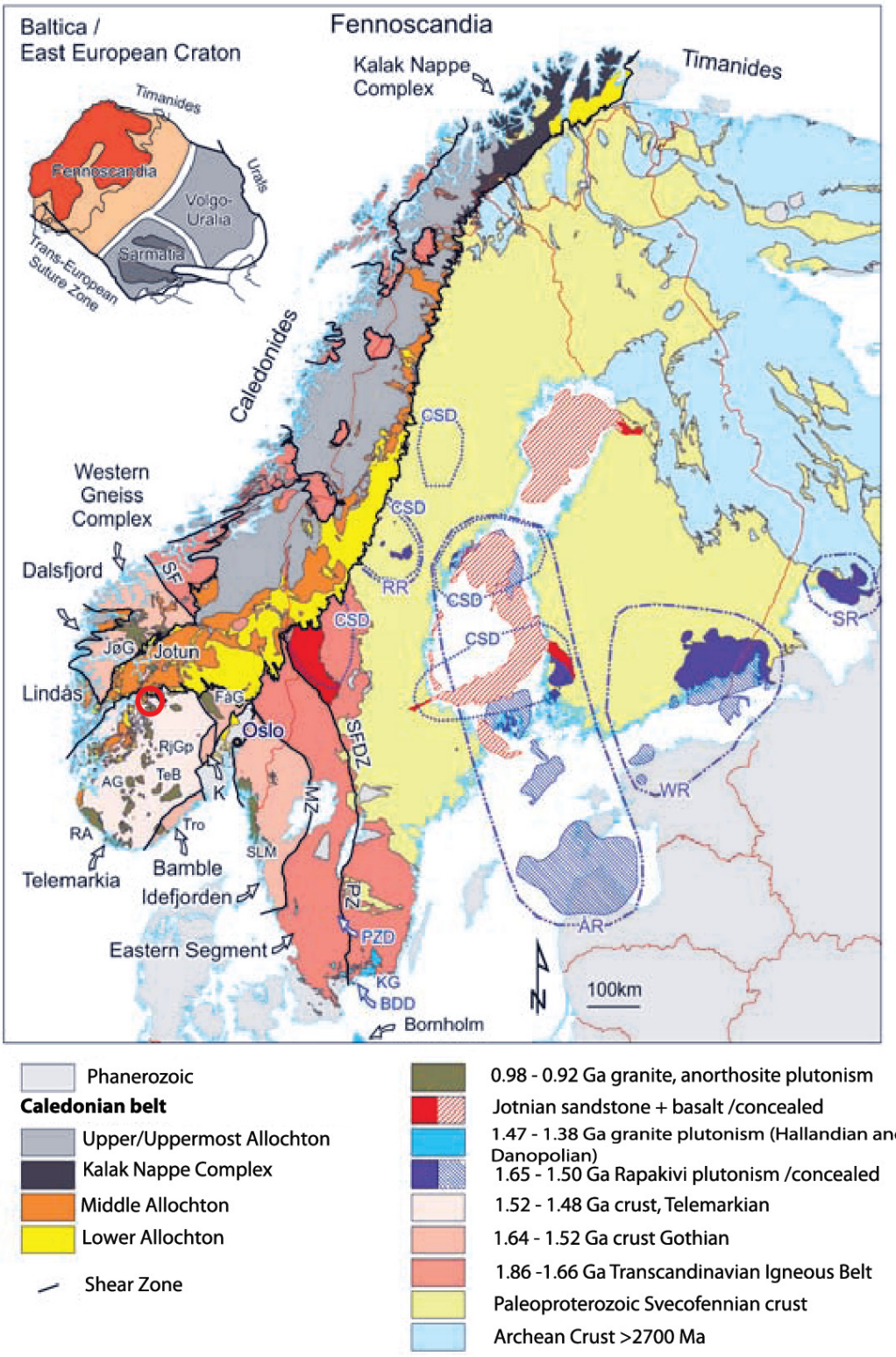

Fig. 1. The illustration shows the different events that have shaped the Precambrian basement in Norway. The study area, Hardangerjøkulen, which is marked with marked a red circle, is situated in the Telemarkia terrane (from Bingen et al., 2008a, slightly modfied by author).

Tectonics is the essential factor controlling how the Earth's crust (either continental or oceanic) has changed, and been destroyed by subduction and collision through time. Continental and oceanic crust drifts on the viscous magma, as a result of convection currents. Subduction zones, island arcs and orogens develop when two plates collide with each other. Some parts of the bedrock located in Norway today are remnants and proof for events happening as far back as the Archean time, more specific approx. 3.1 Ga ago. These events gradually built the Fennoscandian shield (Fig. 1).

The Fennoscandian shield comprises several structural components; Archean core (3.1–2.6 Ga) in the north east, the Paleoproterozoic Svecofennian domains (1.9–1.8 Ga) in the center, and the South west domain, also called the Gothian (1.7–1.5 Ga) in the southwest (Haapala et al., 2005, Bingen et al., 2008b) (Fig. 1). The oldest remnants found at present day in the Archean core are approx. 3.1 Ga (Gaal and Gorbatschev, 1987).

Archean crust

The Archean Crust is subdivided into three provinces: Karelian Province in the West and the Belomorian and Kola Peninsula Provinces (Fig. 1). The age of the Archean crust ranges from approx.3.2 Ga to 2.6 Ga. During this time this crust experienced two orogenies: Saamian~ and Lopian orogeny. Saamian orogeny lasted from 3.1 Ga to 2.9 Ga, and the Lopian orogeny followed from 2.9 Ga to 2.6 Ga (Gaal and Gorbatschev, 1987).

Pre Svecofennian period

After the development of the Archean crust, it began to rift. The following time period, 2.6 Ga to 2.0 Ga involved breakup and development of a passive margin along the western boundary of the Karelian provinces(Gorbatschev and Bogdanova, 1993, Nironen, 1997). This extensional setting led to magmatic activity (Gaal and Gorbatschev, 1987).

Paleoproterozoic Svecofennian crust

In the Svecofennian Orogen model, the pre-Svecofennian ocean was opened at 1.95 Ga. This progressively led to an accretion of two island arc systems with the Archean Craton between 1.91 Ga and 1.87 Ga. This in turn led to thrusting of island arc complexes and marine strata on top of the Archean Craton, and resulted in a thicker crust. A subduction eventually developed and reversed the rotation of the converging plate (Nironen, 1997).

Transcandinavian Igneous Belt

Transcandinavian Igneous Belt (TIB) was a result of a large felsic magmatic event that took place in the Svecofennian crust. According to Gorbatschev and Bogdanova (1993) TIB happened in the period 1.83 Ma to 1.65 Ma.
, and intruded approx. 100 million years older Svecofennian crust, from South-Sweden to Central Norway (Fig. 1). The event is speculated to have developed as a major destructive margin process (Gorbatschev and Bogdanova, 1993).

Rapakivi Plutonism

Magmatic episodes were common during the Mesoproterozoic, and several large events occurred in response to the thinner and weaker crust (Bingen et al., 2008a). The most important magmatic activity (on the Baltica craton) was the 1.670- 1.470 Ga Rapakivi magmatism (Haapala et al., 2005). Large scale plutonism led to felsic granite with a distinct fabric with K-feldspar phenocryst plus albite rim (Dempster et al., 1994). This magmatic event developed due to a "*intracontinental extensional setting"* as a result of extensional collapse of the thicker crust (Bingen et al., 2008a, Windley, 1993).

Gothian Accretion

Near the end of the magmatic activity caused by the TIB, another orogeny initiated 1.64 -1.52 Ga ago and is called the Gothian orogeny (Bingen et al., 2008a). Åhäll et al. (1996) suggested that these two events had to some degree a connection between them (Åhäll et al., 1996, as cited in Nironen, 1997). The Gothian accretion is (one of) the first step of a 500 km reworking of the south-western margin of Fennoscandia (Fig. 1). Several terrains developed in response to the growing and reworking continent, during the Mesoproterozoic. The volcanic, magmatic activity and the sedimentation during the Gothian orogeny developed the Idefjord, Bamble and Kongsberg terrains (Bingen et al., 2008a).

Telemarkia Accretion

The Gothian event ended approximate by the same time as the Telemarkia accretion started, 1.52 Ga ago and lasted until 1.48 Ga ago (Bingen et al., 2008b). This event reworked and built the Telemarkia terrain, with its sub-domains: The Telemark, Hardangervidda, Sulda and Rogaland-Vest Agder. While they all share a substantial magmatic volume dated 1.52 – 1.48, they also have lithological differences (Bingen et al., 2008b).

Hallandian and Danopolonian Orogeny

Brander (2011) created a model for the following Hallandian and Danopolonian orogeny, which took place after Telemarkia accretion. He describes in his model an oceanic plate and a continental block of unknown origin that collide with the Fennoscandian Shield. In response to the collision, a subduction zone develops with several (1450 Ma) felsic pluton, like Bornholm and Skåne (Brander, 2011) The Hallandian and Danopolonian orogeny lasted from 1.45 Ga to 1.42 Ga and the collision originated from south-west, relative to Norway (Brander, 2011).

Pre- Sveconorwegian Interval

The following period, pre – Sveconorwegian interval was in fact relatively quiet. The dolerite group located in central Scandinavian developed 5 large magmatic complexes during 3 events between 1.271 and 1.247 Ga (Söderlund et al., 2006). This interval ends when high grade metamorphism starts to develop. This is the beginning of the Sveconorwegian orogeny (Bingen et al., 2008a).

Sveconorwegian Orogeny

The previously developed and reworked terranes at the Fennoscandia continent were directly involved in the Sveconorwegian orogeny and are an important factor for the progression of this orogeny. The Sveconorwegian orogeny is interpreted as *"a polyphase imbrication of terranes at the margin of Fennoscandia between 1.14 and 0.97 Ga*" (Bingen et al., 2008a).

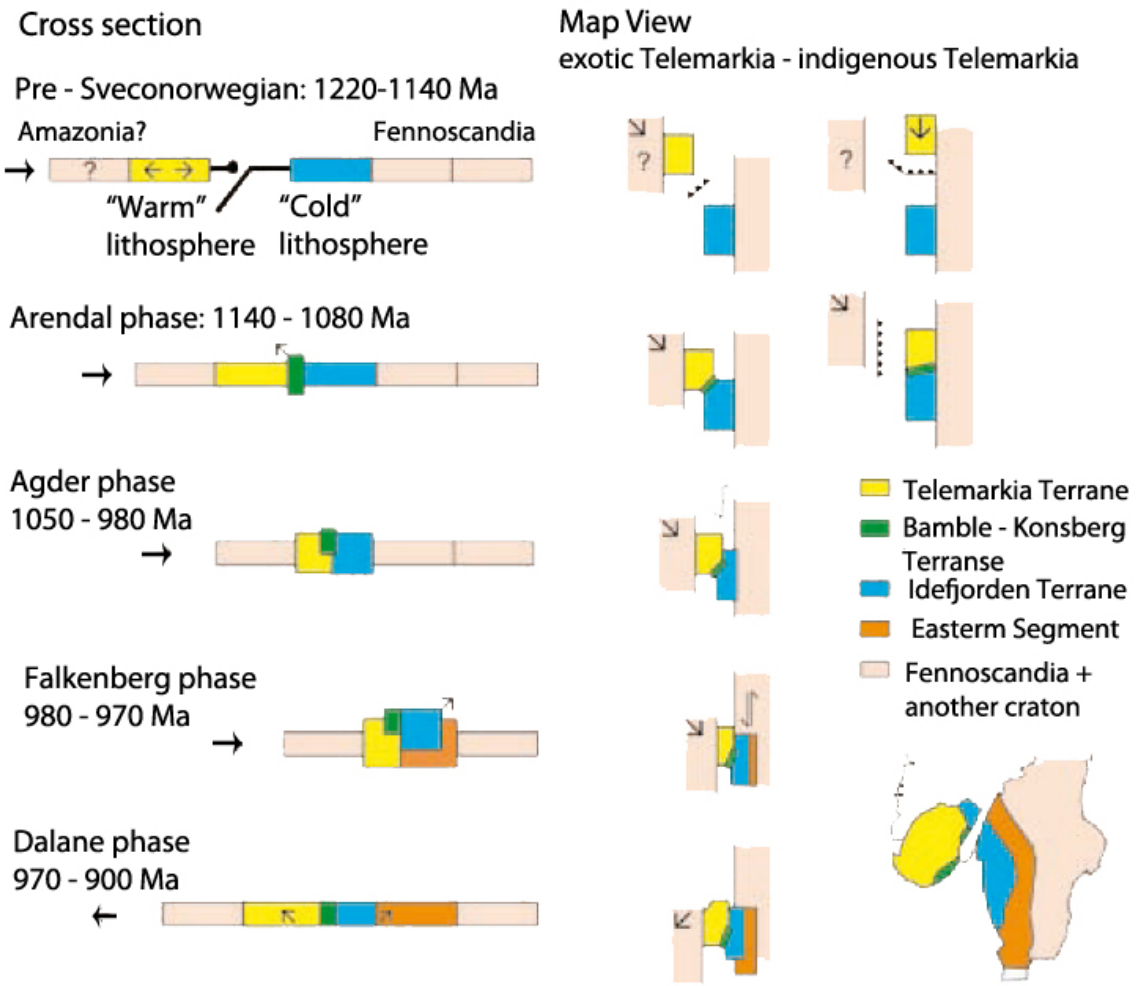

Fig. 2. Illustration shows the progression of the Sveconorwegian orogeny with a four phase model. First phase, Arendal 1140 – 1080 Ma, involves the collision between the Telemarkia Terrane and Idefjorden, and subsequent developing Bamble terrane. Second Phase, Agder 1050 – 980 Ma, progressive collision results in crustal thickening. Third phase, Falkenberg 980 – 970 Ma, the deformation reaches the eastern segment. Last phase, Dalane 970 – 900 Ma, is the extensional phase that involves exhumation and gravitational collapse (from Bingen et al., 2008b).

Bingen et al. (2008b) explains the evolution of this orogeny with a four phase model (Fig. 2).

1. **Arendal phase:** 1140 – 1080 Ma

   This is the earliest metamorphic event during this orogeny and involves a collision between the two terranes: Telemarkia and Idefjorden. The high grade metamorphic product of this collision was the Bamble and Kongsberg tectonic wedge, with lithologies similar to those of the two colliding terranes. Eventually the Bamble terrane was thrusting on top of the Telemark ramp, creating a "*crust-mantle imbrication*". The collision of this first phase reached metamorphic condition as high as granulite facies (Bingen et al., 2008b, Andersson et al., 1996).

2. **Agder phase:** 1050 – 980 Ma

   During this phase Idefjorden and Telemarkia terranes were progressively pushed together, resulting in crustal thickening and imbrication in the central part of the orogen, followed by magmatism. The Agder phase is characterized as the main phase of the Sveconorewgian orogeny (Bingen et al., 2008b).

3. **Falkenberg phase:** 980 – 970 Ma

   The deformation due to the collision eventually reached the Eastern segment High grade metamorphic grade and crustal thickening with deep burial (to approx. 50 km) are the most characteristic processes during this phase (Bingen et al., 2008a).

4. **Dalane phase:** 970 – 900 Ma

   During this period the two continents cease to move towards each other, and entered an extensional period. A gravitation collapse occurred due to the thickened crust. Exhumation of the southern part of the Eastern Segment and the Rogaland –Vest Agder sector in Telemarkia Terrane resulted in two high metamorphic grade domains appearing at shallow crustal depth (Bingen et al., 2008a, Bingen et al., 2006).

At least the progression of this four phase model is well explained, it is still quite uncertain which continent collided with the Fennoscandian shield (Brander, 2011).

The Sveconorwegian orogeny was among one of many other continental collisions that eventually united all the tectonic plates on paleo Earth into one super continent, Rodinia at approx. 1100 Ma (Meert and Torsvik, 2003). The continent Laurentia (which would be today's North America plus Greenland) was the center of this super-continent. Laurentia and Baltica were first situated on opposite sides of the equator, but ended more or less at equatorial latitude before the break up of Rodinia (Torsvik et al., 1996).

Powell et al. (1993) concluded that Rodinia started breaking up at approx. 725 Ma. At 600 Ma, Iapetus oceans started to open when Baltica and Laurentia drifted apart as a result of an asymmetric rifting episode (Torsvik and Steinberger, 2006).. This involved that Baltica rotated clockwise and Laurentia anticlockwise. Baltica and Laurentia in the late Ordovicium were positioned relatively close to the equator, approx. 5000 km from each other (Torsvik and

Steinberger, 2006). At 455 Ma, Avalonia was positioned in Iapetus Ocean, in-between Laurentia and Baltica (Fig. 3) before the next collision was initiated (Torsvik et al., 1996).

Caledonian Orogeny

Except for further movement and rotation of the Baltica continent, there was little that happened after the Sveconorwegian Orogeny. In the late Precambrian, marine transgression eroded the mountains down to a flat "peneplain". Changing water level led to multiple episodes with transgression and regression, which deposited an early Cambrian succession (Bergström and Gee, 1985). The water entered a regressive phase during the Ordovicium, and eventually left the flat basement exposed to an arid climate (Bruton et al., 1985).

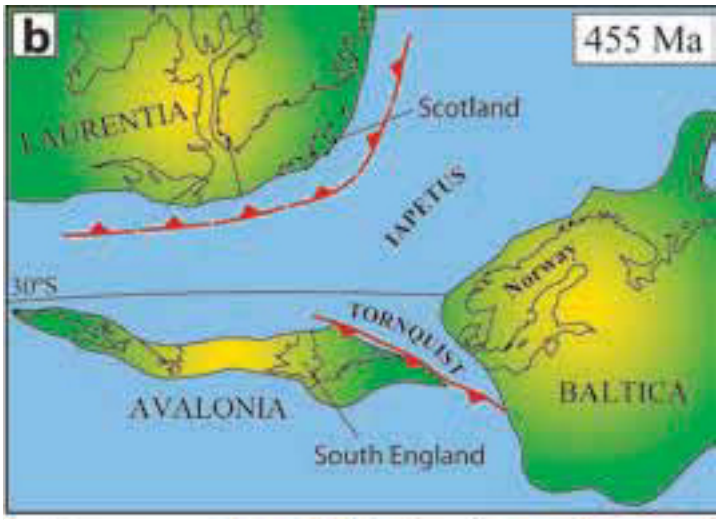

Fig. 3. At 455 Ma Avalonia and Laurentia were progressively pushed towards Baltica, before they collided as part of the Caledonian orogeny. (from Torsvik et al., 1996)

The breakup of Rodinia and the subsequent events could be explained with the Wilson Cycle (Wilson, 1966), which demonstrates the development of an orogeny. The initial stage starts with a stable continent, (like) the supercontinent Rodinia. It is followed by a rifting episode where the continent is divided (for simplicity) into two continents, which will progressively move further and further from each other due to magmatic activity at the rifting site, as seen today at the Mid Atlantic Ocean Ridge. Subduction zones later develop, which lead to a reverse effect were the continents are now being pulled together. The continents eventually collide and unite into one (super) continent to complete the cycle (Wilson, 1966).

The movement and rotation of Baltica continued and pushed it closer to Laurentia. As Wilson (1966) demonstrated in his model, and as discussed by Hossack and Cooper (1986), a subduction zone appeared in the Iapetus Ocean in-between the two continents. The collision between Baltica and Laurentia happened at approx. 425 Ma and marks the start of the Caledonian orogeny and the final step of the Wilson cycle (Torsvik et al., 1996). This orogeny defines most of the mountain chain in Norway today.

Laurentia has moved hundreds of kilometres with respect to Baltica (Fossen, 2010). As Laurentia was pushed on top of Baltica, several nappes developed, and could be seen in western Norway, called the Western Gneiss region (WGR) which is located at the collision front (Fig. 4) (Torsvik et al., 1996). This region in western Norway is an area that underwent high pressure (HP) to ultra-high pressure (UHP) forming eclogites, and defines the part of the continent that was subducted and later uplifted (Koenemann, 1993).

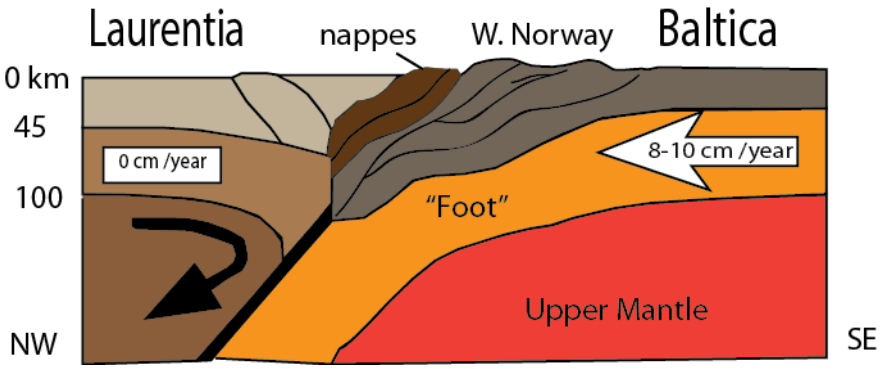

Fig. 4. This illustrates a vertical section of both Laurentia and Baltica, showing how the nappe stacks on top of each other during the collision. Norway is located relative close to collision front. (from Torsvik et al., 1996, modified by author)

The Scandinavian Caledonides are categorized into 6 different geological units: Uppermost Allochthon, Upper Allochthon, Middle Allochthon, Lower Allochthon and Autochthon (Roberts and Gee, 1985).

The Autochthon Pre Cambrian basement as part of the Fennoscandian craton was during the Cambrium overlain by a cover of sediments, which was directly involved in the thrusting. The weak properties of the Palaeozoic sediments acted as a décollement zone, as the thrust sheet could move with relatively little friction over the autochthonous basement (Fossen and Rykkelid, 1992). This thrusting eventually deformed the sediments into a green-schist facies metasedimentary rock (Bergström and Gee, 1985), and is recognized as a phyllite (Bryhni and Sturt, 1985).

The unit above, Middle Allochthon, and to some degree the Lower Allochthon, include locally detached basement derived from the Baltica craton, and defined as the Precambrian crystalline rocks (Bryhni and Sturt, 1985, Koenemann, 1993). Uppermost Allochthon and most of the Upper Allochthon consist of material derived from either island arcs or the Laurentia craton and are defined as exotic (Koenemann, 1993). These two units do not occur in the area of this report, and are located elsewhere in Norway.

As explained in Fossen (2010), during the Devonian (400 – 380 Ma) the Caledonian orogeny entered a post-collision phase with a different kinematic properties. A late stage in an orogeny is well known to develop extensional systems (Fossen, 2010), and due to the great heights of the mountain chain, this also happened in this orogen. The extensional system collapsed the orogen and created detachment faults: Nordfjord –Sogn detachment zone and Hardangerfjord shear Zone which brought higher units to lower ground (Koenemann, 1993, Fossen, 1992) Accommodation spaces developed in the hanging wall of the Nordfjord detachment and sediments from eroding mountains accumulated and created several Devonian basins (Milnes et al., 1997).

Eventually, as modeled by Wilson (1966), the rest of the late Paleozoic continents was assembled into one new supercontinent, Pangaea. One of the responses of this collision was the Oslo-rift. This happened in late Carboniferous around 300 Ma ago. During the Triassic, 251- 200 Ma ago, Pangaea began to break up, and Baltica and Laurentia started to drift from each other creating extensional structures, like basins. In the late Jurassic, the Break-up of Pangaea changed its pattern, and developed rift structure throughout the North Sea and North Atlantic to the Barents Sea. From a petroleum point of view, the famous North Sea Graben was developed in response of this extension, were fault structure and later sedimentation providing source rocks and perfect reservoirs and traps for oil (Ramberg et al., 2006).

2 Methodology

2.1 Introduction

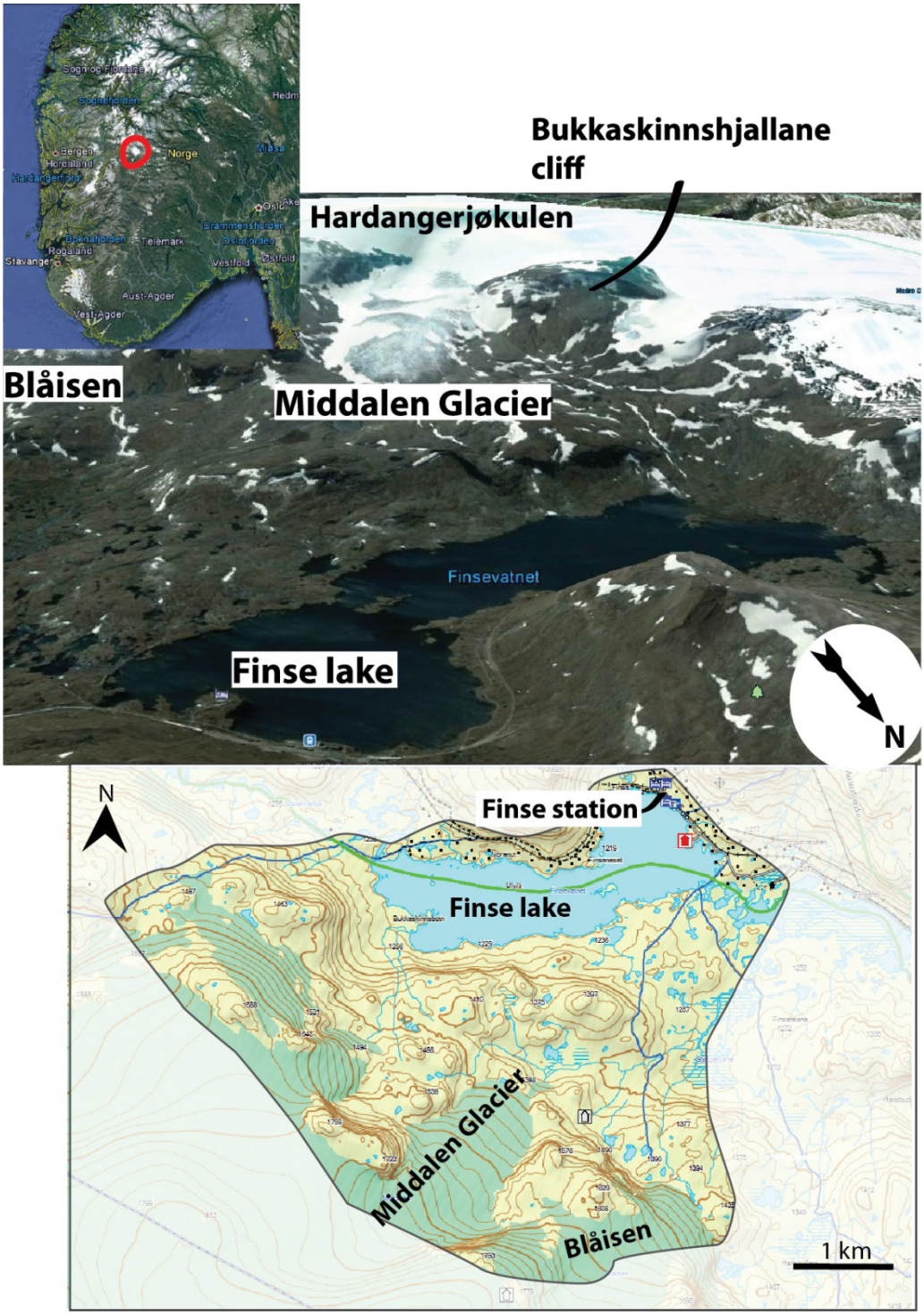

Fig. 5. Picture above: Study area location marked in a red circle. Middle: Google Earth picture of the study area. Below: The marked area is the complete field area. Beside different orientations of the view, the two pictures, middle and bottom cover the same field of view.

This thesis is based on field work around Finse, adjacent to Hardangerjøkulen in the central – south Norway (Fig. 5). The primary goal and methodology during the field work was to

observe and map the main geological elements, and then take sample of the more interesting parts for later analysis.

First week of the field work, was accompanied by supervisor, Fernando Corfu, from 4.July to 9.July 2011. The field work started at the north east side of Hardangerjøkulen, close to DNT (Den Norske Turistforeningen) cabin which was used as accommodation almost the whole trip. A long hike to Rembedalseter (DNT), west side of Hardangerjøkulen, was used as a second place for accommodation during this one week trip. The last day of this trip was a hike from DNT cabin at Finse up Hallingskarvet.
The second field work session was done in the timespan from 22.July to 8.Aug 2011, with accommodation at Finse alpine research center. The primary goal of the 2 weeks field work was mapping and sampling mostly around north-east side of Hardangerjøkulen (Fig. 5). A brief visit from the supervisor, Fernando Corfu during the last days of the 2 week period, led to even greater understanding of the geology of the area.
The third and last session lasted from 28.July to 12.Aug 2012, also with accommodation at Finse alpine research center. This session was to obtain a broader understanding and more measurements. Fernando Corfu shared his experience once more on his 3 days visit how to interpret and distinguish a complex unit (Lower nappe).

The equipment used in the field was personal, while analytical work was done using instrument that was stationed at the University in Oslo

2.2 Field method

During the field work a GPS was regularly used to collect the positions. The GPS data were later converted to WGS 1984 *UTM 32N* as the primary coordinates system used. A Brunton compass was regularly used for measuring strike/dip on a foliation plane, and as well lineations and fold axes.

2.3 Mapping

The coordinates acquired from the GPS, were later exported into Garmin's own software "Garmin Mapsource" (Garmin, 2012). All information was sorted out and exported for the different rock type into ArcGIS version 10, which is the software used for the map making.

Topographical layer, DEM (Digital elevation model), was obtained from the University in Oslo, under the owner of Statens Kartverk (Statens.Kartverk, 2012). This elevation model made it possible to make topographical lines on top of the polygons made in ArcGIS. A geological template was obtained (ESRI.Cartography.Team, 2010), which made it possible to easily create geological contacts. In order to use the correct symbol when mapping, a standard set of patterns was used (Fgdc, 2006). This applies also for names and descriptions on the map of the different features, and is directly obtained from the same document

2.4 Cross section and stereonet

A topographical cross-section was generated in Garmin "Mapsource", and later imported into ArcGIS, as the primary software used to make the cross-section.
The stereonet projections was created using the software by Richard Allmendinger (Allmendinger's, 2012).

2.5 Approximate orientations

Structures, like fold and dikes were repeatedly observed and analyzed in pictures after the fieldwork. So to use these structures, the pictures had to be oriented using the sun and shadow. This implies that exact orientations were not possible, but nevertheless provided a general trend for the fold axes.
All approximate values analyzed with current uncertainty have a (^{Ca}) notation behind.

2.6 Geochronology -TIMS

2.6.1 Theoretical background

"Geochronology is the science of dating and determining the time sequence of events in the history of the Earth" (USGS, 2012).

2.6.1.1 Uranium

Uranium exists as two natural radioactive isotopes: ^{238}U and ^{235}U. Both isotopes have different decay products through time and end up with a different lead isotope (Fig. 6 and Fig. 7). The parent ^{238}U and ^{235}U decay, respectively, to the daughter products ^{206}Pb and ^{207}Pb.

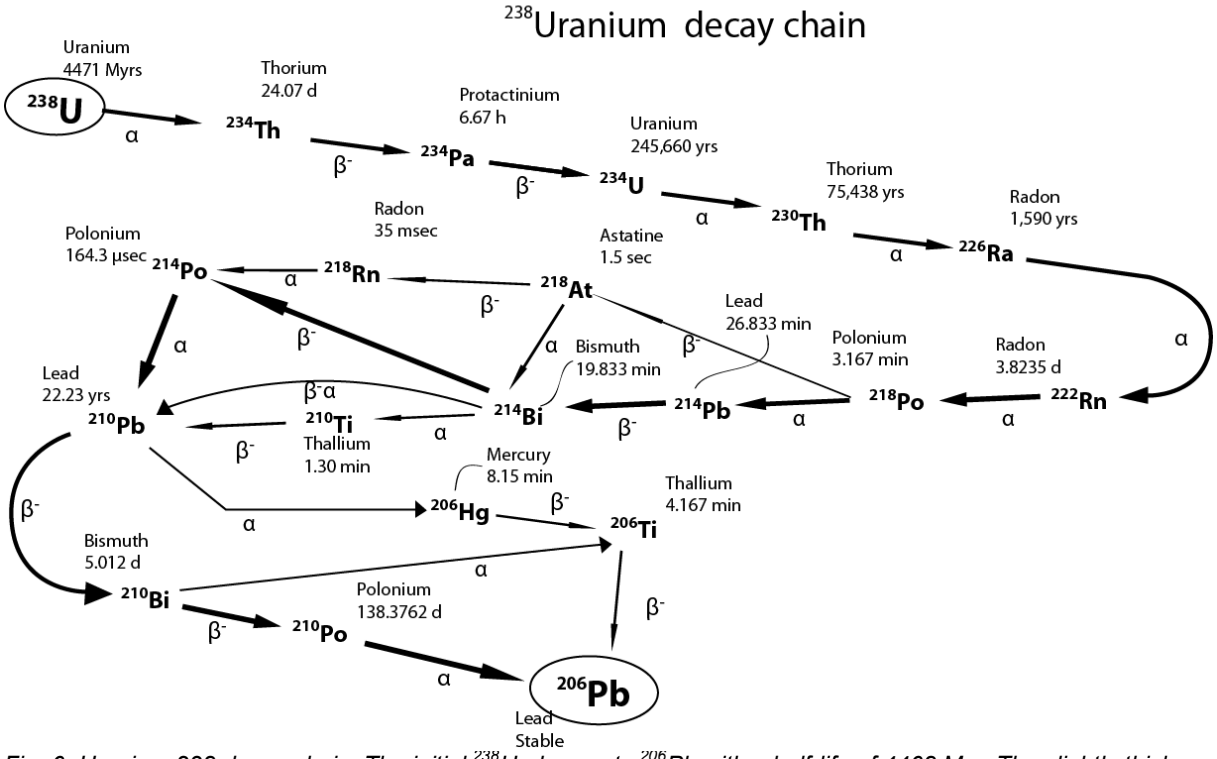

Fig. 6. Uranium 238 decay chain. The initial ^{238}U, decays to ^{206}Pb with a half-life of 4468 Myr. The slightly thicker arrows are the primary chain and contain 13 different decay products after the initial ^{238}U and before the end product ^{206Pb}. (Illustration modifed after Downtheyellowcakeroad, 2012)

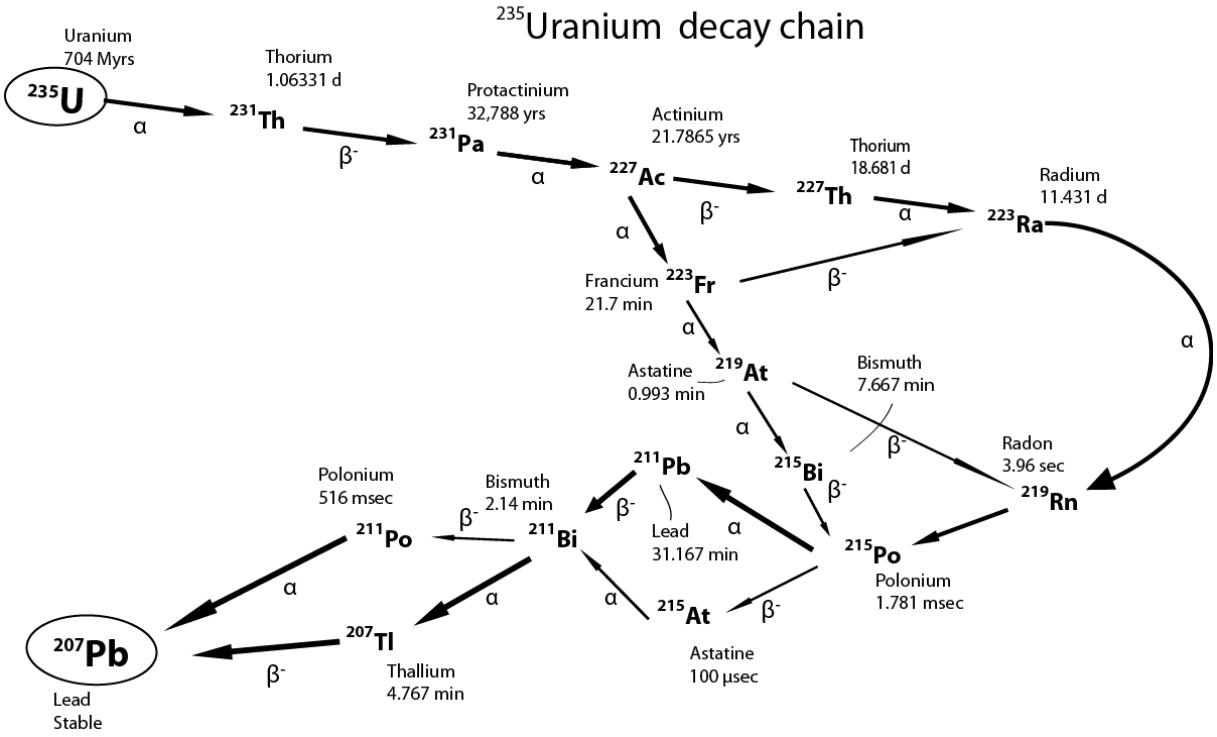

Fig. 7. Uranium 235 decay chain. The initial ^{235}U, decays to ^{207}Pb with a half-life of 704 Myr. The slightly thicker arrows are the primary chain and contain 11 different decay products after the initial ^{238}U and before the end product ^{207}Pb. (Illustration modifed after Downtheyellowcakeroad, 2012)

The half-life of the two different decay chains is also different; ^{238}U decays with a half-life of 4.468 billion years to ^{206}Pb, while ^{235}U decays to ^{207}Pb with a half-life of 704 million years as represented in the following decay formulas:

$$^{238}U \rightarrow {}^{206}Pb + 8\alpha + 6\beta^{-} \ (T_{½} = 4468\ Myr) \quad (1)$$

$$^{235}U \rightarrow {}^{207}Pb + 7\alpha + 4\beta^{-} \ (T_{½} = 704\ Myr) \quad (2)$$

(Davis et al., 2003)

Where α is an alpha particle, which consists of two protons and two neutrons (He^{2+})(Dickin, 2005), and β^{-} is a beta minus particles. After one atom of ^{238}U has decayed and transformed to ^{206}Pb, it has released 8 alpha (α) particles and 6 beta minus (β^{-}) particles (Fig. 6). Similar to ^{235}U, but instead releases 7 alpha (α) particles and 4 beta minus (β^{-}) particles (Fig. 7).

The mathematical representation of equation 1 and 2 shows the amount of radiogenic lead at a given time.

$$^{206}Pb^{*} = {}^{238}U(e^{\lambda_{238}t} - 1) \quad (3)$$

$$^{207}Pb^{*} = {}^{235}U(e^{\lambda_{235}t} - 1) \quad (4)$$

(Halliday, 1997)

Where λ is the decay constant, and defined as $\lambda^{238} = 1.55125*10^{-10}$/yr and $\lambda^{235} = 9.8485*10^{-10}$/yr (Steiger and Jäger, 1977) , t is the time and (Pb^{*}) are radiogenic lead.

2.6.1.2 Zircon

Zircon is usually translucent with some shades of brown color, but also transparent without any color. The chemical composition is $ZrSiO_4$ (zirconium orthosilicate), is made of three basic elements: Zirconium, Silicium and Oxygen. Zircon contains two ionic bonds: ZrO_2 and SiO_2 and constitutes respectively 67.2 % and 32.8 % of the mineral (Klein et al., 2002).

Uranium is a natural element (U), and during the crystallization of the zircon, zirconium can be substituted by uranium. This substitution happens since zirconium has the same charge (4+) and relatively the same size as Uranium (Best, 2009). See Table 1.

Element	Ion	Ionic Charge	Ionic radii (Å)	Coordination
Zr (Zirconium)	Zr^{4+}	4+	(0.72 -) 0.87	8
U (Uranium)	U^{4+}	4+	1.05	8
^{204}Pb		2+	1.32	

Table 1. Datasheet for the elements: Zirconium and Uranium. Both have an identical in ionic charge, and relatively similar ionic radii. In contrast the common lead ^{204}Pb have totally different values to Zirconium. Therefore there are only negligible amounts of common lead in the Zircon.

Trace amounts of uranium will then be incorporated into the zircon structures, and could be used for age determination. In contrast, the common lead isotope ^{204}Pb has different charge and different ionic radio. This means Zircon contains very little (negligible) common lead, which is ideal for U-Pb analysis (Dickin, 2005) .

Zircon is very hard (7.5 on the Mohs hardness scale), robust to weathering and not least resistant to changes during metamorphism, it proves to be a reliable mineral for age determination (Corfu et al., 2003). Despite the small size of the mineral, mostly 20μm to 200μm (Silver and Deutsch, 1963), zircons are typically found in granite but also abundantly found in other types of rocks that contains quartz and feldspar (Mathez, 2004). But in general it is seldom found in large quantities. Zircon is a tough mineral and will re-crystallizes rather than break down if exposed to metamorphism (Mathez, 2004). This crystallization during time develops zoning with slightly different composition. The core can be older than the host rock itself, and rims developed at same time as the host rock was crystallized, represent therefore different geological cycles, like: orogeny- erosion and then burial (Mathez, 2004). Age determination could provide multiple age results when measuring zircons with this core and overgrowth rim structure.

Also taking into consideration that when zircon is (re)heated the chemical composition could be altered, the lead which is a product from decaying uranium diffuses out of the crystal (Mathez, 2004). This ratio between uranium and lead changes, and would give a wrong or meaningless age of the current rock (Davis et al., 2003).

Since the different potential miscalculations have to be taken into consideration, both isotopes are measured and compared. If the age gathered from these two isotopes deviates considerably, it is said to be discordant and might not be reliable (Davis et al., 2003).

A zircon that is not affected by radiation damage is transparent with light yellow color, while zircons that are affected from decay damage have a darker color, usually gray and are non-transparent (Corfu et al., 2003). Zircons that contain both relatively high quantities of uranium and lead have been strongly damaged by the radioactivity, are called *metamict* (Publishing and Rafferty, 2010). This provides a dilemma, where higher amount of uranium makes the analytical work easier since it gives more readings, but at the cost of more radiation damage which will affect the credibility of the results. To prevent this dilemma, zircons with less uranium is chosen on the cost of more difficult analytical part.

2.6.1.3 Titanite

Titanite is another mineral used for age determination. This mineral in its purest form has a chemical composition: $CaTiSiO_5$, and is composed of Calcium, Titanium, Silicium and Oxygen. The ionic bonding developed from these elements is TiO_2, SiO_2 and CaO, which respectively constitute 40,8%, 30.6 % and 28.6% off the mineral (Klein et al., 2002). Titanium could be substituted by Uranium during crystallization, as they have same charge (4+) and relatively similar ionic radii. This gives trace element of uranium in the Titanite.

Element	Ion	Ionic Charge	Ionic radii (Å)	Coordination
Ti (Titanium)	Ti^{4+}	4+	0.61	8
U (Uranium)	U^{4+}	4+	1.05	8

Table 2. Datasheet for the elements: Titanium and Uranium. Both are identical in ionic charge, and quite similar in ionic radii.

The major difference between Titanite and Zircon is how easly the mineral responds to heat during metamorphism. The blocking temperature for titanite is 625°C degrees, which means that titanite requires less temperature than zircon (> 625°C) to resets its internal clock (ratio lead/uranium) to zero. Results from Titanite could (also) be totally differente from Zircon, and might tell the metamorphic age rather than the formation age (Dickin, 2005). It might not give any meaning to correlate the age aquired from the Zircon with the age from Titanite, since it is likely that they tell two different stories (or contamination has altered one or both of the samples). But Titanite and Zircon could also provide same age which would be a reliable age for the current sample.

2.6.2 Analytical Preparation

The samples gathered from Finse during the field work, had to be prepared before it could be analyzed using the method described in (Krogh, 1973), (Corfu and Grunsky, 1987) and (Dickin, 2005).

The solid rock fragments were first crushed into smaller pieces and later washed on a wilfley board to remove all lighter mineral while keeping the heavier ones. The main fractions had to be reduced substantially in size with Frantz magnetic separation and heavy liquid separation using methylene iodide. While the magnetic separation separates based on its magnetic properties, the heavy liquid separates all mineral heavier or lighter than approx.[1] p=3.32 from each other.

The next phase of the preparation work was to pick the best zircons by using a microscope. In this case the best zircon would be the minerals that are least subjected to radiation damage and has a clear red color and is homogenous. The zircons with greyish color and a lot of inclusions from other minerals are removed. Also Zircons with cores are not preferable and filtered out. The selected minerals were transferred to an abrasion chamber, where the rim of the zircon was abraded away to remove radiation damage domains that may be present and alter the age result. Pyrite was also injected into the chamber to prevent zircon from destroying each other. A washing process followed by using a solution with Nitric Acid (HNO_3) to remove foregin minerals or particles attached to the zircon mineral. Some zircons went through a chemical abrasion, where the mineral is first annealed at 900°C and then subjected to a HF solution for a day. This process removes all the softer part, while keeping the harder clear, non- metamict zircons.

The minerals were subsequent weighed (on a microbalance) and transferred into a solution of 1 drop Nitric Acid and 12 drops of hydrofluoric acid. To determine the ratio between U and Pb correctly, a reference solution called a spike was united with the zircon. The reason for using a spike is that lead ionizes easier than uranium which gives a higher value from the mass spectrometry of lead compared to uranium. All values had to be calibrated according to the spike, to get the correct ratio. The spike consists of two isotopes: the artificial ^{205}Pb and the natural but enriched ^{235}U. The ratio between ^{238}U and ^{235}U is 137.88 (Steiger and Jäger, 1977), while the spike, ^{235}U and ^{238}U is 1400:1 and the ratio between ^{205}Pb and ^{235}U is 1:100. This solution (spike + zircon) was added to a Teflon bomb. The Zircon was dissolved in these bombs containing Hydrofluoric acid at a temperature of 184 °C for five days (Corfu, 2004, Krogh, 1973). A chemical separation process (chromatography) removes any other unwanted

[1] Methylene iodide has ideally a density of p=3.32. Repeated usage reduces the density of the heavy liquid.

chemical components, as described by Krogh (1973). This process involves using HCl to separate Lead (Pb) and Uranium (U) from the rest of the solution. The solution which only contains lead and uranium is loaded onto Rhenium (Re) filaments with Silica gel and phosphoric acid (H_3PO_4).

2.6.3 Analytical work

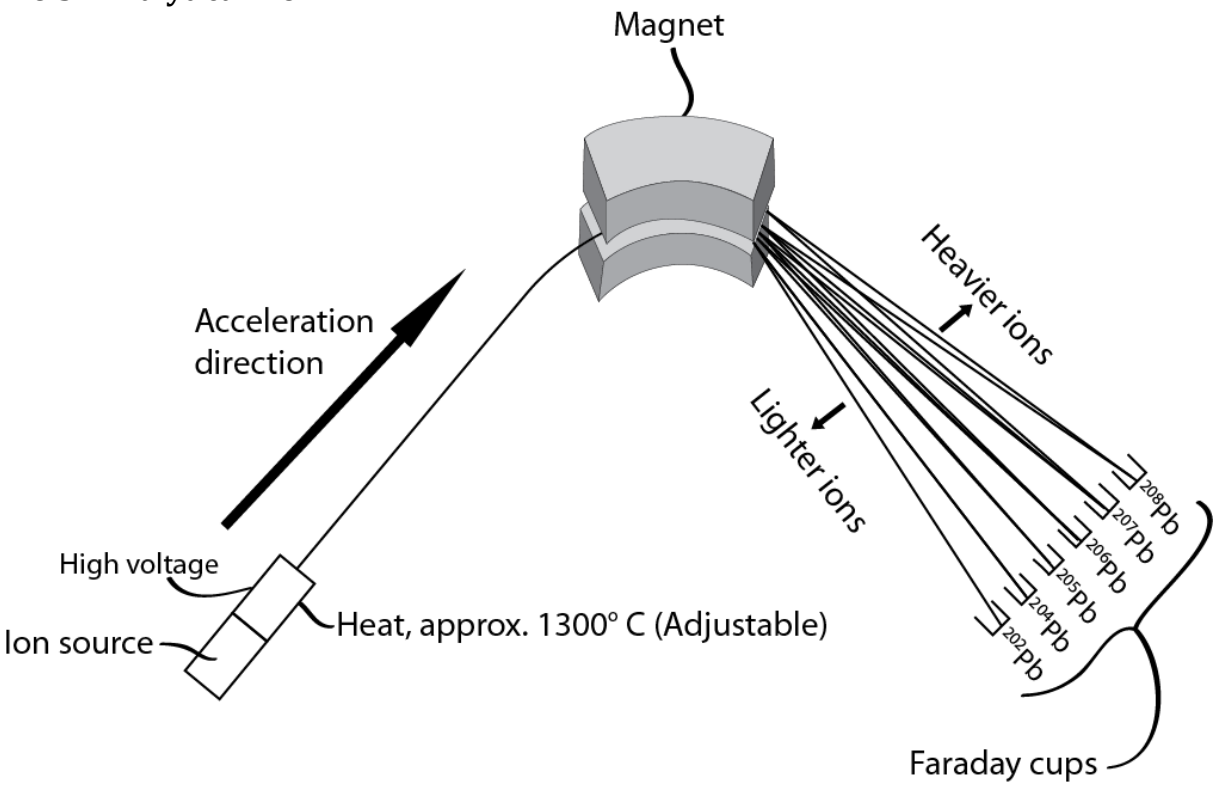

Fig. 8. The mass spectrometer. First module is the Ion source where samples are placed. Next is the heat source, which heats the sample to approx. 1300° degrees (variable) and ionizes the U and Pb. The ions are accelerated by an 8- 10 kV potential and speed up along the flight tube. The magnet module in the middle deflects the ions, the trajectory changes depending on the mass of the ion and is collected by 8 faraday cups. These cups represent (from lighter to heavier mass): ^{202}Pb, ^{204}Pb, ^{205}Pb, ^{206}Pb, ^{207}Pb and ^{208}Pb

The filament with the sample incorporated into the hardened silica, was placed into a part of the mass spectrometer called "the source" (Fig. 8). A variable amount of electric current was applied to the filament that heated it up to approx. 1300 °C. When the filament were heated up, the lead and uranium in the sample were ionized and started to emit Pb^+ and UO_2^+ ions. The silica gel used in previous prepartation, is to produce a stable and efficient ion emission (Cameron et al., 1969). The positive ions are set in motion due a high voltage module, and the trajectory of the ions is changed from a magnetic field were the mass influences the amount it changes the curvature (Dickin, 2005). The mass spectrometer consists of eight different faraday detectors which would collect different ions based on their masses (Fig. 8).

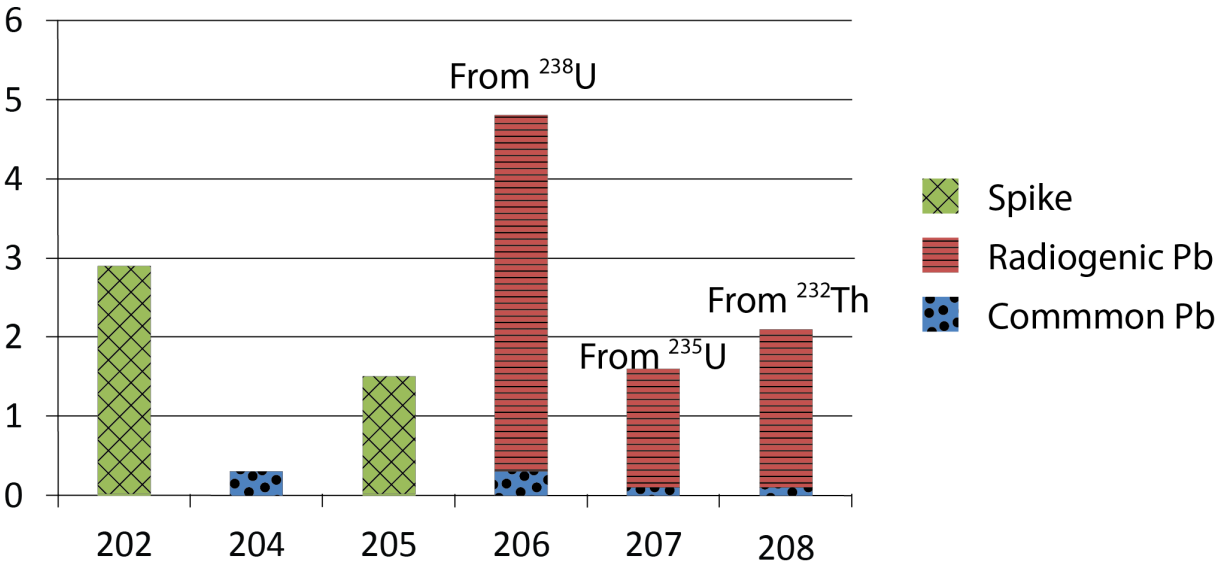

Fig. 9. A fictive result diagram from the mass spectrometer. Each column represents current/ion intensity collected from each faraday cup. 202(Pb) represent only spike, 204(Pb) are only common lead, 205(Pb) are only spike, 206(Pb) consists of a small fraction Common Pb and rest radiogenic Pb and are acquired from ^{238}U, 207(Pb) consists a small fraction of Common Pb and rest radiogenic Pb and are acquired from ^{235}U, last is the 208(Pb) also consists of a small fraction of Common Pb and rest radiogenic Pb produced from ^{232}Th.

Fig. 9 presents a fictive result from the mass spectrometer. Each column is a current intensity from the different faraday cups (Fig. 8) positioned to receive from ^{202}Pb to ^{208}Pb, where ^{203}Pb doesn't exist. While ^{206}Pb, ^{207}Pb and ^{208}Pb are composed of mainly radiogenic Pb and a small fraction of common lead, ^{202}Pb and ^{205}Pb is spike (tracer) and ^{204}Pb is Common lead. Common lead, ^{204}Pb is lead from other sources than decaying uranium, and is defined as contamination. *Initial lead* is not generated from decaying uranium, and *blank* is lead contamination from other source under the analytical work. This contamination (blank + initial) has to be mathematically removed (Dickin, 2005, Kober, 1986). The challenge with ^{204}Pb, is that it only exists in small quantities which make it very difficult to measure. To get proper readings while analyzing with mass spectrometry, a *secondary electron multiplier* was used to multiply the electrical current, where the quantity is too small to be measured with Faraday cup method.

2.6.4 Calculations

The basic goal was to acquire all concentration quantities of the different isotopes and subtract the common lead which gives the radiogenic quantity. The following procedure gives the radiogenic ratios:

First is to acquire the concentration of ^{207}Pb and ^{206}Pb by using the spike.

Spike concentration	Spk_c (pg pb/mg)
Spike quantity	spk_q

Table 3. Values for the spike concentration and spike quantity. The spike concentration are usually a given value.

Results from Mass spectrometer	
Isotopes	**Ratio**
$^{207}_{Pb}/^{206}_{Pb}$	Pb_1
$^{206}_{Pb}/^{205}_{Pb}$	Pb_2
$^{206}_{Pb}/^{208}_{Pb}$	Pb_3
$^{205}_{Pb}/^{202}_{Pb}$	Pb_4
$^{207}_{Pb}/^{204}_{Pb}$	Pb_5
$^{238}_{U}/^{235}_{U}$	U_1

Table 4. This table represents results aquired from the mass spectrometer. The different ratios between each isotopes are given as Pb_x.

1. The total solution ^{205}Pb, equals the amount of spike used times the concentration: Spk_c

$$spk_q * spk_c = {}^{205}Pb \qquad (5)$$

2. The ratio between ^{206}Pb and ^{205}Pb are Pb_2 : 1, which means the amount of ^{206}Pb is Pb_2 times the amount of ^{205}Pb.:

$$Pb_2 * {}^{205}Pb = {}^{206}Pb \qquad (6)$$

3. The ratio between ^{207}Pb and ^{206}Pb are Pb_1: 1.

$$Pb_1 * {}^{206}Pb = {}^{207}Pb \qquad (7)$$

The calculated ^{206}pb and ^{207}pb are adjusted in respect of the spike.

Contaminations which are common lead (initial + blanks) have to be corrected for. The ^{206}Pb and ^{207}Pb contains relative to the radiogenic Pb, a minor fraction of common lead (Fig. 9). While the quantity is unknown and has to be calculated for, the ratio between the common lead fraction of ^{206}Pb/^{204}Pb and ^{207}pb/^{204}Pb are always constant and known. This means by knowing the quantity of ^{204}Pb, the amount of common lead in ^{206}Pb and ^{207}Pb are 1:18:15 respectively. In other word: ^{206}pb/ ^{204}Pb = 18 and ^{207}Pb/^{204}Pb = 15. The quantity of common lead from each isotope (Fig. 9) can now be mathematically remove to get the proper radiogenic value of either ^{206}Pb or ^{207}Pb. Since the radiogenic lead concentration represent the amount of decaying lead, this will be used to calculate the age of each isotope. Equation 3 and 4 has to be rearranged:

$$T_1 = \frac{1}{\lambda_{238}} \ln\left(\frac{^{206}Pb^*}{^{238}U} + 1\right) \qquad (8)$$

$$T_2 = \frac{1}{\lambda_{235}} \ln\left(\frac{^{207}Pb^*}{^{235}U} + 1\right) \qquad (9)$$

Where (Pb^*) are radiogenic lead (Halliday, 1997, Wetherill, 1956).

Wetherill (1956) developed a graphical system that plots the two different isotopic ratios (^{207}Pb/^{235}U and ^{206}Pb/^{238}U), and easily read the age of the diagram, where the x- axis is ^{207}Pb/^{235}U and y-axis is ^{206}Pb/^{238}U. For the pre-defined concordant line, it's calculated for every *t* value starting at 0 age. This displays concordant ^{206}Pb/^{238}U and ^{207}Pb/^{235}U values as a continuous curve. As every point represent a certain age, it's easy to read the age from a samples that has concordant values and put into this diagram (Fig. 10) (Dickin, 2005, Wetherill, 1956)

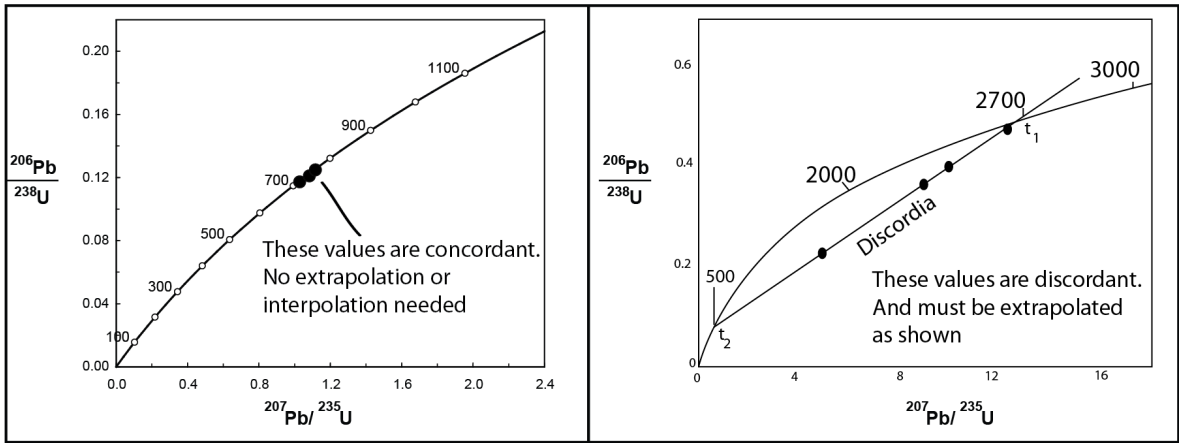

Fig. 10. Concordia diagrams were x–axis is the ratio ^{206}Pb/^{238}U, and Y-axis is ^{207}Pb/^{235}Pb. Left: The values are defined as concordant, since they fit on the "Concordia curve". (Illustration modfied from Dickin, 2005) Right: The values are defined as discordant since they don't fit on the "Concordia curve, and has to be extrapolated. Modified lecture from Fernando Corfu, After Tilton(1960)

If equation 8 and 9 yield similar ages ($T_1 = T_2$), they are defined as concordant, and could be simplified:

$$\frac{^{206}Pb^*}{^{238}U} = (e^{\lambda_{238}t} - 1) \qquad (10)$$

$$\frac{^{207}Pb^*}{^{235}U} = (e^{\lambda_{235}t} - 1) \qquad (11)$$

(Wetherill, 1956, Dickin, 2005)

However the true nature of a rock cycle may be far more complex than just obtain true concordant values.

Wetherill (1956) suggested several assumptions for the given ages to be concordant, otherwise they are defined as discordant:

a) "*There have been no gains or losses of uranium or lead during the time since the formation of the system*"
b) "*There have been no gains or losses of intermediate members of the radioactive decay scheme, for example, radon, or ionium*"
c) "*Proper corrections have been made for the initial concentration of* Pb^{206} *and* Pb^{207}"
d) "*The Chemical analyses have been properly performed and the correct decay constants* λ_1 *and* λ_2 *have been used*"

As assumption (a) states, it is a problem when the lead or the uranium concentration increases or decreases by other factors than natural decaying. Fig. 10, right picture illustrates a Concordia diagram where the points might reflect a later geological event, ex. metamorphism and re-heating. In this case the ages are discordant (Equation 8 and 9: $T_1 \neq T_{2)}$ and cannot be simplified in the same way as if it was concordant. Extrapolation and further calculations are needed to achieve the correct age (Wetherill, 1956).

2.7 Thin Section

Four samples were sent in to make thin section. The thin section contains a slice of rock that is glued on a 2.7 cm x 4.7 cm glass piece, and polished down to size of 0.3 mm. The equipment used to analyze the thin section sample was a petrographic microscope stationed at the University in Oslo. This microscope consists of several optical devices, like: polarizer,

Bertrand lens, stage, (with more) that was used to analyze the thin section and identify different minerals and the metamorphic properties of selected minerals.

2.8 Terminology

Color coding

The units on the map and in the description are marked with different colors.

Upper nappe is yellow

Lower nappe is purple in the map and dark purple in the description

Phyllite is green

Basement: Regolith are marked as red or red line

Basement: Granite are always marked as orange

Pegmatite are marked as darker orange

Gabbro and amphibolite are marked stippled black on the map, and gray in the description

Crystal sizes

A classification table of the different crystal sizes, use to describe the different lithologies.

Name	**Size range**	**Visible without optical instrument**
Very fined grained	< 0.1 mm	No
Fine grained	0.1 mm - 0.5 mm	Some minerals, but the matrix are not visible
Medium grained	0.5 mm – 1 mm	Yes, but some are too small
Coarse grained	1 mm - 5 mm	Yes
Very coarse grained	5 mm – 1 cm	Yes
Pegmatitic size	> 1 cm	Yes

Table 5. This table is a classification of the different grain sizes used in the description.

Décollement zone

This zone contains weaker rock units which are parallel to the bedding, and separates the deformed rocks from (sometimes) the undeformed basement. This reduces the friction between the basement and the moving thrust front, and enables the trusting to move even further. The fault which separates the weak rock with the thrust front, is called décollement (Twiss and Moores, 2007).

Accretion

"*The addition of continental material to a pre-existing continent, usually at its edge*".

As stated above, accretion general involves all situations were plates converge and meet without the thrusting or subduction involved (Allaby and Allaby, 2003).

Klippe

Klippe is an isolated erosional feature (Fig. 11). While the erosion has removed the surrounding area beneath the thrust fault, an isolated cliff (hence the word klippe) sometimes remains. Later faults could also be the reason for how these structures are developed.

The opposite feature is a window, where erosion has carved a hole in the thrust sheet, below the thrust fault exposing the rock below. (Twiss and Moores, 2007)

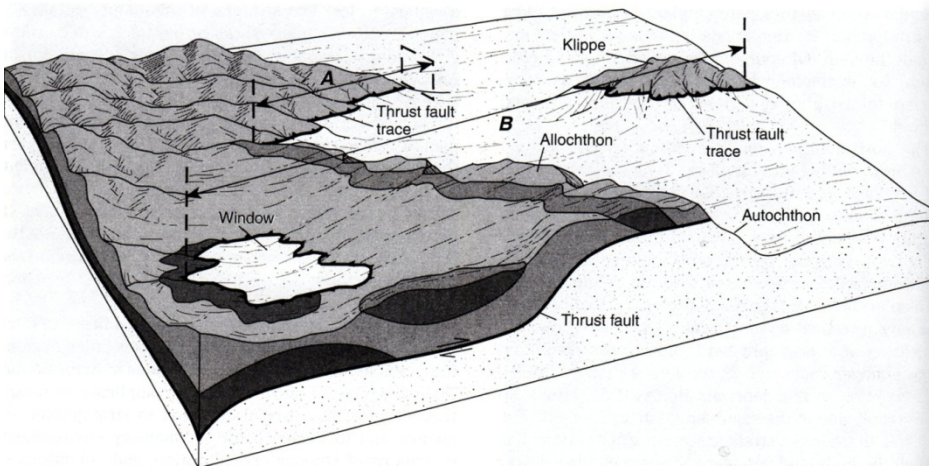

Fig. 11. The klippe as illustrated is the same geological features as seen in the study area, and developed as an isolated erosional feature. (from Twiss and Moores, 2007)

Fold tightness describes the fold based on the interlimb angle, *i*.

Gentle, Open, Close, Tight, Isoclinal are definition based on various tightness angles (Fig. 12).

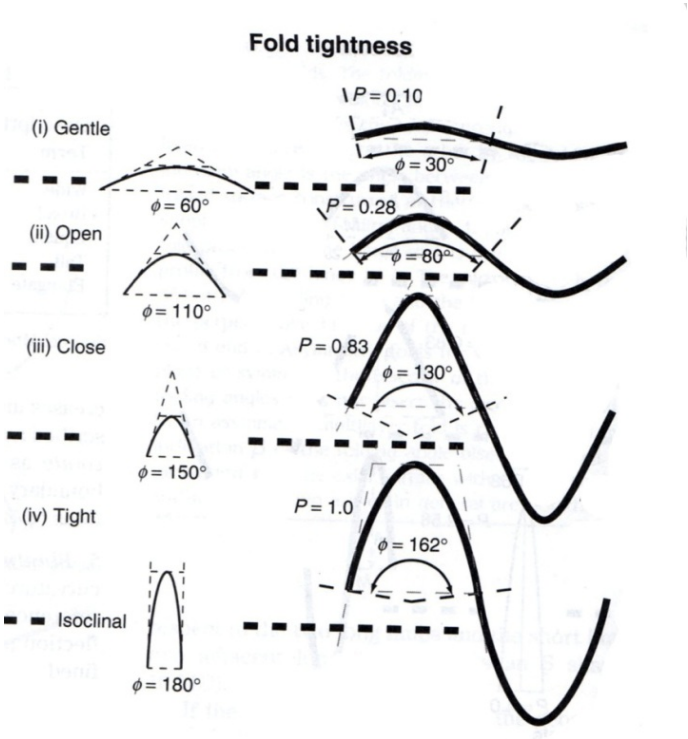

Fig. 12. Fold classification based on their tightness. (from Twiss and Moores, 2007)

Relationship between the plunge of the hinge and the dip of the axial surface:

The folds are also classified depending on the plunge of either the axial surface or the fold hinge. A *recumbent* fold would according to the classification have 0°degrees plunge fold and between 10° and 0° dip of axial surface, while a gently inclined has axial surface dip between 30° to 10°.

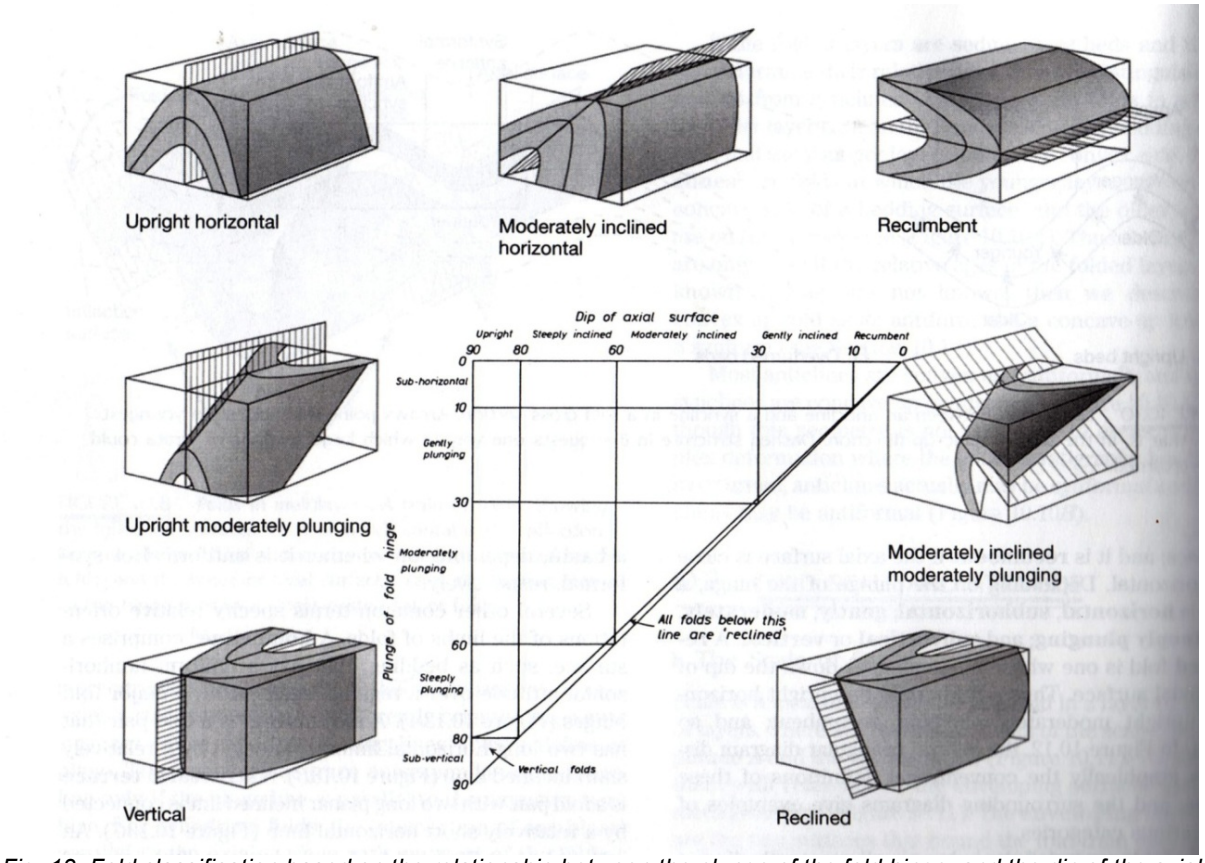

Fig. 13. Fold classification based on the relationship between the plunge of the fold hinge, and the dip of the axial surface. (from Twiss and Moores, 2007)

Asymmetric and symmetric folds:

A fold is defined either as asymmetric or symmetric whether if the fold has a mirror image on the opposite side relative to its center (Fig. 14).

Symmetric folds are defined "if the hinge is a mirror image of the shape on the other side and if adjacent limbs are identical in length".

Asymmetric fold "have no mirror plane of symmetry and the limbs are of unequal length".

If the short limb has rotated clockwise with respect to the long limbs it is defined as a z-fold or a clockwise fold. And it is defined as s-fold or counterclockwise fold when the short limb has rotated counterclockwise in respect to the longer limbs. (Twiss and Moores, 2007)

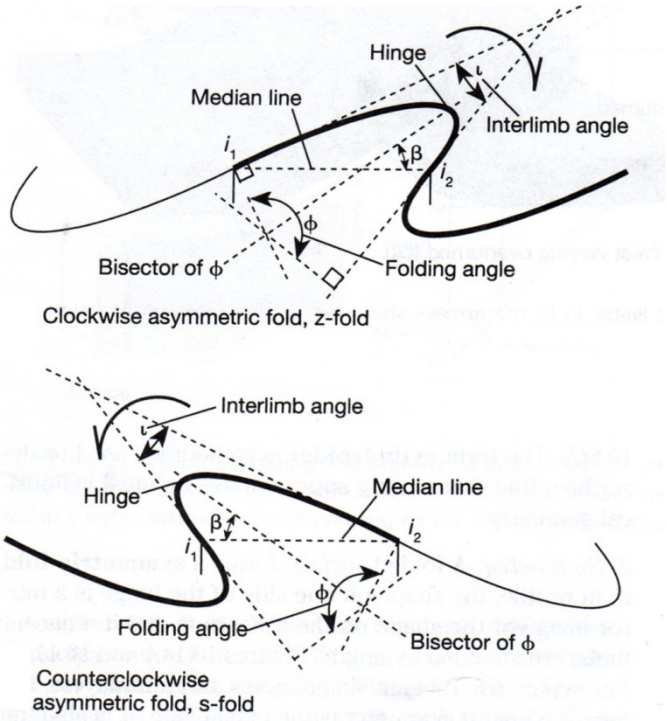

Fig. 14. Asymmetrical fold, as there is no mirror images around the fold hinge. The fold above is defined as a Z.-fold since it has rotated clockwise, and the fold below is rotated anticlockwise, and are defined as a S-fold.(from Twiss and Moores, 2007)

Beta axes

All acquired strike and dip measurements might reveal the fold axis orientation if plotted into the stereonet. The place where (nearly) all measurements cross each other, are the Beta point and equals the fold axis orientation (Fig. 15). (Twiss and Moores, 2007)

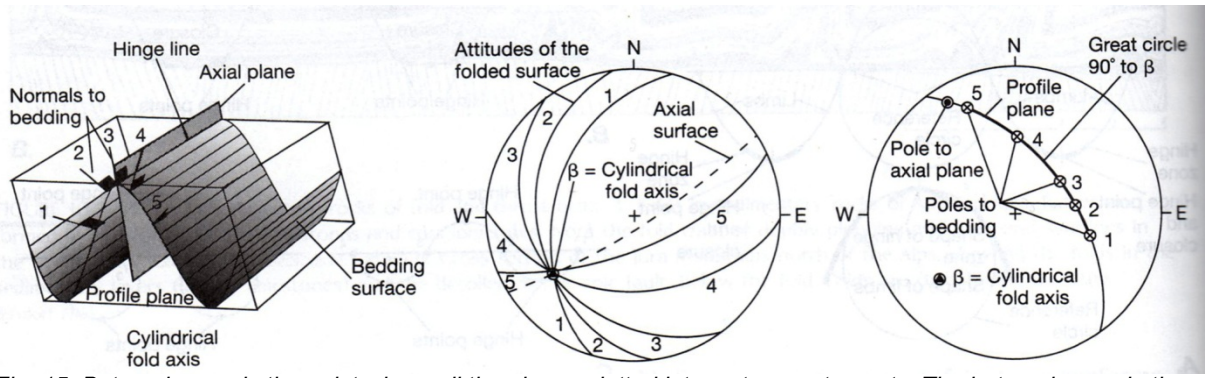

Fig. 15. Beta-axis equals the point where all the planes plotted into a stereonet, meets. The beta-axis equals the fold-axis. (from Twiss and Moores, 2007)

Nappe

Nappe is defined as a large scale recumbent isoclinal fold. The word nappe is French and means "tablecloth", and illustrates sheet that are move on top of a low dipping surface (Twiss and Moores, 2007).

Flinn diagram

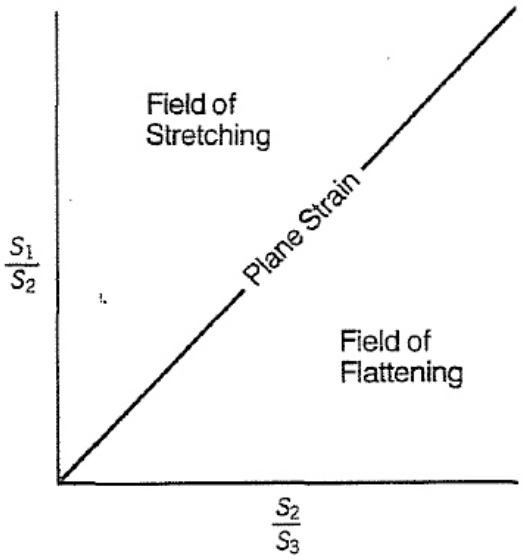

Fig. 16. Flinn diagram. In three dimensional strain this diagram is used to visualized the different possibilities of deformations. Constrictional strain are occurring in the "field of stretching".(from Davis and Reynolds, 1996)

The Flinn diagram is way to visualize the possibilities in three-dimensional strain (Fig. 16). X and Y axis of this diagram are respectively X/Y (S1/S2) and Y/Z (S2/S3) ratio to the three axes in the strain ellipsoid. Constrictional strain, also known as cigar shape is occurring in the "Field of stretching" area (Davis and Reynolds, 1996).

3 Description

3.1 Introduction

Finse and surrounding area, including Hardangerjøkulen, have 2 fundamental tectonostratigraphic units. These units are categorized on depending whether they result from Caledonian thrusting, hence a long distance movement, or static which implies that it was overall unaffected during the Caledonian orogeny. These tectonostratigraphic units are defined as Autochthon and Allochthon. The stratigraphically lowest unit, the basement is a static unit and hasn't moved in response to the orogeny. The next unit, (para) Autochthon, is the sedimentary layer that has been metamorphically changed to phyllite during the orogeny. This unit has moved a relative short distance (only tens of km, in contrast to the 300 km the nappe has been pushed (Ramberg et al., 2006)), so it's not defined as allochthon, and it's not entirely static as autochthon. Therefore the author would avoid any confusion, and name this unit just for phyllite. Above the phyllite is the first evidence of the tectonic Nappe, and is defined as the Middle Allochthon. This unit is the crystalline basement derived from Baltica itself. But as observed from the field, there is another unit that doesn't fit in as either phyllite or the Middle Allochthon. To resolve this, an unofficial term "***Lower nappe"*** is introduced to describe the local unit that appears in this field area. Lower nappe is therefore placed as part of the lower part of Middle Allochthon. Above is yet another unofficial name: "***Upper nappe"***, which is the documented crystalline basement and would be the upper part of Middle Allochthon. This tectonostratigraphic setting is shown in Fig. 17.

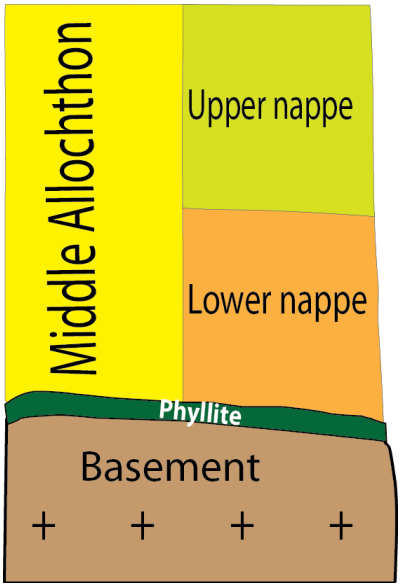

Fig. 17. This is the general stratigraphic setting at the Field area. Besides the known Basement and Phyllite, Middle Allochthon are dived into two further unofficial sub-units: Lower nappe and Upper nappe

While describing each unit, the same chronological order will be used, starting with the stratigraphic lowest unit and ending with the top most units that are found at Finse and surrounding area.

Appendix 1 is a map of all the localities.
Color coding and classification of the different mineral sizes is explained at chapter 2.8
For values with ([ca]) behind, referred to chapter 2.5.

3.2 Rock description

3.2.1 Basement

The autochthonous basement is exposed over a large area, general in places below 1320 m - 1360 m: The basement consists of different lithologies, as follows:

Granodiorite

Granite

Gabbro/Amphibolite

Pegmatite

Besides the pegmatite and amphibolite, the different lithologies tend to be found in more isolated areas. The study area is characterized by a felsic dominated area and a mafic dominated area which respectively are located north of Hardangerjøkulen and north-east of Hardangerjøkulen. The felsic area is primarily granodiorite and granite, and the mafic area is primarily gabbro. However in the felsic dominated area, it is very common to find larger (tens of meter) isolated areas with mafic lithologies, usually with intermixing structures area often observed. Pegmatite is also another common feature, which intrudes both mafic and felsic lithologies more systematically.

Roughly estimated the basement in the study area consists of 50% fine grained granodiorite, 20% coarse grained granodiorite, 20 % granite and 10% amphibolite/gabbro. The late dikes intruding basement are mostly pegmatite, but coarse grained granodiorite dikes have also been observed.
The granite however is still the primary felsic lithology when comparing the basement outside of the field area. In a larger view, Finse, Hardangerjøkulen and surrounding areas of the basement constituted of approx. 95 % granite.

3.2.1.1 Granodiorite

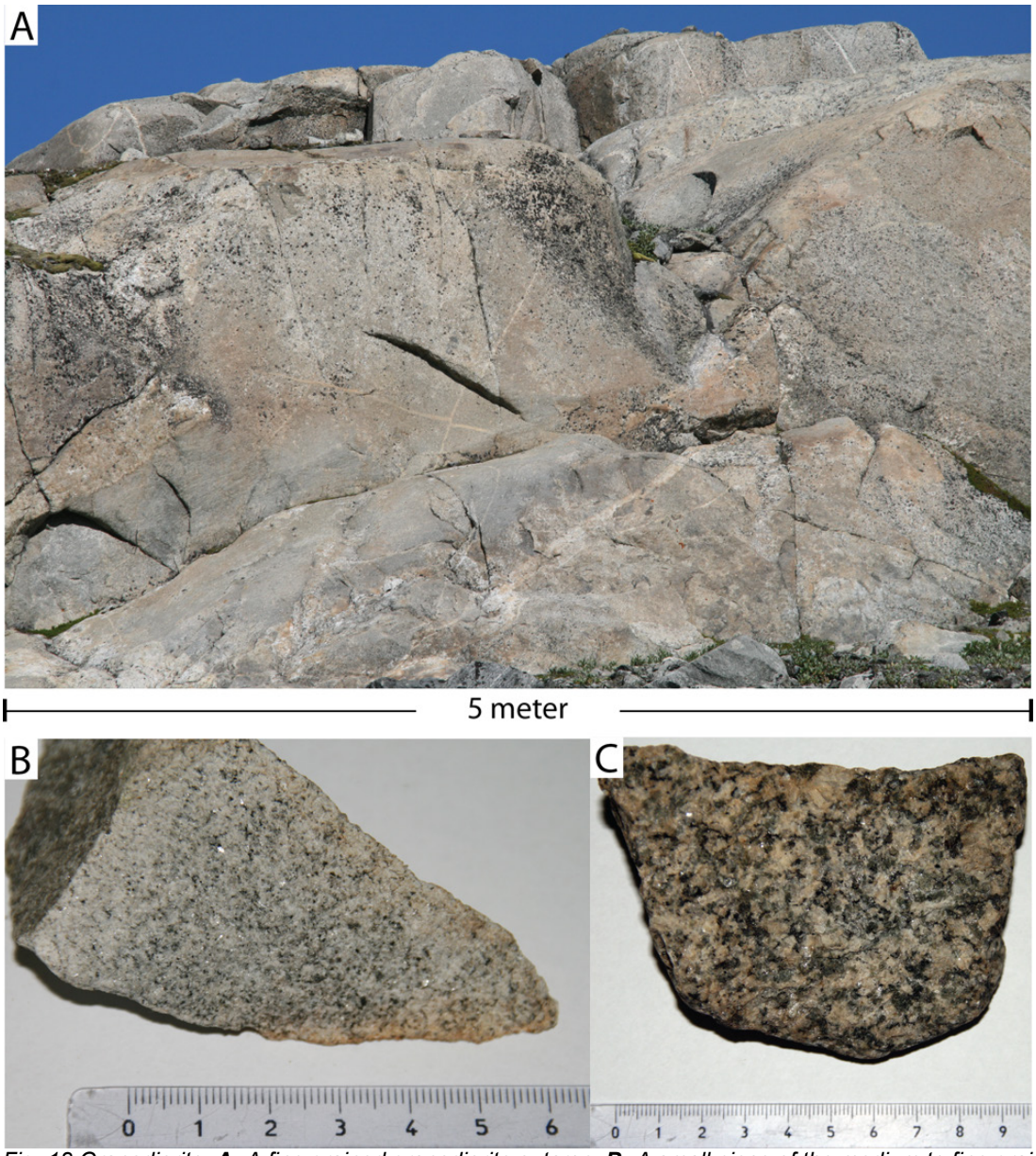

Fig. 18.Granodiorite. ***A:*** *A fine grained granodiorite outcrop.* ***B:*** *A small piece of the medium to fine grained granodiorite. The grain size ranges from 1 mm to below 0.5 mm.* ***C:*** *The very coarse grained granodiorite with grain size from 1mm to 1 cm.*

The first granitic type is a medium to fine grained granodiorite (Fig. 18 A & B), where each crystal is 1 mm and smaller, and barely visible without an optical instrument. Very massive and homogenous rock type, and are the dominated basement lithology in the study area. The granodiorite has been highly affected by glacier erosion due to the polished outcrops, and not least weathered surface, which makes the appearances for the granite and coarse grained granodiorite surface similar, and sometime a challenge to distinguish.

The thin section reveals a high amount, 50- 70 % of plagioclase and K-feldspar, and only 10 – 20 % quartz. According to the Streckeisen classification diagram, this light felsic type is a

Granodiorite, almost tonalite. Mafic minerals as mica (biotite), contributes 10 – 30 % of the rock. Titanite was found sometimes as large grains and also as secondary feature as it has grown around the biotite.

Another type, is a "very coarse grained" granodiorite (Fig. 18 C). It is quite similar to the fine grained granodiorite. But here the crystals have been able to grow to size where it's easier to distinguish each one with the bare eye. The size of the minerals ranges from 1 mm up 1 cm. The distribution between felsic and mafic minerals is quite similar to the fine grained granodiorite approx. 60/40.

3.2.1.2 Granite

The second granitic type is the widely distributed granite, and is the primarily type found in the basement. However at the study area, the granodiorite is the primary lithology.

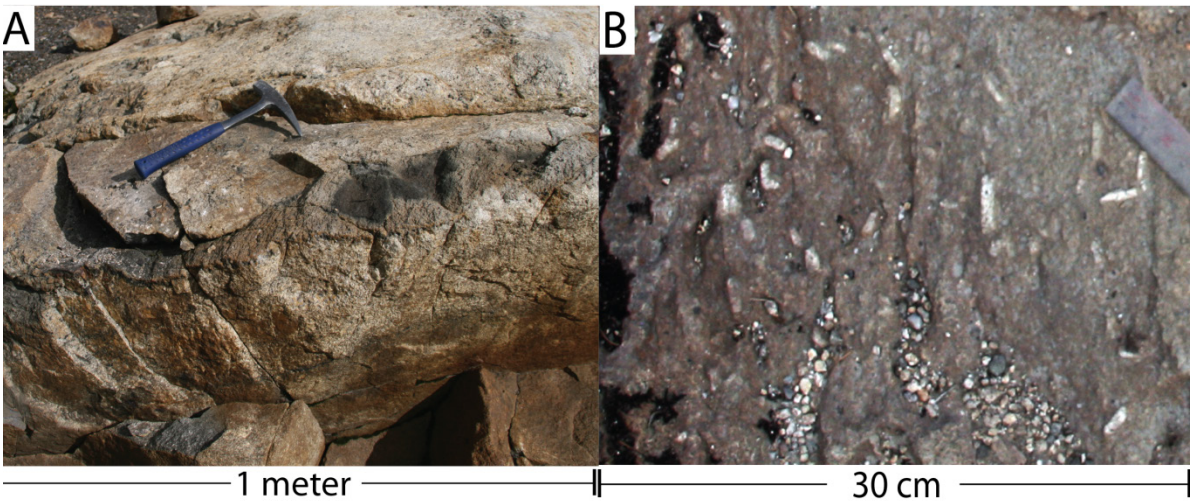

*Fig. 19. Granite. **A:** A granite outcrop. **B**: The characteristic feldspar megacryst appearing in the granite. These crystals are 1-2 cm long.*

This granite has often many similar appearances to the coarse grained granodiorite and is often very homogenous and massive. This is granite like the granodiorite is little affected by Caledonian orogeny and besides erosion, weathering and intrusions it is quite unaltered without any foliation plane. In Fig. 19 A, the regolith contact is close due to the slightly red colored lithology.

The granite is light colored felsic and with very coarse grained minerals. The megacrysts of feldspar have grown to centimeter sizes, and are easily observed without any optical instruments. The lithology has many similarities to the very coarse grained granodiorite, and contains microcline, plagioclase and 50% quartz. The plagioclase has inclusion of microcline. Calcite was also observed.

3.2.1.3 Amphibolite and gabbro

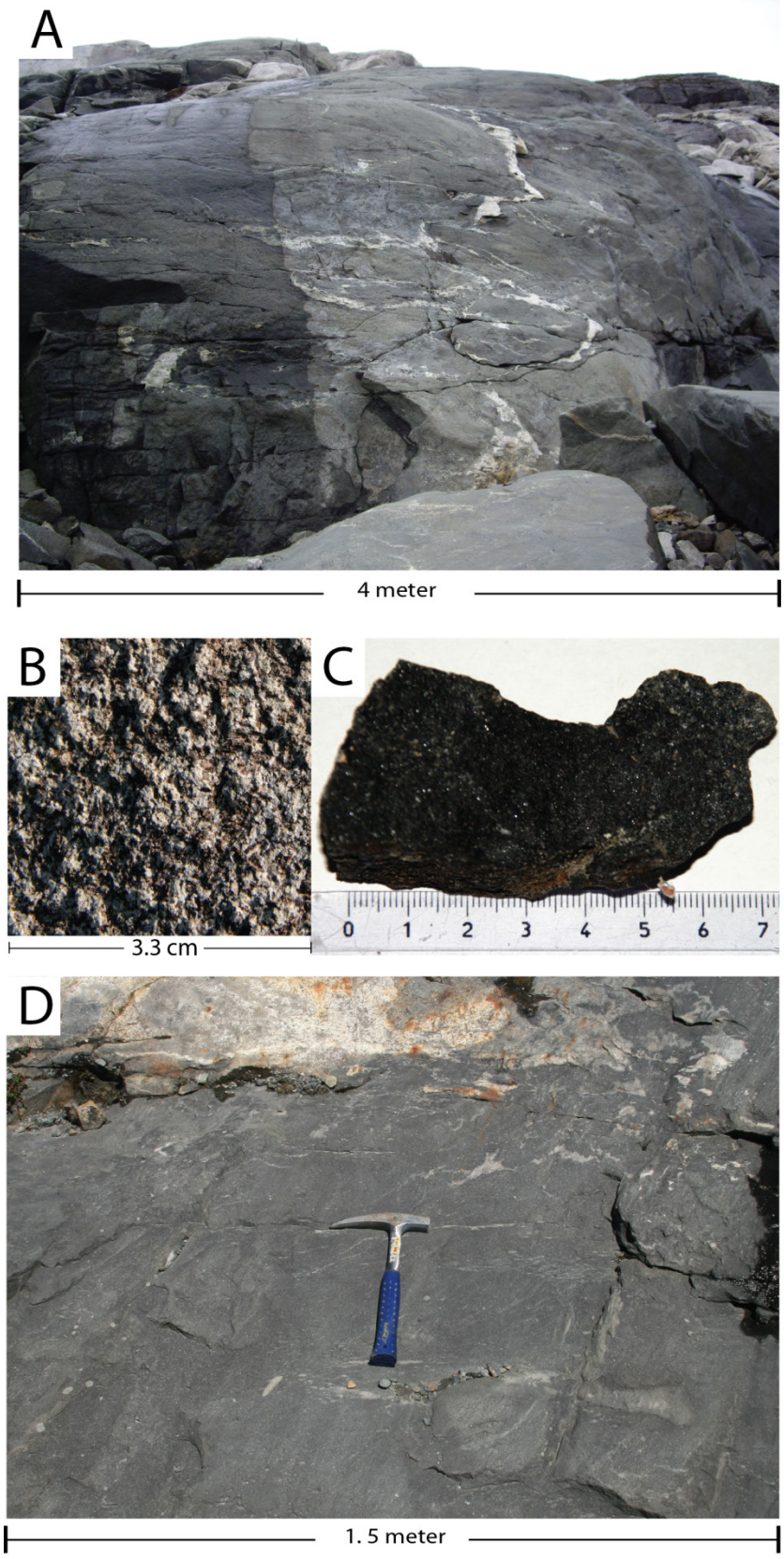

Fig. 20. Two mafic lithologies occurring in the study area. ***A:*** *Gabbroic outcrop with a felsic vein. Picture provided by Fernando Corfu* ***B:*** *Gabbroic weathered surface with feldspar minerals visible without any optical aid.* ***C:*** Amphibolite is the dark mafic variant that often is occurring in the basement. The size of the grain ranges from *"Very fine" to" fine grained", and are difficult to see without optical instruments.* ***D:*** *Outcrop with amphibolite and granodiorite*

Among the mafic rocks observed in the basement there were two rock types observed: Amphibolite and gabbro. The first one is a dark mafic rock type with minerals size from "fine grained" to "very fine grained" (Fig. 20 B & D), and it's hardly possible to observe the minerals without optical instrument. Amphibolite are very common, but at more specific places, and also usually in places were the granitic bedrock dominates. Dikes are rare in this lithology, but more common are felsic mixing intrusion without any preferred orientation

The other mafic rock type is the gabbro (Fig. 20 A & C), compositionally it's more or less the same as amphibolite, but the grain size differs and is distinguishable with the bare eye. Gabbro is found mainly at the north side of Hardangerjøkulen, **Locality 1**. The extent of the gabbroic body is quite large and might extend from 100's to 1000 meter as far seen at this area. Gabbro intrudes in same manner as the granitic lithology and amphibolite, and mixes with the granite. Pegmatitic dikes are very common feature that intrude the gabbro, both as dikes with a preferred orientation and as random mixing.

Thin section reveals a high amount of feldspar, nearly 70 % of the sample. Among these percentages, the majority are plagioclase that constitutes approx. 50 % and K-feldspar around 20 %. Mica, biotite and sericite constitute 25 % of the sample. The last 5 % would be quartz, chlorite amphibole. Quartz is very rare, and is nearly non-existence.

3.2.1.4 Pegmatite

The basement, both felsic and mafic are intruded by pegmatitic dikes, and are very common over the study area.

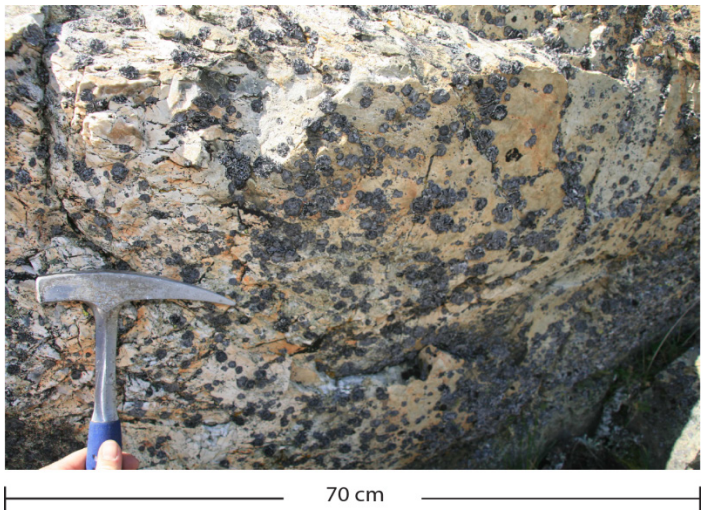

*Fig. 21. A characteristic pegmatitic dike, but this one is intruding the Lower nappe at **locality 14**. Besides its unusual large grain size, it is very common to find similar dike elsewhere in the study are. The more common dikes are usually up to 10 -15 cm thick. Note the dark spot, these are biological lichens and are not crystals. Orientation of the dike: NW-SE (Ca)*

It is common to observe several generation of pegmatite cutting each other, which means there was several magmatic events with different ages that underwent after the basement was developed.
The grain size ranges up to pegmatitic size with feldspar crystals that are of centimeter size and more, but sizes as the one intruded the Lower nappe at **Locality 14**, shown in Fig. 21, are very uncommon. Usually the dikes are only 5- 20 cm thick and intrude all the lithologies, (granite, granodiorite and gabbro) as seen in Fig. 22 & Fig. 23. Among feldspar there are nearly 50%/50% between plagioclase and microcline, and the remaining composition is mostly quartz.

3.2.1.5 Dikes and intermixing

Some of the rocks that appear in the basement tend to be very homogenous without any intrusion or dikes. But there are two types of intrusion that often occur in the basement:

Dikes with preferred orientation

Intrusion with random mixing structures

The distribution among them would be approx. 60 % dikes and 40 % intrusion with random mixing structure.

Intrusion with random mixing structures

There are several places that display such feature, either in the gabbro or the granitic dominated area. In general a felsic coarse grained lithology, often as pegmatite, intrudes the basement lithology in a very random fashion. Amphibolite tends to intrude in such manner in the granitic dominated basement, but it is slightly more uncommon than felsic intrusion. In Fig. 22 A, the amphibolite is mixed with a felsic unit, but it not easy to determine the age relation between the two.
Fig. 22 B & C displays a intermixing between the coarse and fine grained granodiorite, which appears to be in a random fashion with no preferred orientation and no obvious relationship between the two lithologies. This makes it very hard to determine which magmatic body is intruding, and which one is the host rock,
Fig. 22 D, the pegmatite is intruding the gabbroic lithology in more or less a random fashion. However there are still some dikes at this picture that could give the impression of a preferred orientation.

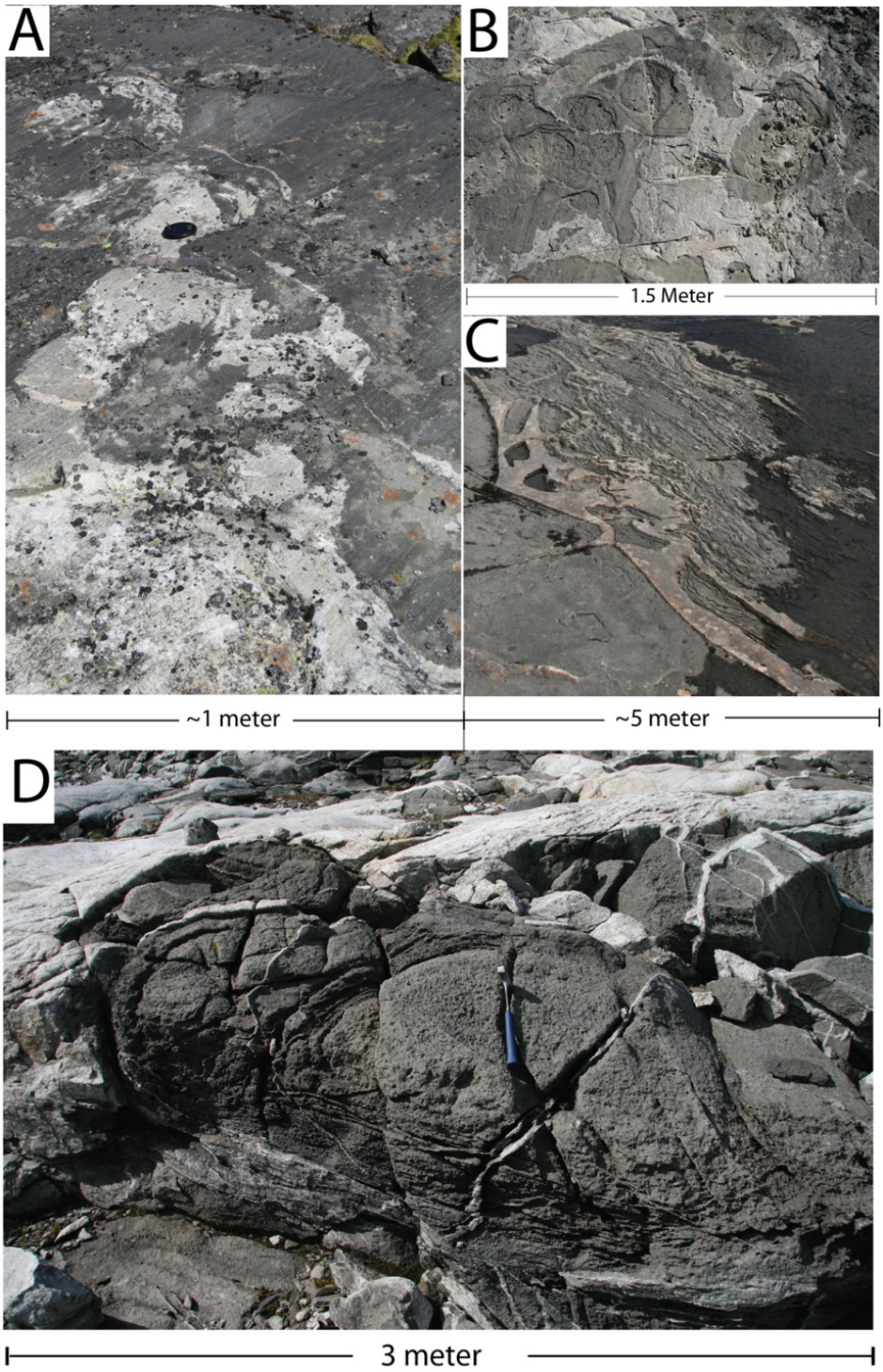

*Fig. 22. Different aspect of random intrusions in the basement. **A**: Amphibolite and fine grained granodiorite intermixing **B**: Fine and coarse grained granite" intermixes in a relative random manner. It is very difficult to say which magmatic body that intrudes the other, and which one is the host rock body. **C**: Another variant of random intrusion of pegmatite into the granitic basement. **D:** Felsic lithology intruding gabbro with same random mixing appearances.*

Dikes with preferred orientation

In contrast to random mixing structure, the "very coarse grained" granitic lithology often as pegmatite, is systematically intruding the "fine grained" granitic lithology or the gabbro. This could be seen in Fig. 23 A, which represents at least two different generations of dikes. The first orientation is trending 60° - 240° (NE-SW) and the other is oriented 284° - 104° (NW-SE) (Fig. 23 B). Since the NE-SW dike is superimposed on the pre-existing dike, this would represent the youngest generation, which means the oldest among them would be the NW-SE.

Multiple generations of dikes and intrusions are a common feature in the study area. Fig. 23 C & D, shows these overprint of pegmatite, coarse grained granodiorite and amphibolite. The surrounding fine grained granodiorite is the oldest which are cut by a pegmatite dike, and both are later intruded at cut by the amphibolite. The rim of the "fine grained" granitic body appears as bits and pieces in the amphibolite. Orientation of the pegmatite dike is WNW – ESE ($^{ca.}$)

At the north side of Hardangerjøkulen, **Locality 1** similar pegmatitic dikes are systematically intruding the gabbro in a larger scale with an NW-SE orientation, 125° and dip 45-55° (RHR) Fig. 23 (E & F). The dikes are quite different in thickness but would be in average 0.5m to 1m thick

There is a consistency observed among the dikes at the basement, as most to them tends be either oriented NE-SW or NW-SE.

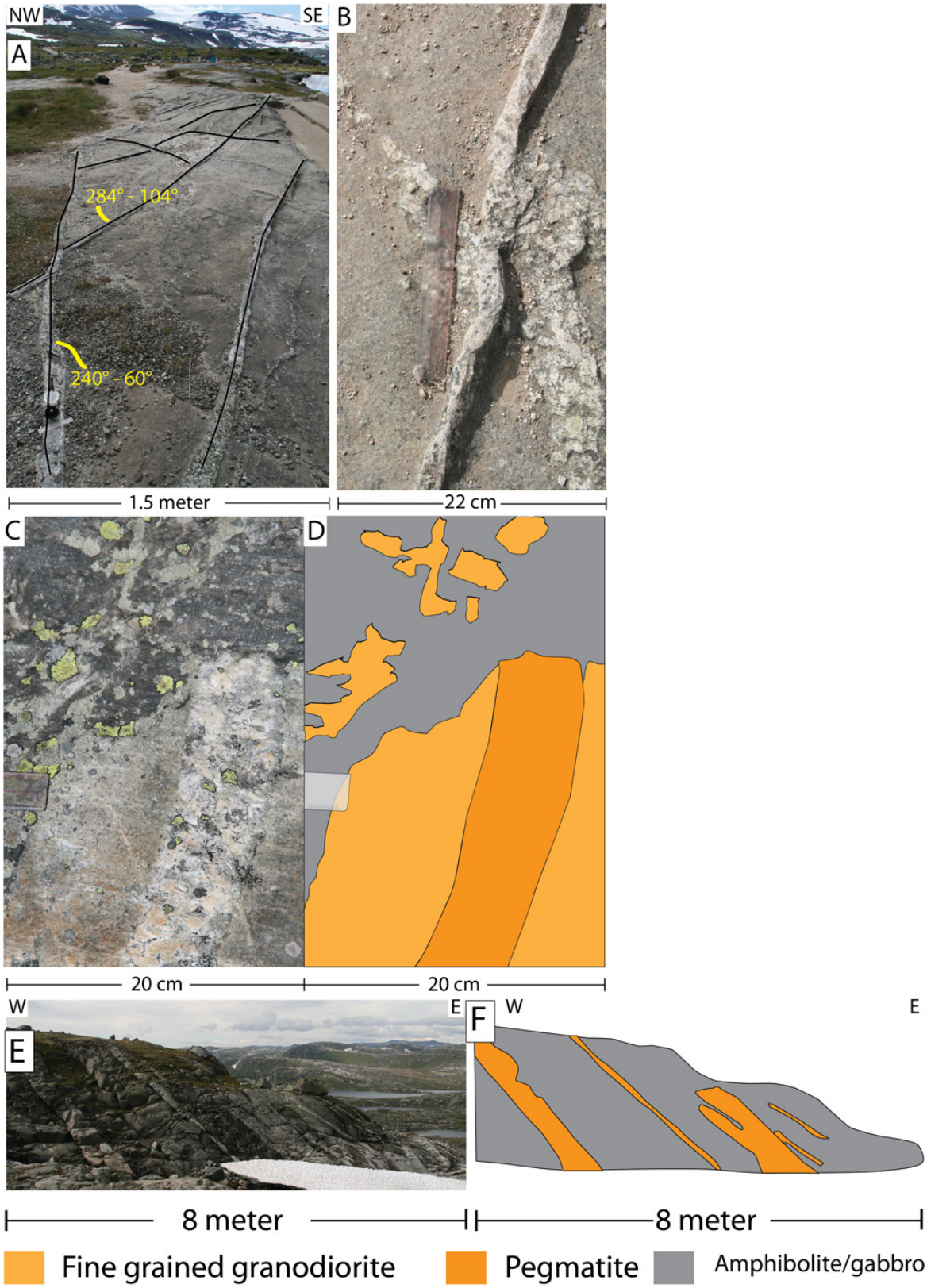

*Fig. 23. Different dikes with preferred orientations occurring in the basement. **A**: Systematically intruding dikes like these ones, are a very common feature. Usually the very coarse grained, also up to pegmatitic size intrudes the (very) fine grained granite. The majority of the dikes seem to follow a preferred orientation, either NW-SE (240° - 60°) or NE-SE (305° - 125°). **B**. A close up view from picture A showing the intersection point where the two generation of dikes cut each. **C & D**: This relatively small scale feature (20 cm) represents three different events. The age relation between these three rocks types are quite easy to determine. The "(very) fine grain" granite is cut by a pegmatitic dike, and both are later intruded and cut by the amphibolite. Orientation of the pegmatite is WNW-ESE (^{ca}). **E & F**: Locality 1. The outcrop is a vertical section, showing pegmatite systematically intruding the gabbro with an orientation NW-SE.*

3.2.1.6 Top of the basement

This study area contradicts that the basement is a flat peneplain, as the contact is far from horizontal and fluctuates to a relatively high degree. A cross section from Blåisen (A), north east of Hardangerjøkulen to north of Hardangerjøkulen (A') (**Appendix 1, see also map**) shows the fact that the basement occurs at different altitudes. To the east of Middalen glacier, or SE on Fig. 24, there were observed significant changes of the basement contact over a relative small distance (1 km), which is interpreted as fault zone(s), explained in chapter 3.2.1.7. Stepwise shift of the basement contact were observed as the basement rapidly decreased from 1378 m down to 1320 m, and climbing up again before it reaches 1420 at NW (Fig. 24). Highest altitude to the basement (contact) at SE is 1390 m and to NW it is 1420 m, while the lowest point is 1325 m.

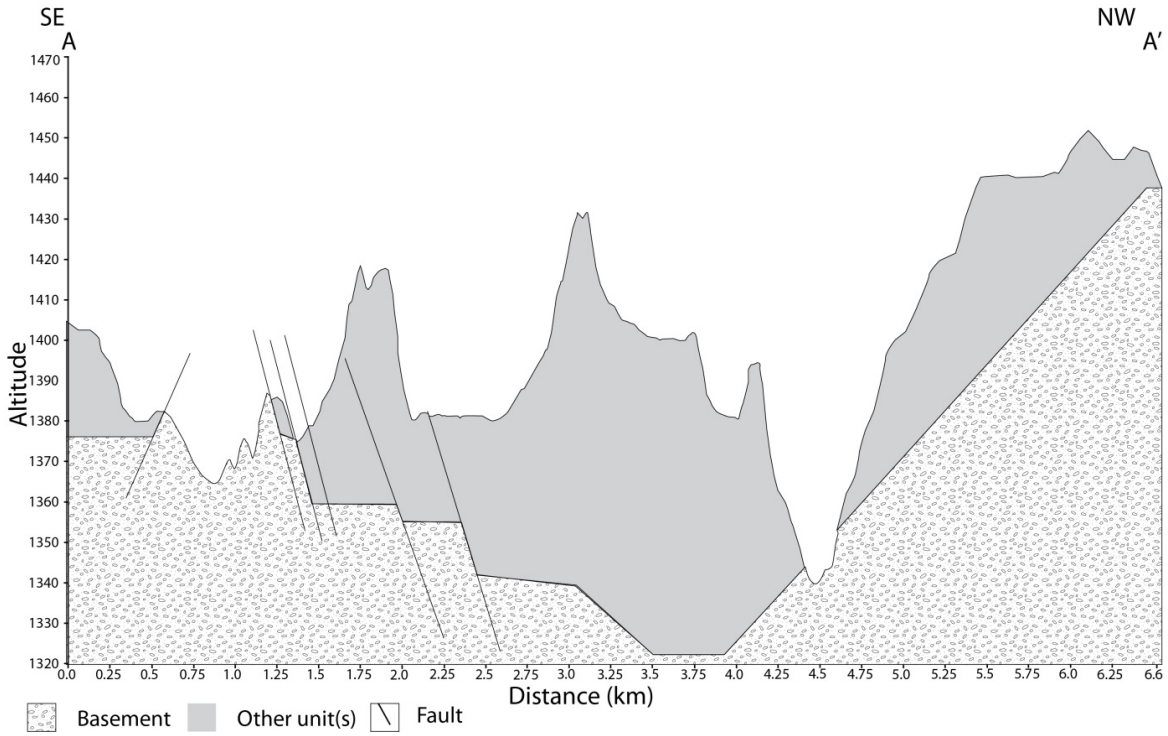

Fig. 24. A cross section (A-A') of the basement plus the overlaying units, are made with a SE-NW direction. The basement is far from horizontal (peneplain) and fluctuates to some degree. Faults do contribute for the shifting basement, is not an feature observed further towards NW. Note the horizontal and vertical scale are not the same.

The contact between the Basement and the unit above, Phyllite is very distinct, and is possible to follow even from greater distance. There are several features that define the contact between the basement and the Phyllite.

First it's the lithological different between the Basement and the Phyllite. The basement which are light colored, massive, are easily distinguished from the Phyllite which has a dark color and are also highly schistose. There are several places that mark a clear contact with this kind of feature, were the Phyllite is stacked on top of the Basement.

The **second** feature is a result from the erosion of the (Sveconorwegian) mountain chain during the Neoproterozoic and Cambrian. The bedrock, which is todays basement was exposed to tropical weathering and turned-gradually into a soil profile (Fig. 25, left). While the "soil" defines the topmost layer, the Regolith is defined as "*particles of weathered and un-weathered parent rock, clay minerals, iron and other metal oxides, and other product of weathering*" (Press et al., 2003). In contrast to the soil, the regolith does not contain any organic matter and therefore doesn't support any life.

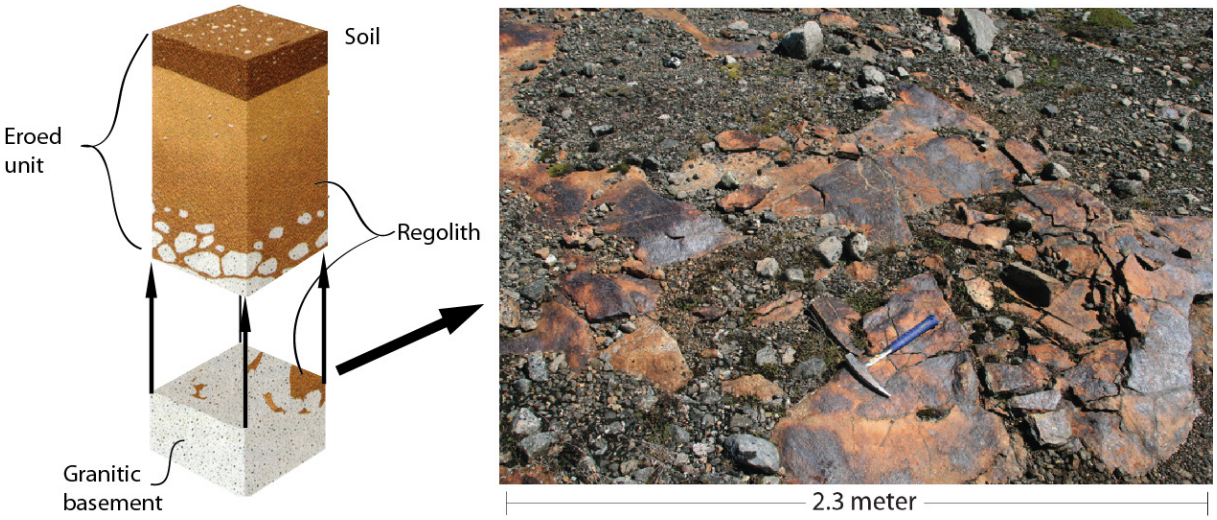

Fig. 25. A typical soil profile. Left: The regolith which are the unit below the soil, are developed during arid climate and leaves a characteristic trace on the basement. As the illustration shows, most of the sedimentary cover that once where deposited during Neoproterozoic and Cambrian where almost completely eroded away.(Illustration modifed from Press et al., 2003). Right: A typical regolith outcrop, with red, rusty colored outcrop. This features are only seen at isolated areas in the in the granitic basement, but nevertheless, they are very easy to see.

This Regolith is observed in several places as a rusty (red) colored outcrop (Fig. 25, right), in the top parts of the basement. Despite the recognizable color, the regolith also tends to fracture more easily than the fresh granodiorite. The thickness of the regolith around Finse is observed to be very thin, probably just 1 meter thick. This would be highest part the soil profile, and therefore could be used to determine the top of the Basement. This method is a very efficient way, since the upper unit, Phyllite does not need to be present to find the contact.

And the **third** and last feature is more for distant observation, from a scenery overview. The eroded Precambrian peneplain is very easy to see in the field from a distant view, and clearly marks the contact between the basement and the Phyllite. Often at places where the peneplain

is exposed it is also possible to find the Regolith, but the peneplain itself is a good way to tell the contact to the top of the Basement even if the Phyllite is not clearly exposed (Fig. 26).

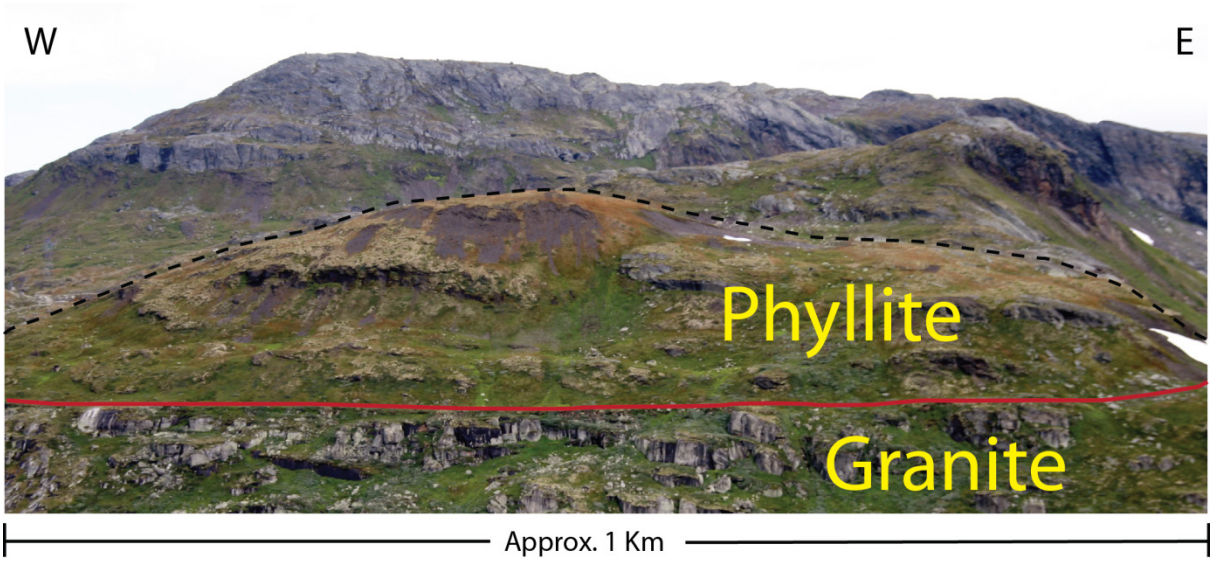

Fig. 26. A scenery view, looking towards North. The red line represents the "peneplain" and is a clear contact to the Phyllite above.

3.2.1.7 Faults and folds

In general large scale faults and also folds are very uncommon to observe in the basement. But still there is evidence that it exist. The faults that were observed and marked into Fig. 24 had to some degree different displacement and magnitudes. The displacement for each fault was approx. 5-10 meter, but still there are some faults with even greater displacement ranging up 20 meter displacement. Usually there were large crack in the overlaying strata were the basement and Phyllite displaces, but it was not always evidently if this was related to these faults. Fig. 27 A, illustrates the fault systems appearing at SE at Fig. 24, which is in-between Blåisen and Middalen glacier. The relatively large fault (Fig. 27, B) displaces the basement upwards relative the footwall, while the rest displaces the basement and the overlaying strata downwards relative to the footwall, all as normal faults. Still without the strike and dip of the fault planes, the orientations are between NNE-SSW (^{Ca}) and NE-SW (^{Ca}). Fig. 27 C, represents a small scale faulting, 4 meter wide, with a stepwise shift of the strata, and represents the structural feature undergoing in large scale (Fig. 27 A).

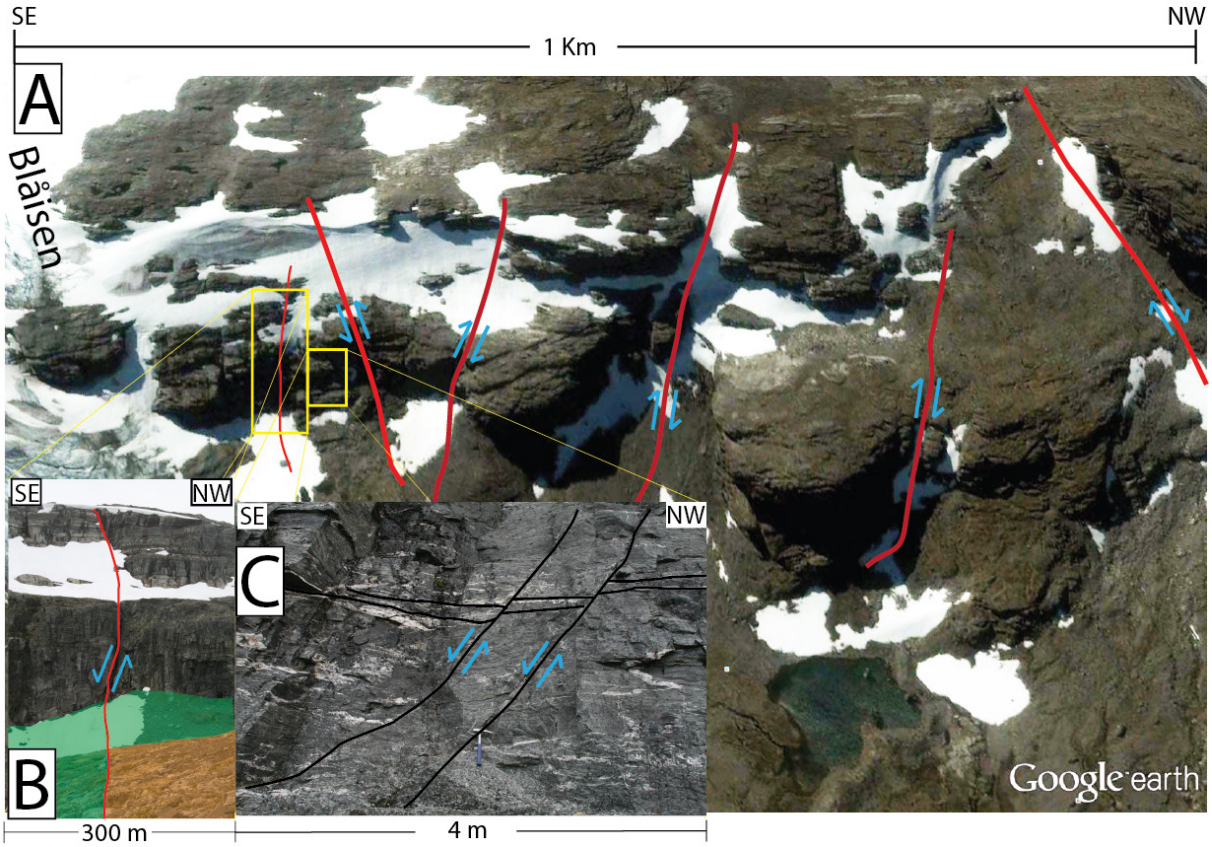

Fig. 27. The faults as marked in the cross-section (Fig. 24) are located in-between "Blåisen" and Middalen glacier. ***A****:The Google (2012) background image are supposed to represent a vertical section of the current area. The red lines are faults (not orientation of fault plane!) and displaces vertically with direction as noted in blue, either as normal faults or reverse fault.* ***B****: The image bottom-left is a larger normal fault that displaces the basement upwards, and the Phyllite unit downwards.* ***C:*** *Bottom-right image are smaller scale faulting, as exactly happening in larger scale. Orientations of the fault are NE-SW.*

The basement contacts (regolith) towards NW (Fig. 24) were mapped for all exposed outcrops, usually for every tens of meters. It was not recorded any sudden displacement, so faults are less likely to have occurred at this side. The climbing basement was instead interpreted as the topography that gradually increases towards NW.

Folds, which are even more uncommon to observe than faults, was found at **Locality 1.** The structural feature at this locality showed a highly folded and schistose top layer of the basement as gabbro and granite folds into each other with a nearly overturned geometry (Fig. 28 A). Close to this folding structure the regolith appears as a contact between the granite and the Phyllite. A small scale parasitic folding incorporated in the gabbro which is also incorporated in between the granite as shown in Fig. 28 C. The highly schistose granite, nearly mylonitic is folded with gabbro incorporated around (Fig. 28 D & E). Fold axis are trending NE-SW ($^{ca.}$) with vergence towards NW (^{ca}).

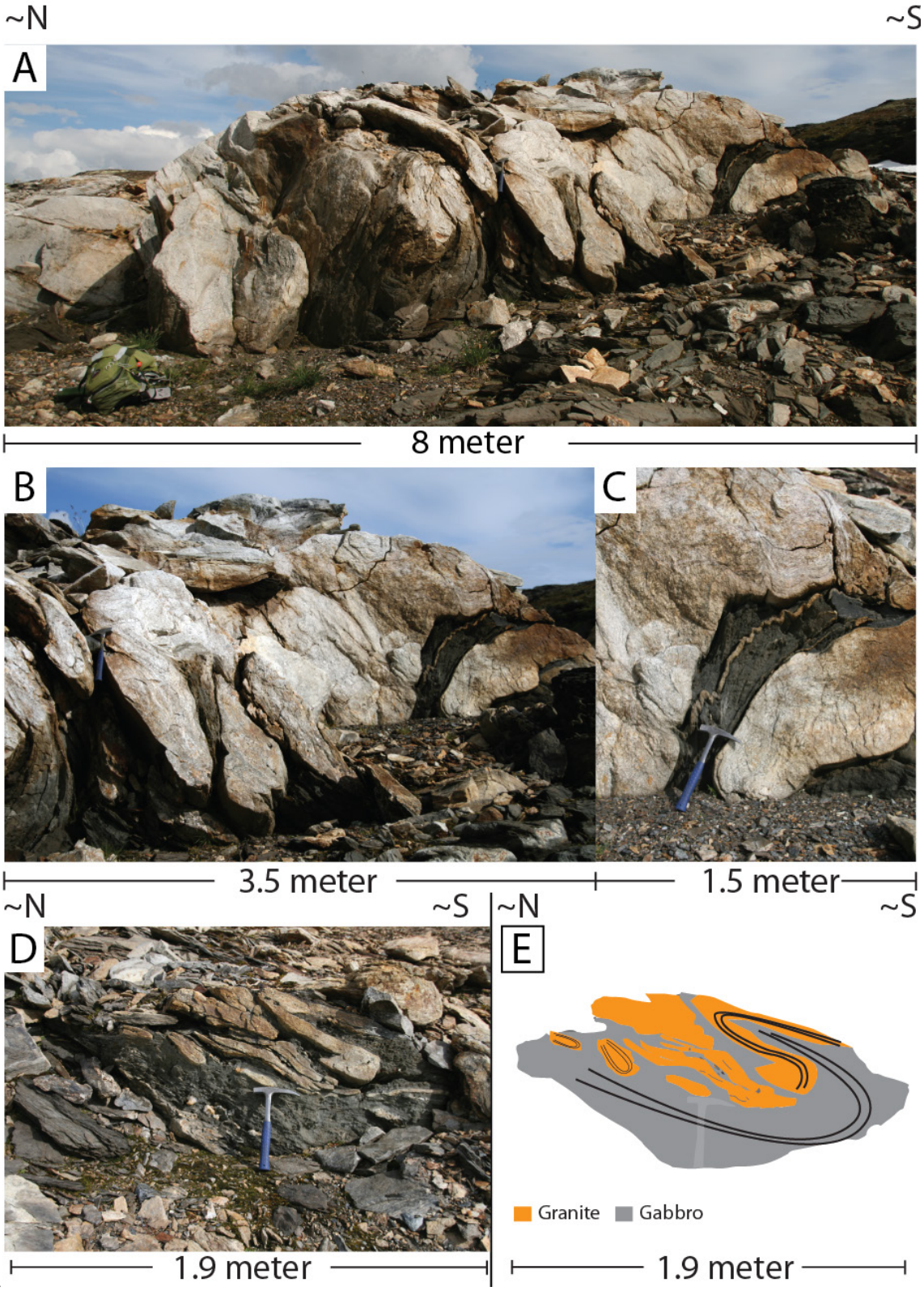

Fig. 28. ***Locality 1. A & B:*** *This is a granitic outcrop which is still part of the basement. But this has been deformed, folded and transformed into gneiss or schist, a feature that is very uncommon to observe in the basement. This outcrop is also 100 meters higher than the exposed basement 3 km further to the SE (middle of Fig. 24) The approximately orientation of the fold axis are NE-SW(ca.) with vergence towards NW (ca). **C: A c**loser view of the smaller scale feature in this fold. Gabbro is incorporated in the granite and with same fold-axis orientation. Inside the gabbro there is a small scale parasitic fold with felsic lithology. **D**: The folded basement is broken up into fragments. Fold axes are NE-SW (ca) with vergence towards NW (ca).**E:** This is a graphical illustration that highlights the structure on picture D.*

While these represent a large scale faulting and folding, but small scale features such as dikes have also been subjected folding and faulting, which represent a later event relative to the intrusion age. These features are very common to observe among the dikes, and follows all over the basement dominated part of the study area.

Fig. 29 A & B, a pegmatite intruding the amphibolite and later has become sheared and rotated. The outcrop displays three pegmatitic dikes where two of them are relatively unaffected with an orientation NNE-SSW. While the third one in the middle is trending NNW-SSE and here the dike has broken up in four larger pieces, which has slightly rotated. It is likely a shearing has occurred which has affected the middle pegmatitic..
Fig. 29 C & D, a pegmatitic dike intruded the granite has become folded. The surrounding lithology is the typical granite with phenocrysts of feldspar. Fold axis are E-W trending (265°-85°), which means a later north-south (355°-175°) oriented stress regime has deformed the fold.
Fig. 29 E & F is a typically small scale, 3 cm wide pegmatitic dike cutting the gabbro. The coarse feldspar minerals in the surrounding gabbro are visible in this picture. Two small scale share zone displaces the pegmatite with only 10 cm displacement for the bigger and 1 cm displacement for the smaller. This would be part of an even later event. Orientation of this dike is NNW – SSE ($^{ca.}$).

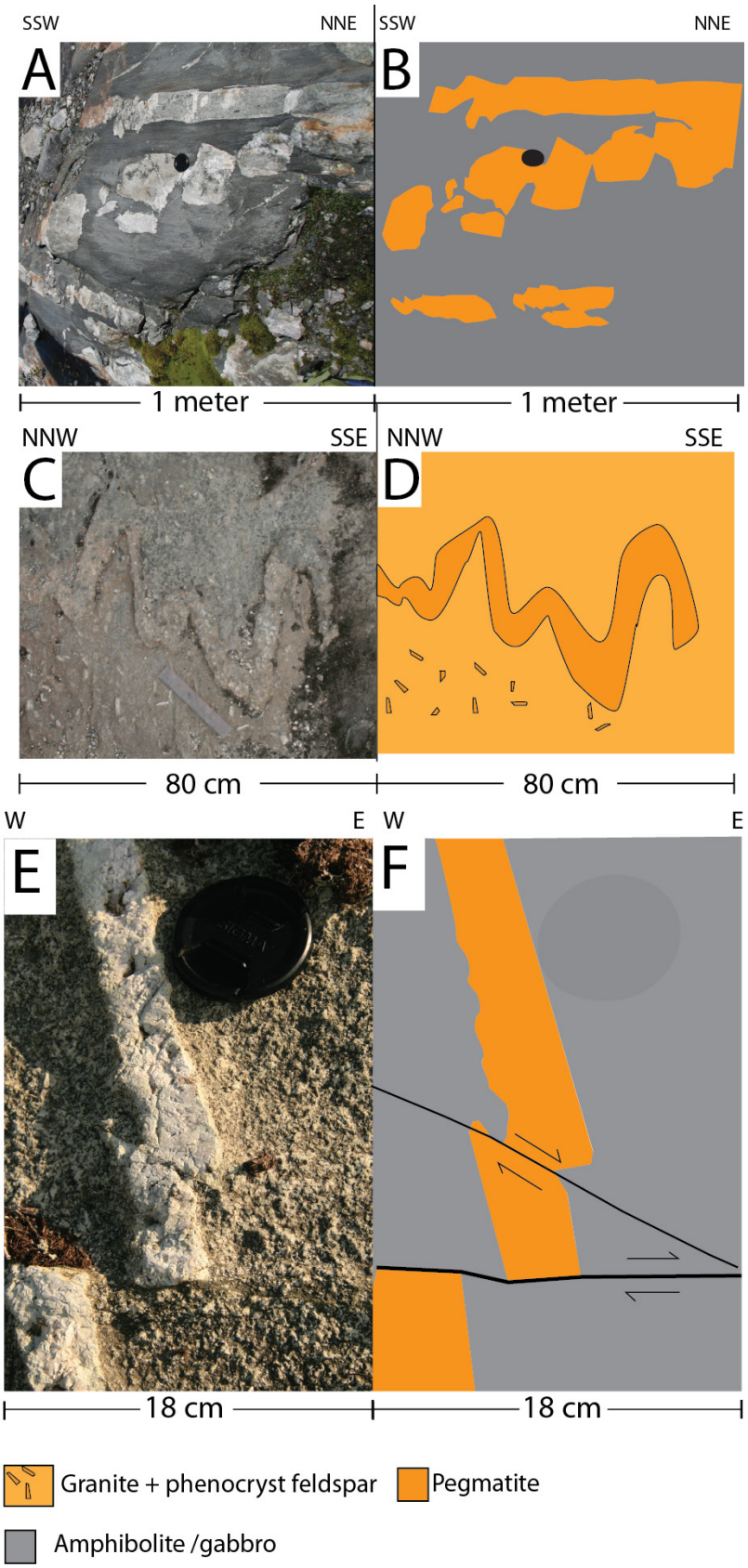

*Fig. 29. Pegmatitic dikes subjected to later stress. **A & B**: The pegmatite intruded the amphibolite, has later been broken into fragments due to shearing and subsequently rotation. **C & D**: The pegmatite appearing in the basement has been subjected to compression that's has folded the dike. Fold axis are E-W (265°-85°). The surrounding rock is the granite with phenocrysts of feldspar. **E & F:** A pegmatite is later displaced by two small shear zones with a 10 cm displacement for the bigger and 1 cm for the smaller .Orientation of the dike is NNW-SSE ([Ca])*

3.2.2 Phyllite

The tectonostratigraphic unit above the basement is the Phyllite. The lithology of this rock has a distinctly different appearance from the basement, and there is a sharp contact between the two units. Phyllite is by definition a result from a metamorphic event, were the proto rock was a sedimentary rock of some sort. The nappes during the Caledonian orogeny slide with relatively little friction on top these sediments and altered the sediments to a meta-sedimentary rock type (Fig. 30), and is put in a category in-between slate and schist of (low grade) foliated rocks. While there is a relatively small difference between three of them, phyllite is recognized of having glossy sheen and crinkly cleavage in contrast to the others. The sheen occurs when microscopic grains of mica, chlorite and graphite recrystallize during the metamorphism and grows a little larger (Press et al., 2003). Phyllite breaks easily into well-developed sheet (but not as well developed as slates). As observed, the Phyllitic outcrop tends to be significantly more fractured compared to both unit above, Lower nappe and the unit below, the basement. The way that it is weathering and breaks along well developed sheets, is some of the reasons that the outcrop are rougher with jagged corners.

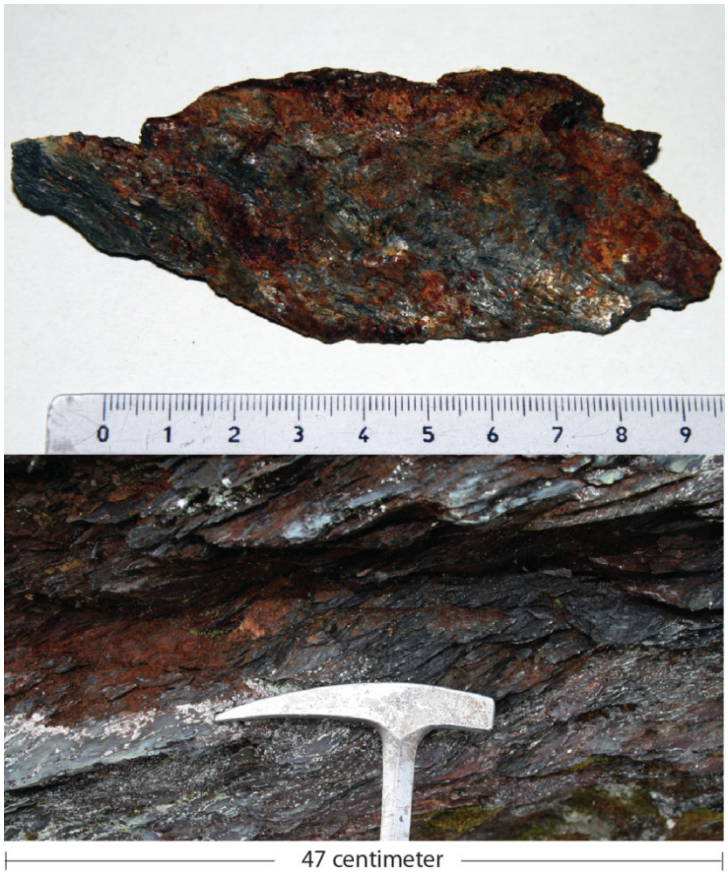

Fig. 30. Phyllite outcrop and fragment. Above: This rusty, red colored surface with a distinct sheen is very characteristic features of Phyllite. Below: A typical phyllitic outcrop, very schistose that break along thin sheets. The red rusty surface with this sheen is also visible on this picture.

During the field work the Phyllite is observed to have two minor different appearances. The one that dominates which would make it “the Phyllite” is the one that has a really dark red color, kind of rusty appearances (Fig. 30). This rock has a very distinct sheen and is easily recognized. While the “other” phyllite has a little lighter color and the sheen is not so distinct. The differences between them are very notable, and the lighter version of the phyllite is very similar to rocks in the unit above, Lower nappe. This lighter version is only observed at 5 % of all phyllitic outcrops. The geological map, further description and discussion, the darker version (Fig. 30) is generalized to be the primary phyllitic rock type.

The Minerals in the Phyllite have obtained a preferred orientation during the metamorphism, and developed a foliation plane. This plane is sometimes easy to observe and measure, and sometimes is wavy or complex folded. Quartz lenses are often found in the Phyllite unit with various sizes, and the minerals in the matrix tend to range down to “very fine grained”. While the contact between basement and Phyllite is very distinct, the contact between Phyllite and Lower nappe often are very uncertain. This is because the appearances between Phyllite and Lower nappe are sometime are very similar. The Phyllite tends to be highly folded without any preferred orientation, because of that it is not possible to use the altitude for guidance where to expect a contact, in contrast to the basement-Phyllite contact. Still there are several localities that show clear contact between the two rock types (Fig. 31). But this outcrop represents a stratigraphic anomaly. Phyllite in principle should be located under the Lower nappe (Fig. 17), but as illustrated in the picture, it is over. These kinds of structural setting where which includes both Phyllite and Lower nappe are further described in chapter **3.3**.

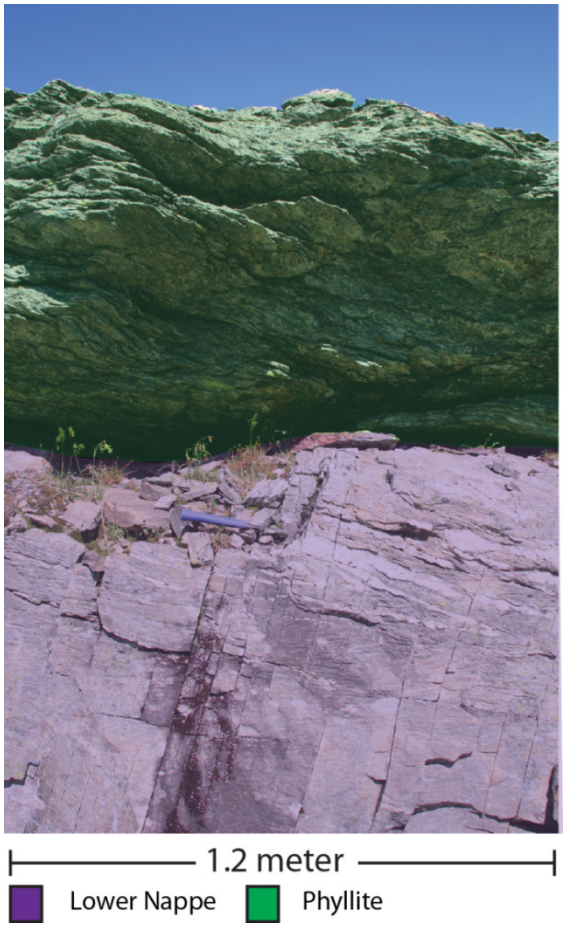

Fig. 31. This is a vertical section showing the clear contact between Phyllite and Lower nappe. This outcrop represents the complexity in this field as Phyllite is over Lower nappe.

3.2.2.1 Measurements

Map with stereonet measurements of Phyllite foliation planes

Because of the erosion, the Phyllite foliation planes tend to be more complicated to measure than expected. So certain areas have fewer measurements than others.

With the knowledge that the fold-axes changes at certain places, the Phyllite measurements are divided accordantly into defined areas.

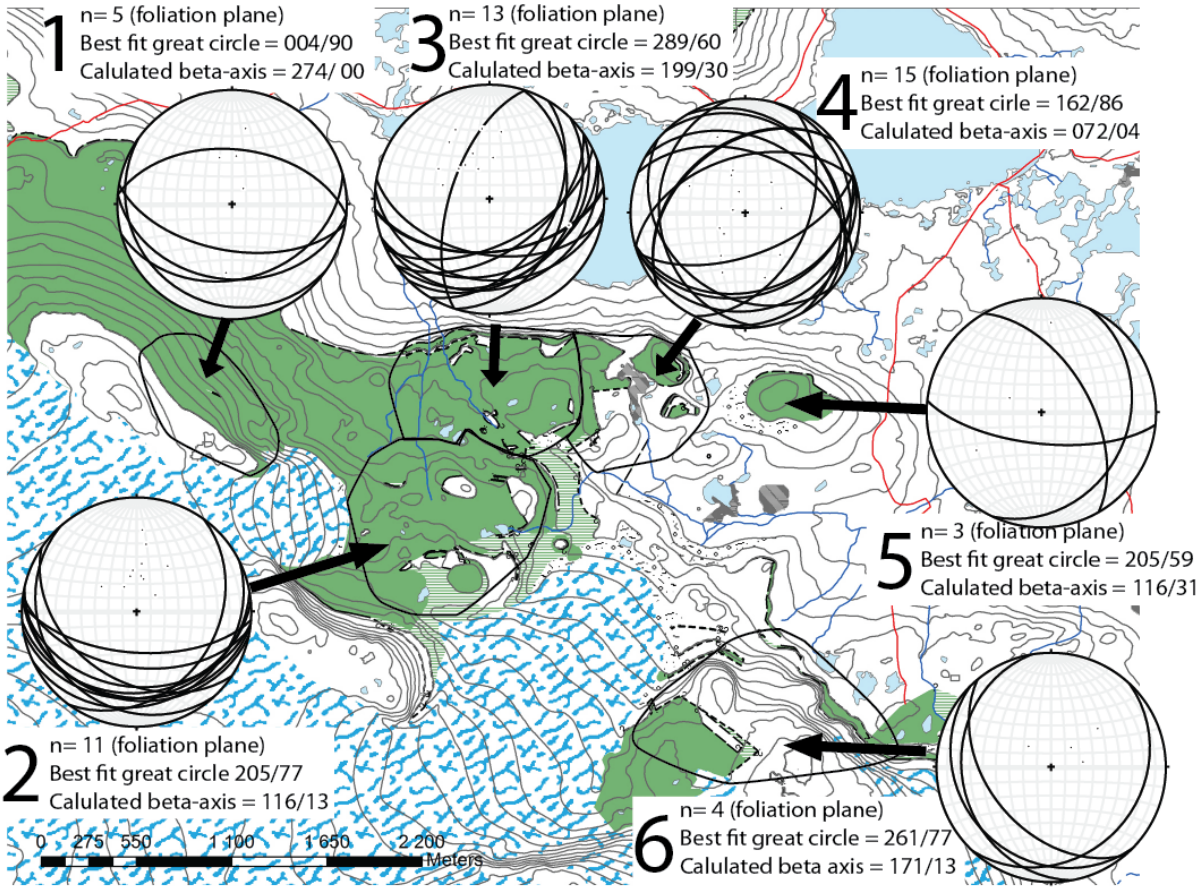

Fig. 32. Stereonet map of Phyllitic foliation plane measurements. Each stereonet represents a cluster of measurements in the classified, numbered areas.

Fig. 32 is based on all Phyllite foliation plane measurements in the study area.

The first area (Fig. 32 stereonet nr. 1) gives horizontal east-west trending fold-axis, the second area (Fig. 32 stereonet nr. 2) the beta axis is plunging 13° towards south-east, the third area (Fig. 32 stereonet nr. 3) it plunges 30° south-west, the fourth (Fig. 32 stereonet nr. 4) it plunges 4° north east, the fifth (Fig. 32 stereonet nr. 5) it plunges 31° south – east, and the sixth (Fig. 32 stereonet nr.6) it plunges 13° south.

All Phyllite foliation measurements

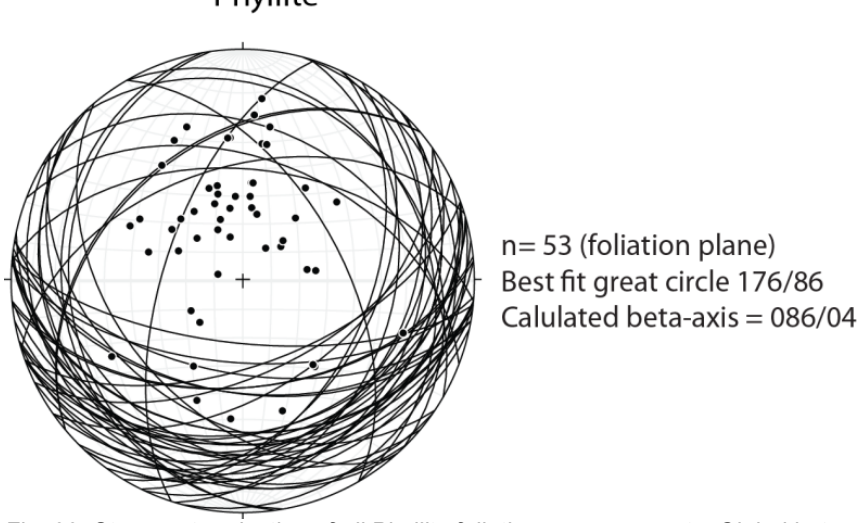

Fig. 33. Stereonet projection of all Phyllite foliation measurements. Global beta-axis is 086/04

Fold axes measurements in the field (Appendix 2) and the beta axes calculations from foliation plane (Fig. 32 and Fig. 33) are compared in the following table (Table 6), with number according to the area classification (Fig. 32)

1	Beta axis:	274/00	4	Beta axis:	072/04
	Fold axes:	NO DATA		Fold axes:	NO DATA
2	Beta axis:	116/13	5		
	Fold axes (both directions):			Beta axis:	116/31
		290° - 110°		Fold axes (both directions):	
		300° – 120			200° – 18°
		310° - 130°			218° – 38°
3	Beta axis:	199/30	6	Beta axis:	171/13
	Fold axes:	NO DATA		Fold axes :	NO DATA
Global beta-axis: 086/04					

Table 6. Comparisons table of beta-axes calculations based on foliation plane and fold-axes measurements done in the field. Each number represents the different areas defined in Fig. 32.

3.2.3 Lower nappe Unit

The next unofficial tectonostratigraphic unit above the Phyllite is the allochthonous Lower nappe, part of the Lower Middle Allochthon. Lower nappe is in fact a whole unit and involves several more or less different rock types. To describe the Lower nappe a stratigraphic log from **Locality 2**, will explain each rock type of this unit.

All pictures including the illustrations are oriented with NE to the right and SW to the left.

3.2.3.1 Lithostratigraphic log

Nr.	Thickness (cm)	Lithology picture	Lithology illustration
11			
10	15	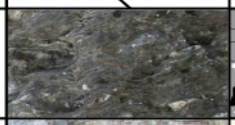	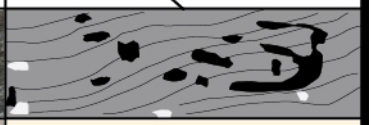
9	20		
8	15		
7	26		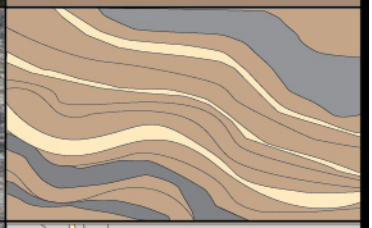
6	11		
5	20		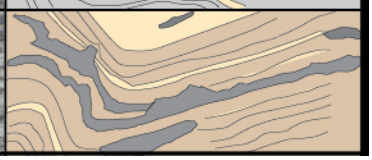

4	7		
3	22		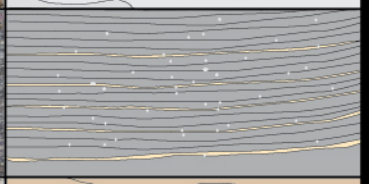
2	40		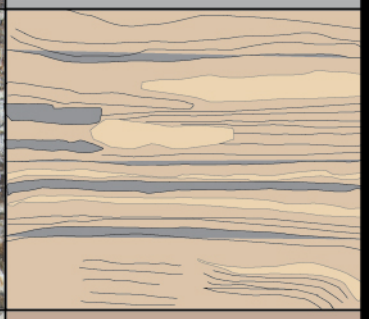
1	38		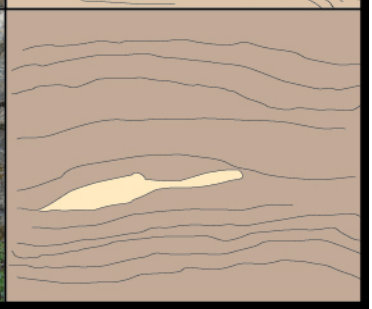
-	?		

Table 7. A stratigraphic log over the rock types within the Lower nappe unit. It appears that the lithological differences in most of these "layers" are either as: coarse grains almost sand sized, mica or carbonate rich. The brighter colored areas represent lithology dominated by felsic minerals, while in contrast the darker would represent mafic minerals. Whether this units repeats (nr.11) in a systematic ordering or random ordering are not clear. Color represents either mafic or felsic minerals. Black are carbonate holes. Keep in mind that the illustrations often represent a slightly different area of the same lithology picture, this to highlight the important features. The different pictures also the illustrations are oriented with NE to the right side and SW to the left side.

Detailed log description

Starting with the stratigraphic lowest rock (1).

Stratigraphic nr:

1. The stratigraphically lowest unit in this log is a mica rich rock. It breaks up in sheets almost in same manner as the Phyllite does, which means that the outcrop tends to be irregular with jagged corners. Large quartzitic lenses are incorporated into the matrix, and are approx. 1 cm thick and 6 cm wide. The matrix is black and fine grained, where each grain is hardly visible with the eye. The layering or foliation plane is either poorly developed or it is weathered so it's hardly seen. Still the bandings that is visible is more curved and seems to bend around these lenses of quartz.
2. This rock type is quartz rich with sand sized minerals. It has a well-developed layering, almost horizontal banding, where it alternates between light colored minerals

and darker minerals. The darker bands contain amphibole and mica, and the lighter are quartz-rich felsic minerals. Each band is approx. between 2 mm to 5 mm thick. Lenses of quartzite are incorporated in this rock type as well. The whole rock type appears to be more massive and weathering resistant than the mica rich unit below (nr.1).

3. This rock type has darker appearances than the previous rock types (nr. 1 & 2). The banding is nearly completely horizontal and harmonic. The surface of this rock is exposed to more weathering than the previous rock unit (nr. 2), which could be one of the reasons why the bandings are less visible. Still it seems that the rock contains more mafic minerals, and less felsic ones. It appears that the lighter felsic bands are only 1 to 2 mm thick, but the darker mafic bands are approx. 4 mm thick. The coarse grained matrix has several feldspar phenocrysts incorporated approx. 20 – 40 %, and is interpreted as volcanic tuff layer. The age of the zircons at this "layer", are 997.3 ± 3 Ma, and the age of the titanite are 940 Ma (Roffeis and Corfu, 2012).
4. This is a thin "layer" only 7 cm thick. Basically it is a huge quartzitic vein. But the lithology around the quartz has weathered in a selective fashion, which means it is a carbonate rich rick type. This non-quartzitic rock is dark very fine grained rock with a lot of carbonate weathering holes.
5. This rock has a very similar lithology compared to rock type nr.2, but one of the biggest differences are the bandings are folded and not horizontal and harmonic as it nearly appears in rock nr.2. Darker mafic and lighter felsic layers alternates, with coarse grained mineral sizes. Quartzitic veins are incorporated in to the structure.
6. This "layer" appears as a mafic rock type in between lighter ones (nr. 5 & 7). Grain size is coarse grained.
7. This rock is quite similar to the one at nr. 5, but slightly more mafic minerals and the bands are not as folded.
8. This is another mica rich rock type. The outcrop weathers and breaks along sheets and leaves a characteristic appearance. Quartzitic lenses are also incorporated here.
9. Another banded rock type with more felsic minerals than mafic. Rock type is light and the bands are quite horizontal.
10. A small (15 cm thick) carbonate layer with these characteristics weathering holes.
11. The rock types from this point above are more unclear and difficult to distinguish. As carbonate layer is found at different location at different topographic altitudes that

could both means a cyclic ordering or random pattern. So further topographical upwards it is unclear what to expect.

The small scale folding in this stratigraphic log, displays a vergence towards NE ([ca.]).

In general the different stratigraphic units in Lower nappe are very difficult to distinguish in the field. There have been some localities with good outcrop that shows the variations, but the majority outcrops in the study area are glacier polished (Fig. 34 A). Beside the carbonate rich "layer" (stratigraphic unit nr. 4 & 10) and mica rich "layer" rock (stratigraphic unit nr.1 & 8) it is very difficult to determine what exact lithology that appears in the most of the outcrops.

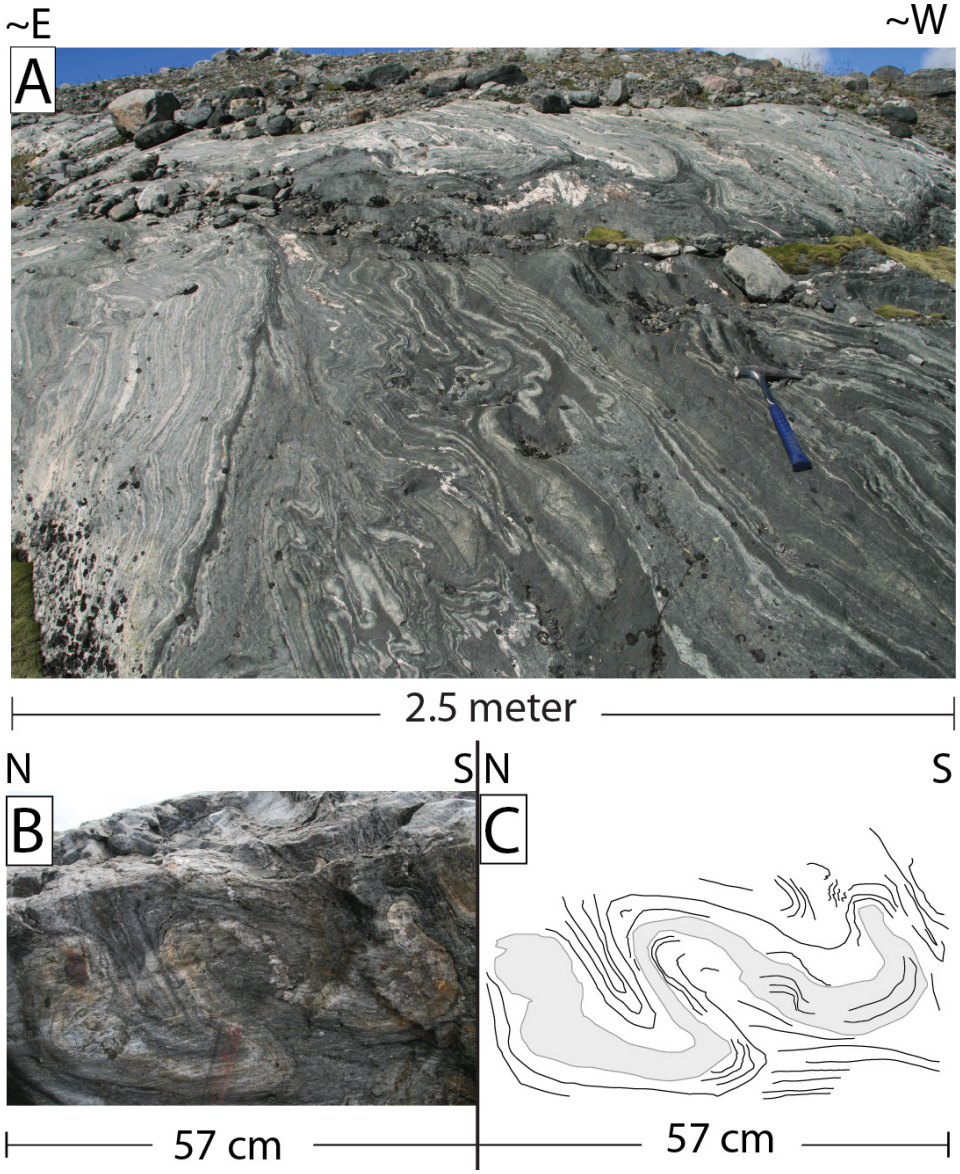

Fig. 34. Several small scale folding appearing in the Lower nappe unit. ***A:*** *This unit is recognized as a dark massive unit, but still lighter than Phyllite, mylonitic and highly folded. Lithology with different competence gives parasitic folding.* ***B & C****: This is the more representative smaller scale folds appearing in the Lower nappe unit, asymmetric S-fold. Fold axis 276°- 96° (WWN- EES), vergence towards NNE.*

Lower nappe and Phyllite are from time to time very similar, but the key differences between them are that the Lower nappe is lighter and more massive (Fig. 34 A). The whole unit also shows from time to time a higher deformation grade compare to the Phyllite, but still lower than the Gneiss (Upper nappe). The banding, either the lighter or the darker are complexly folded often as parasitic, not uncommon as multiple generations. Microstructures also appear on centimeter scale, and involve small scale duplex/in sequence thrusting, sigma blast, folding and faulting. The small scale folding (57 cm) are usually assymmetric s-fold, as seen Fig. 34 B & C. The fold axis are 276°- 96° with vergence towards ~NNE.

The general grain size of the Lower nappe is to some degree very similar to the lithology of the Phyllite, and is "fine grained" and difficult to see without a hand lens.
Macro scaled folding is very common and has been observed to be from meter to at least tens of meters large. This also involves complex folding different geometries, like *recumbent* and *gently inclined*. Some folds involve only Lower nappe, while other has involved Phyllite into the folded structure. This will be further described in the chapter **3.3**.

Since Lower nappe has many similarities to Upper nappe, and some to the Phyllite, the contacts are sometimes a challenge to interpret. But still the lithological differences between Lower nappe and Phyllite are often very distinct and make a clear contact.
Pegmatitic intrusion locally intrudes the Lower nappe unit (Fig. 21) at **locality 14**. This is very uncommon in contrast to the intrusions in the basement. Still 1-2 meter thick pegmatitic intrusion, with well-developed feldspar crystal have been seen. Approximately orientation of the dike is NW-SE ($^{ca.}$).

3.2.3.2 Measurements

Map with stereonet measurements of Lower nappe foliation planes

The Lower nappe measurements are divided in same way as the Phyllite. With the knowledge that the fold-axes changes somehow at certain places, the Lower nappe measurements are divided accordantly to this, into areas.

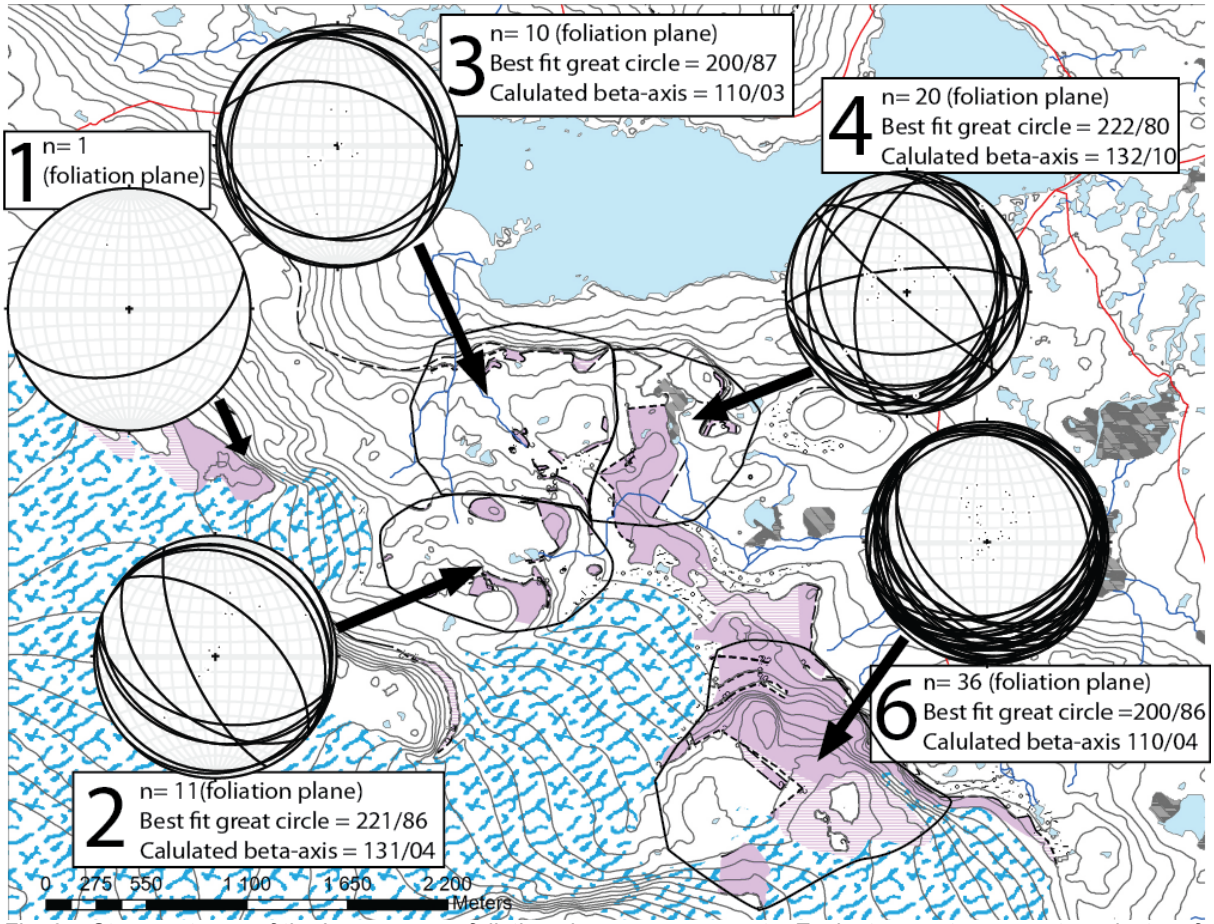

Fig. 35. Stereonet map of the Lower nappe foliation plane measurements. Each stereonet represents a cluster of measurements in the classified, numbered areas.

The first area (Fig. 32 stereonet nr. 1) is not representable, and has only one measurement, the second area (Fig. 32 stereonet nr. 2) it plunges 04° south-east beta-axis, the third (Fig. 32 stereonet nr. 3) it plunges 03° south-east, the fourth (Fig. 32 stereonet nr. 4) it plunges 10° south-east, the fifth area are only Phyllite and no measurements from there, the sixth (Fig. 32 stereonet nr. 6) it plunges 04° south – east.

All Lower nappe foliation measurements

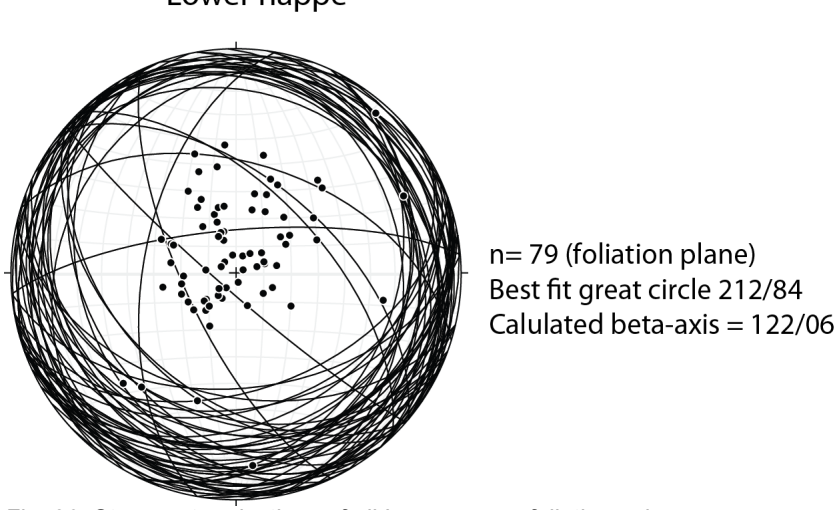

Fig. 36. Stereonet projections of all Lower nappe foliations plane measurements.

Fold axes measurements in the field (Appendix 2) and the beta axes calculations from foliation plane (Fig. 35 and Fig. 36) are compared in the following table (Table 8), with number according to the area classification (Fig. 35)

1	Beta axis:	NO DATA	4	Beta axis:	132/10
	Fold axes:	NO DATA		Fold axes (both directions):	
					355° - 165°
					340° - 160°
					310° - 130°
					190° - 37°
2	Beta axis:	131/04	6	Beta axis:	110/04
	Fold axes (both directions):			Fold axes (both directions):	
		250° - 70°			210° - 30°
		290° - 110°			215° - 35°
		300° - 120°			260° - 80°
		310°- 130°			300° - 120°
		325° - 145°			305° - 125°
					310° - 130°
					315° -135°
					326° - 146°
3	Beta axis:	110/03			
	Fold axes (both directions):				
		300° - 120°			
		310° - 130°			
		320° - 140°			
Global beta-axis: 122/06					

Table 8. Comparisons table of beta-axes calculations based on foliation plane and fold-axes measurements done in the field. Each number represents the different areas defined in Fig. 35.

3.2.4 Upper nappe

The last tectonostratigraphic unit appearing around Finse, is the Upper nappe, and is part of the Upper middle Allochthon. This unit appears first at high altitudes (approx. 1600m) and was quite difficult to reach because of the glaciers. There were only four places where it was possible to observe the Upper nappe due to the glacier**.**

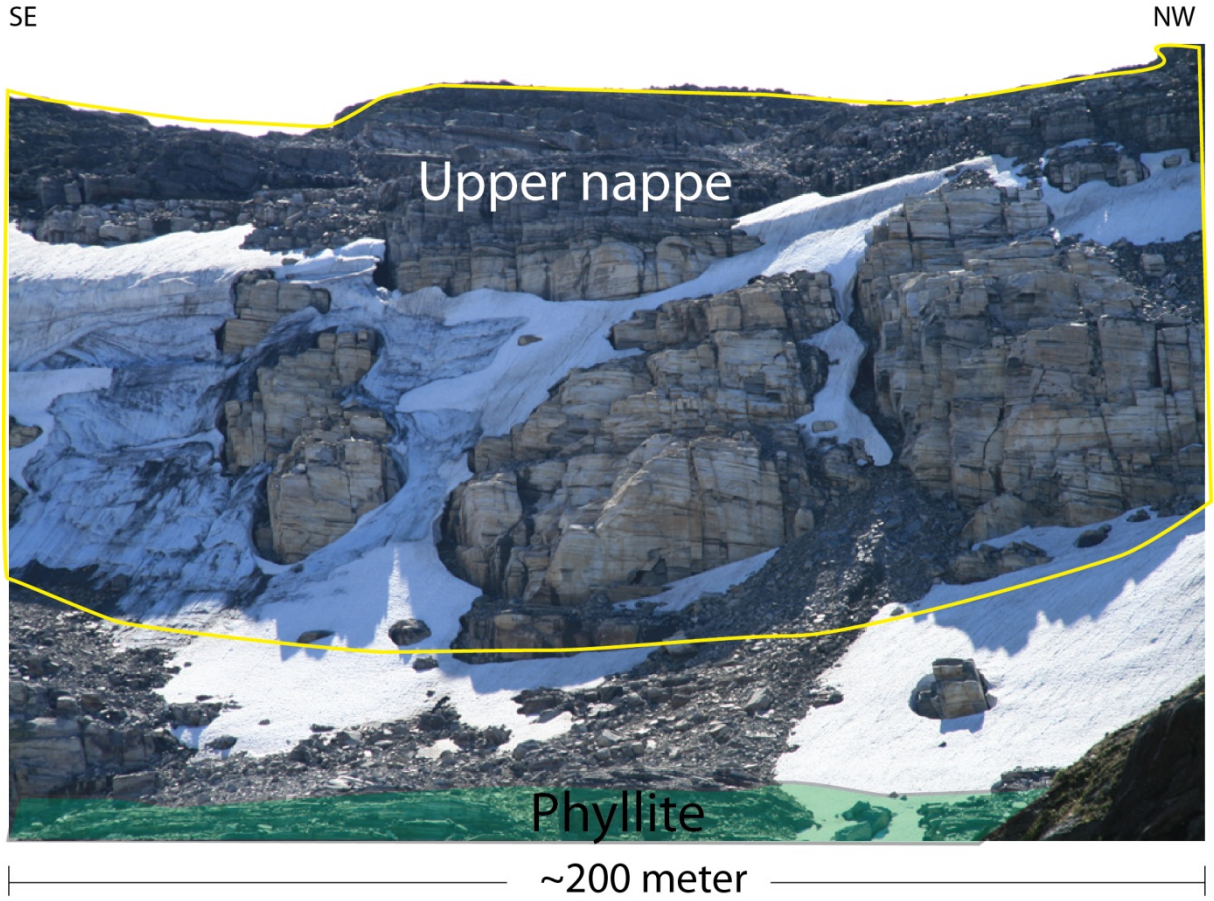

Fig. 37. ***Locality 3****.Scenic view of the Bukkaskinnshjallane. The light colored rock type is the crystalline rock part of the Upper nappe. The bottom below the snow is Phyllite, which makes the two units in direct contact.*

Bukkaskinnshjallane cliff, west of Middalen glacier (**locality 3**) is place were the crystalline Upper nappe is easily seen from a remote distance as an outstanding light felsic rock type (Fig. 37). Since the area to the SE of this locality was not visited, it was assumed that a thin Lower nappe gradually wedges out (Fig. 37). As observed the Upper nappe is in direct contact with the Phyllite unit at the North- west side of the same cliff. The lithology difference between the Phyllite and Upper nappe makes a sharp contact

This cliff (Fig. 37) represents a mylonitic and sheared rock type (Fig. 38). The bands are nearly horizontal and very harmonic. The lighter felsic bands are feldspar and quartz rich, and the mafic bands are amphibole rich. The mineral size is fine to coarse grained with phenocryst of feldspar up to 3mm to 5 mm in size. The pink/red K-feldspar phenocryst is the biggest difference between Upper nappe and some rock types in the Lower nappe, where the overall

mineral size to the latter is very fine grained. Also the feldspar crystals tend to be sheared and they act as elongated minerals, sometimes as sigma clast.

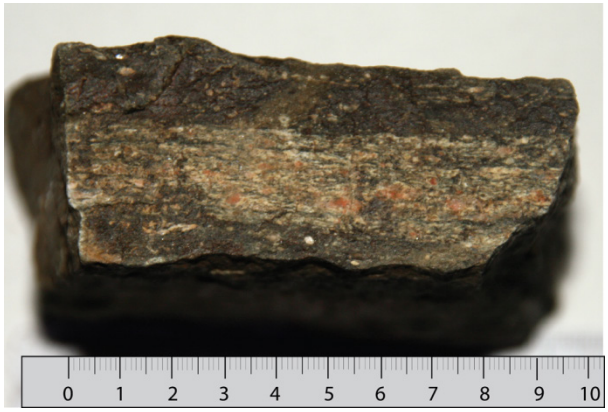

Fig. 38. ***Locality 3.*** *A rock sample from Bukkaskinnshjallane. Pink/red phenocrysts mineral is K- feldspar and are horizontal banded with mafic minerals in-between. This view is from the weathered side of the rock, because it better highlights the color of the various minerals. .*

Among the horizontal bandings, folds were observed as *gently inclined* to *recumbent* (Fig. 39). Approximately axis is oriented NW-SE ($^{ca.}$). The vergence is very difficult to determine sine everything appearing so harmonic, but one kinematic indicator could fit with NE ($^{ca.}$) direction.

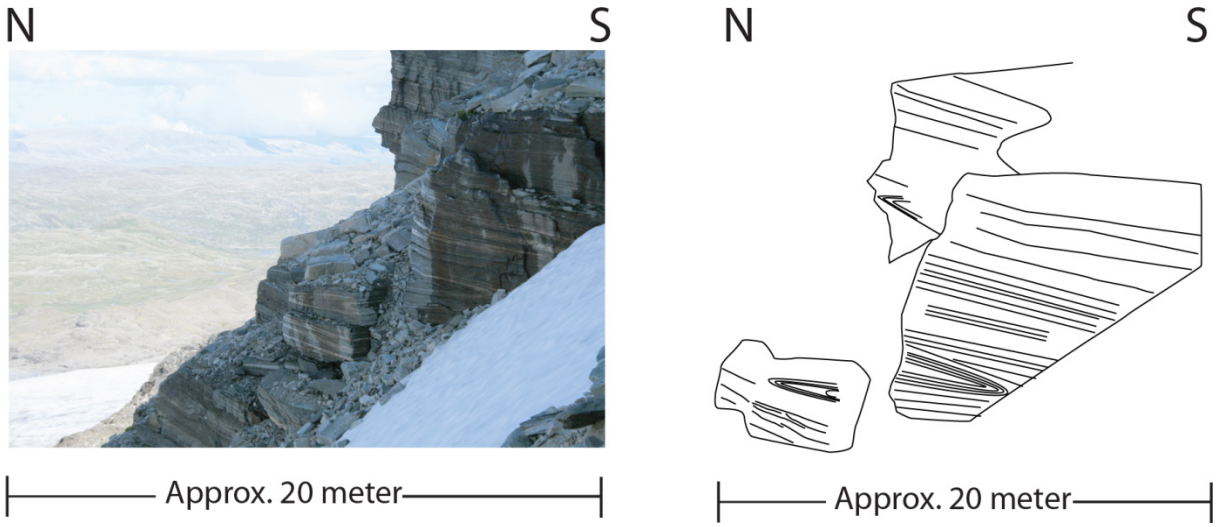

Fig. 39. ***Locality 3.*** *Folds that appear in the Upper nappe unit at this location are overturned to recumbent. The fold axis is approximately NW-SE ($^{ca.}$), and might have a vergence towards NE, but this is very uncertain due to lack of good kinematic indicators.*

In contrast, the east side of Middalen glacier displays a very different lithology (**locality 4**). Still this is the Upper nappe with mylonitic fabric. A light rock type, almost grey/white colored dominates this area (Fig. 40). This rock type is very strongly folded, with bands which are less visible than of Bukkaskinnshjallane. Fold axis and lineation are orientated towards NW-SE.

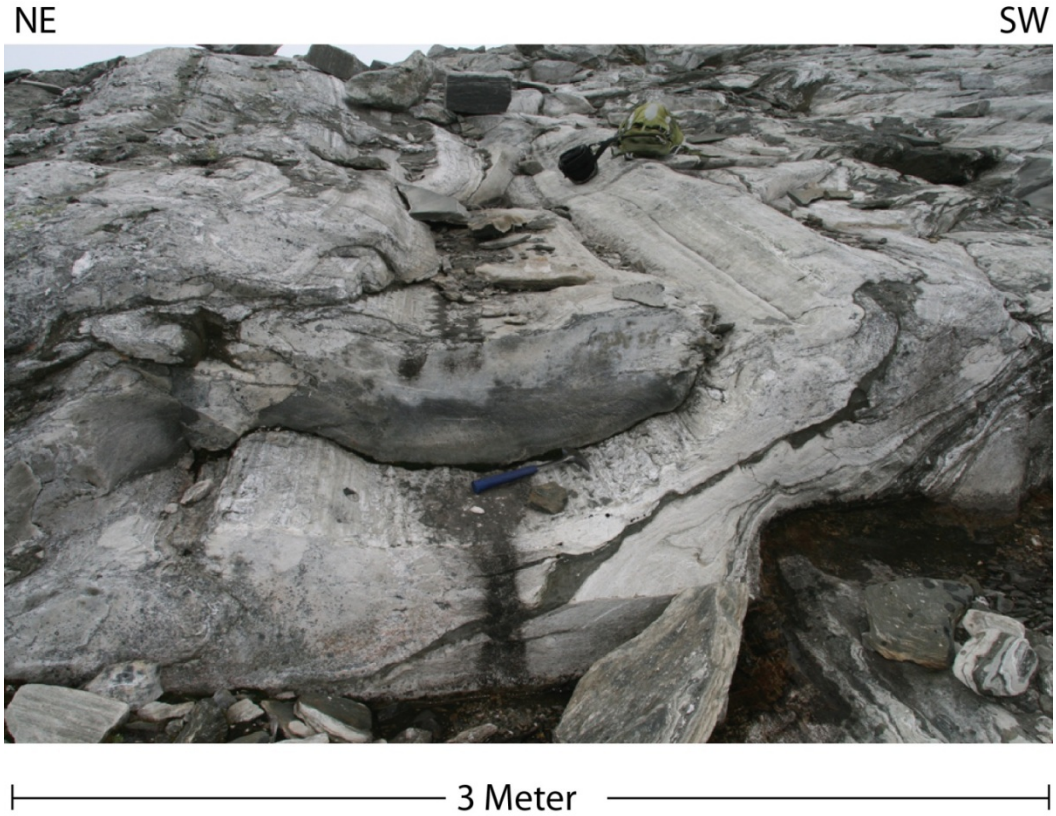

Fig. 40. Locality 4. This Upper nappe unit is very different from the normal rock type in Upper nappe. Light, white to greyish color, the bandings are not so clear and defined. This rock type is folded with fold axis oriented NW-SE.

Fig. 41. Locality 4. Upper nappe with a different lithology. Mafic bands separate the more felsic lithology. The rock lithology in between the two mafic bands cotain epidote, as being slightly more green.

The second rock type appearing in this locality appears to be transitional between mylonitic and less mylonitic rock types (Fig. 41). Darker to black layers of amphibolite, with rusty iron rich mineral incorporated, separates the different gneissic layers. The pink are the felsic, quartz and feldspar rich, and the slightly green "layer" appears to be mostly the same, but contain also epidote. Large feldspar crystals have crystalized to pegmatitic size, at centimeter scale sizes. The overall matrix is a coarse grained size, from 1 mm to 2 mm.

The more homogenous fabric beneath the pegmatitic sized feldspar (at the bottom of Fig. 41)., has slightly larger crystal size from 3 mm to 4 mm, and appear to be less sheared compare to the rest of the fabric in this rock.

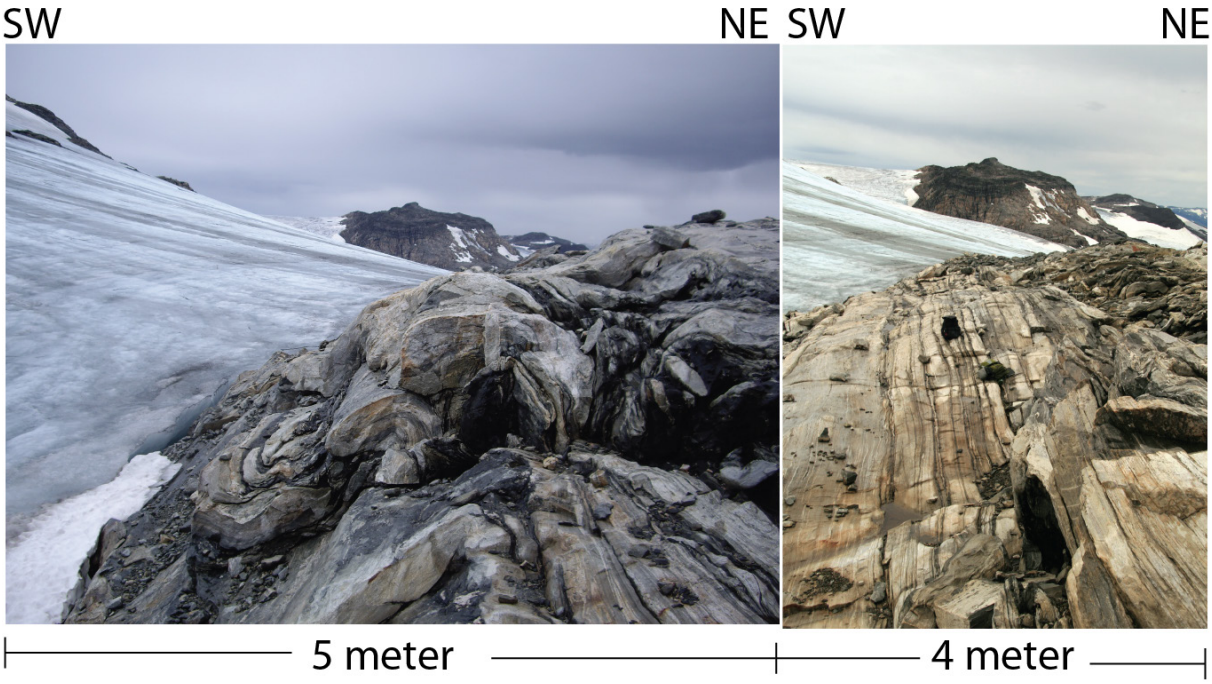

*Fig. 42. **Locality 18**. Upper nappe. Two pictures are taken in the same direction. The left picture shows the highly folded upper nape, with felsic and mafic lithology. Fold axis are trending NW-SE. As this is very complexly folded, the vergence appears to be towards SW (ca.), but this could also be a local feature. The right picture is taken 10 meters further NW and looking along the fold-axis.*

Further topographically upwards relative to Fig. 40, the lithology becomes very similar to the Bukkaskinnshjallane (Locality 3), and it appears to be part of the same rock type. Highly mylonitic and sheared bedrock, and some places are more folded than other. Fold axis are NW-SE (310° - 130°). This locality appears to have a vergence towards SW(ca.), but this could also be a local feature, since it is the only one found and it contradicts the general NE vergence.

Upper nappe is the crystalline basement and would have many compositional similarities to the Basement. Light colored, felsic, coarse grained crystal to phenocryst and also compact. The biggest notable difference between the Upper nappe and the Basement is the lithology. Upper nappe is characterized as a gneiss, and are usually highly deformed with bandings either as complex wavy or almost horizontal. Alternating pink and green color, and with a thinner mafic layer. Most of the unit consists of K-feldspar and plagioclase, chlorite and some epidote, with these darker bands of amphibole. This unit are in various degree highly folded, but still less complex than the Lower nappe.
Due to more horizontal bands, the deformation grade appears to be higher than the Lower nappe. The sheared and mylonitic fabric tends to be only the “lowest” part of Upper nappe.

Fig. 43. A rock sample of the less mylonitic upper nappe. The felsic part of the rock appears much more homogenous and less shared, and constitutes 70 % of the rock fragment. Feldspar crystal appears as pegmatitic sizes. In other hand, the mafic minerals are banded and sheared with gneissic fabric.

The fabric appears to be less mylonitic at higher altitudes[2].

This rock type (Fig. 43) is the closest in fabric (as observed) to the basement. The feldspar has grown very large, pegmatitic size at centimeter scale, and contributes with quartz approx. 70 % of the rock. Still there as some mafic composition that has mylonitic fabric.

The contact to Upper nappe is locally difficult to distinguish, as there are similarities between Lower nappe and Upper nappe. Most of the Upper nappe is either covered by the glacier or it's just inaccessible to reach, therefore amount of contacts and observation are very limited.

3.3 Lower nappe and Phyllite structures

This field area involves complex layering of both Lower nappe and Phyllite which are the reason to split the structurally description into a chapter for itself.

Both units are observed to be complexly involved in folding at various scales, and are exposed very differently on EAST side and WEST side of Middalen Glacier (Fig. 44).

Lower nappe constitutes about 70 -80 % of the area and the rest is Phyllite that are observed as usually 1 meter thick "layers". The thickness for the Phyllite situated on top the basement, changes to some degree but overall quite thickness is only 1 – 5 meter. In this case faults are observed to be to either what seems to be thickening or thinning of the unit (Fig. 24 and Fig. 27). The other "layers" of Phyllite, are found further topographically upwards and appears to be "cutting" through the Lower nappe unit.

[2] These areas are not reachable and are only observed and interpret from a distance. The precise altitude is not possible to determine.

3.3.1 The general structure of the East and the West side at Middalen glacier

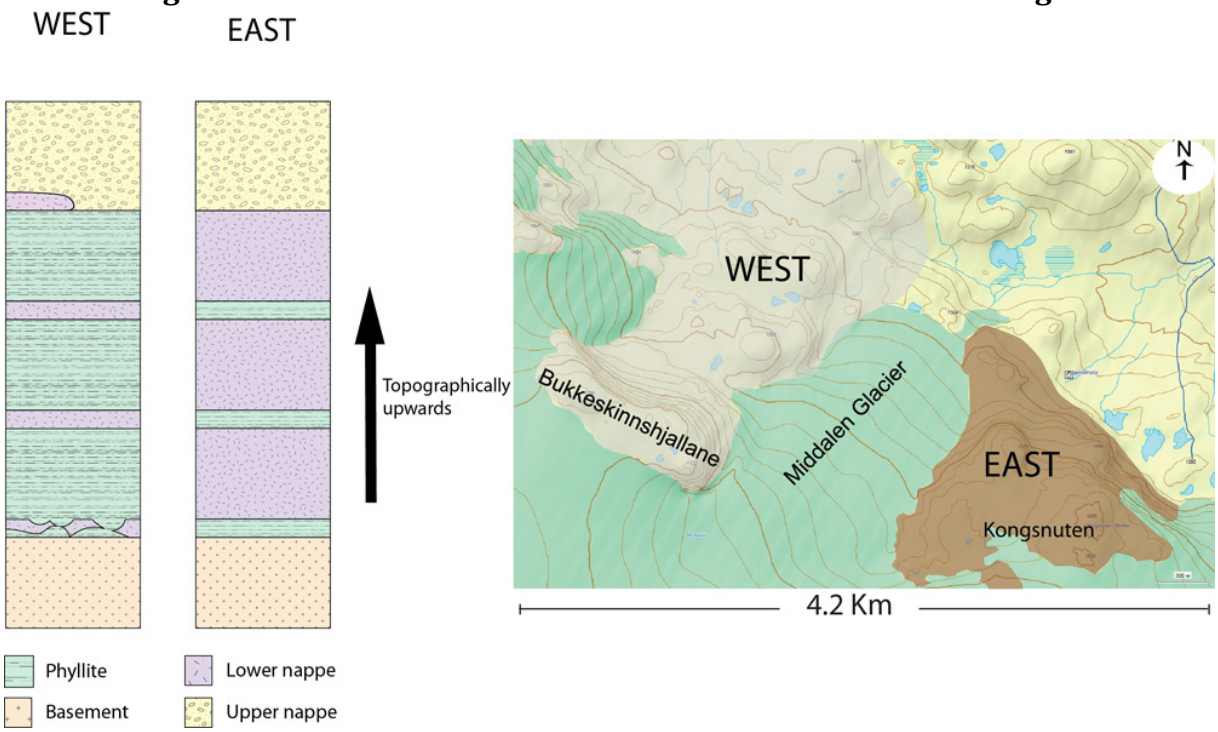

Fig. 44.Generalized stratigraphy of both east and west side of Middalen glacier. Upwards at the illustration is topographical upwards in the field. Left picture: The dominant rock unit is Phyllite with Lower nappe appearing as "Layer". Bottom, close to the contact to the basement, are lenses of Lower nappe directly on top to the basement. Right picture: The main rock type here is Lower nappe with "layers" of Phyllite in-between. Note this is an illustration displaying the structural differences, the thicknesses is therefore generalized and likely not always valid.

The east side

The whole 200 meter stratigraphy appears as 3 "layers" of Phyllite, and 3 significantly thicker "layers" of Lower nappe, from 20 – 100 meter or even more(Fig. 44, right illustration).. Above the third Lower nappe "layer" there is a flat area that is mainly dominated by Phyllite. This area could still be one of these "layers", but erosion might have cut more horizontal rather than vertically. This exposes the whole "layer", instead as usually seen as incorporated "layer" in the Lower nappe

The west side

In contrast to the East side, the West side is very different and quite the opposite. The Phyllite dominates in this area, and nearly constitutes 80 -90 % of the outcrops West of Middalen Glacier. The rest of the outcrops are Lower nappe.

The number of layering on this side is very difficult to determine, in contrast to the East side, since the Lower nappe is exposed in what appears to be more random places. But still there seems to be a pattern, as interpret (Fig. 44, left illustration).

3.3.2 Structural description

The dominant structural phenomena are folds and are observed practically everywhere from small scale to larger scale at tens of meter. Both illustrations (Fig. 44) display a homogenous "layering", but in reality it is far from as horizontal as illustrated.

Locality 5

The cliff located between Blåisen and Middalen glacier, represents a fold which is nearly 10 meter high and almost 10 meter wide, and contains alternating "layers" of Phyllite and Lower nappe **(**Fig. 45**)**. The sequence starts with Phyllite, which would part of the rock unit that is normally stratigraphically below Lower nappe. Next is a small "layer" of lower Nappe that is 20 cm thick, and above a slightly thicker layer of Phyllite which is 1 meter thick. Two more Lower nappe "layers" appearing with a 63 cm thick Phyllite in-between. The first have a thickness of 1.3 meter, the latter would be part of the dominant structures above. A quartzitic vein is incorporated between the Phyllite the top-most Lower nappe unit. The fold is characterized by *gently inclined*, and with *close* fold tightness, with fold axis trending 215°-35°, and vergence towards NW.

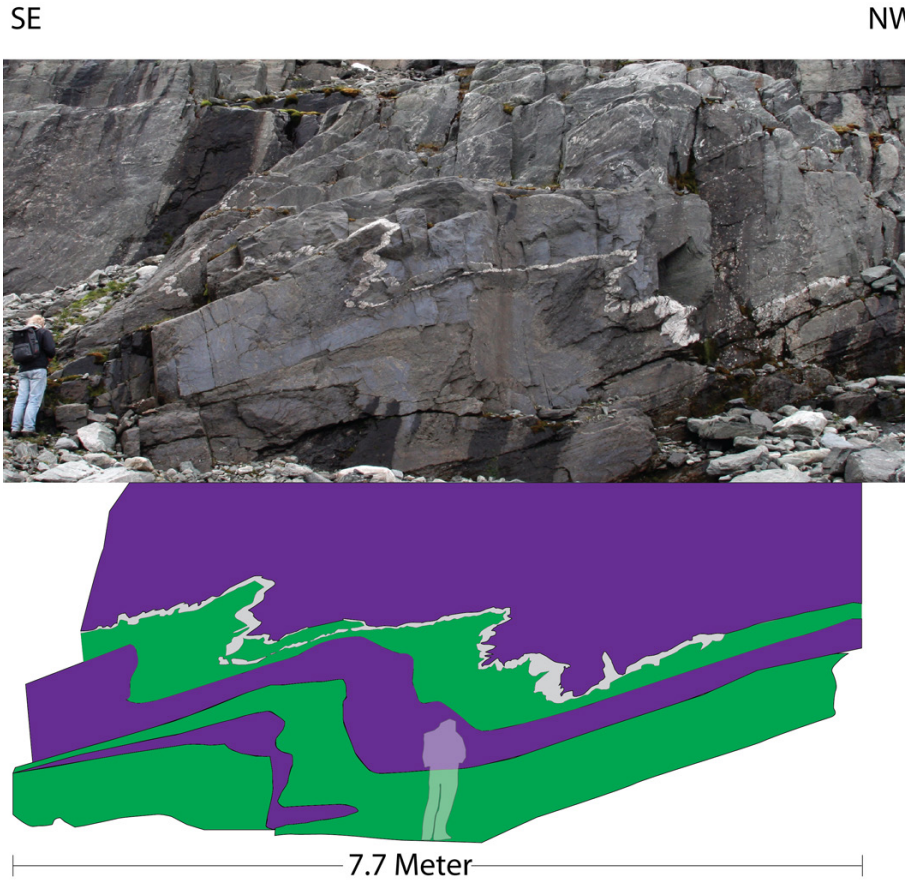

Fig. 45. ***Locality 5****. A moderately sized fold. Phyllite and Lower nappe are folded together, and appears as three alternating "layers". A quartzitic vein separates the topmost Phyllite layer and topmost Lower nappe unit. Fold axis 215°- 35° with vergence towards NW. Note: the view area for the illustration are slightly shorter compare to the picture above, and to maintain a reference point, the person where moved.*

Locality 6

This locality is located west of Middalen glacier, and north of Bukkaskinnshjallane (Appendix 1). The cliff represents a large scale folding which is 20 meter wide and 3 meter high. This large scale folding has a fold-axis orientated NE-SW, and vergence towards NE. Mylonitic fabric with lenses of quartzite that has rotated in response to the folding, but hasn't developed perfect sigma clast. The fold geometry changes from a small scale folding at centimeter scale to a larger scale folding at meter scale. This Lower nappe contains carbonate "layers" (Fig. 46 B, the slightly darker area, with red line), and would be part of either rock type 4 or 10 according to the Lower nappe stratigraphic log (Table 7).

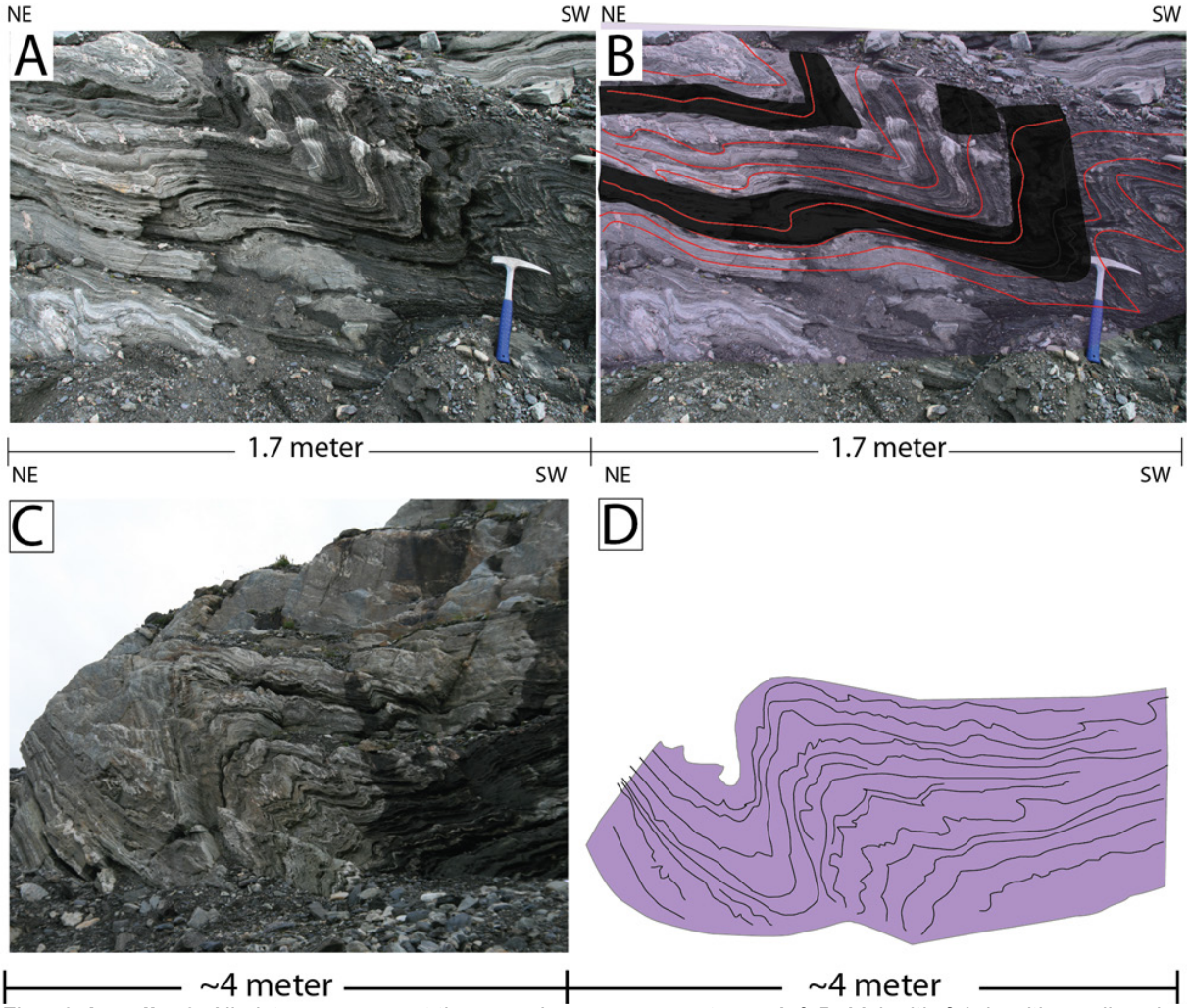

Fig. 46. ***Locality 6.*** *All pictures represent the same Lower nappe outcrop. A & B: Mylonitic fabric with small scale folding, carbonate layer is mark in black. C & D: the fold geometry changes to a moderately sized fold, with fold axes oriented NW-SE, and with vergence towards NE.*

Locality 7

This locality is located west of Middalen glacier, and south of Bukkaskinnshjallane and slightly north –east of Locality 19 (Appendix 1). This small hill is only 5-7 meter high relative to the surroundings and approx. 50 meter wide, has similar features as seen in locality 6 (Fig. 46**).** Phyllite and Lower nappe are alternating, but with greater magnitude.

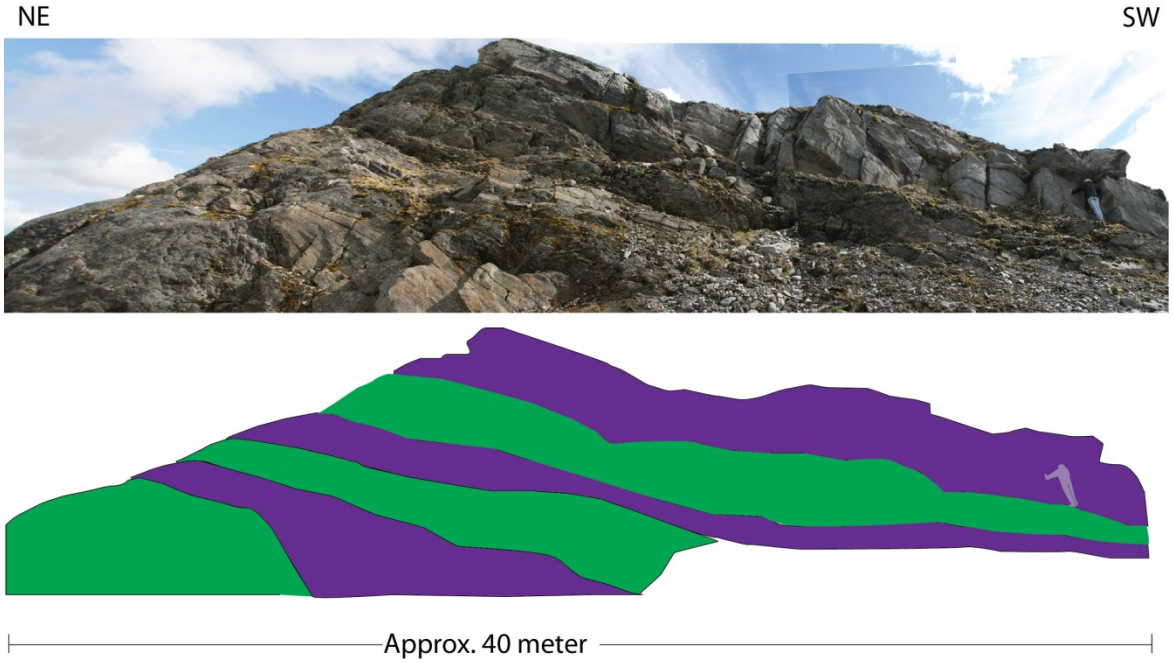

Fig. 47. ***Locality 7.*** *This hill represents the alternating Phyllite and Lower nappe "layering. Each lithology alternates three time within each other, expect the lowest Phyllite and the topmost Lower nappe unit. Phyllite and Lower nappe alternates with three different "layers". Green color are Phyllite, and purple are Lower nappe.*

Alternating layering of both Phyllite and Lower nappe is also display at this locality (Fig. 47). Three "layer" of each lithology, where the lowest Phyllite at this hill would be correlated to the one stratigraphically below Lower nappe, and the uppermost Lower Nappe "layer" would be stratigraphically above Phyllite. While not display at this picture, the first and second Lower nappe "layering" from bottom is connected and folded together.

The fold axis for the Lower nappe unit are oriented NE-SW with vergence towards NW. In contrast to the NE side of the same hill, the Lower nappe appears more complex folded (Fig. 47) and with a different fold –axis NW-SE (^{ca}). This hill represents two vergence directions, towards NE and NW (^{ca}), this further are discussed in next chapter: 3.3.3.

Since the top of the hill is Lower nappe, this is projected to be Lower nappe at the map.

Locality 8

This locality is located west of Middalen glacier, and south of Bukkaskinnshjallane and slightly south-west of Locality 8 (Appendix 1). The cliff is approx. 150 meter wide and 3 meter high. The majority of the folds observed are either *isoclinal* or *close* with either *sharp* or *angular* bluntness. The fold geometry is *recumbent* with nearly horizontal axial surface. Lower nappe folds (Fig. 48) with Phyllite existing both around and inside the structure. The fold axis is 120°.

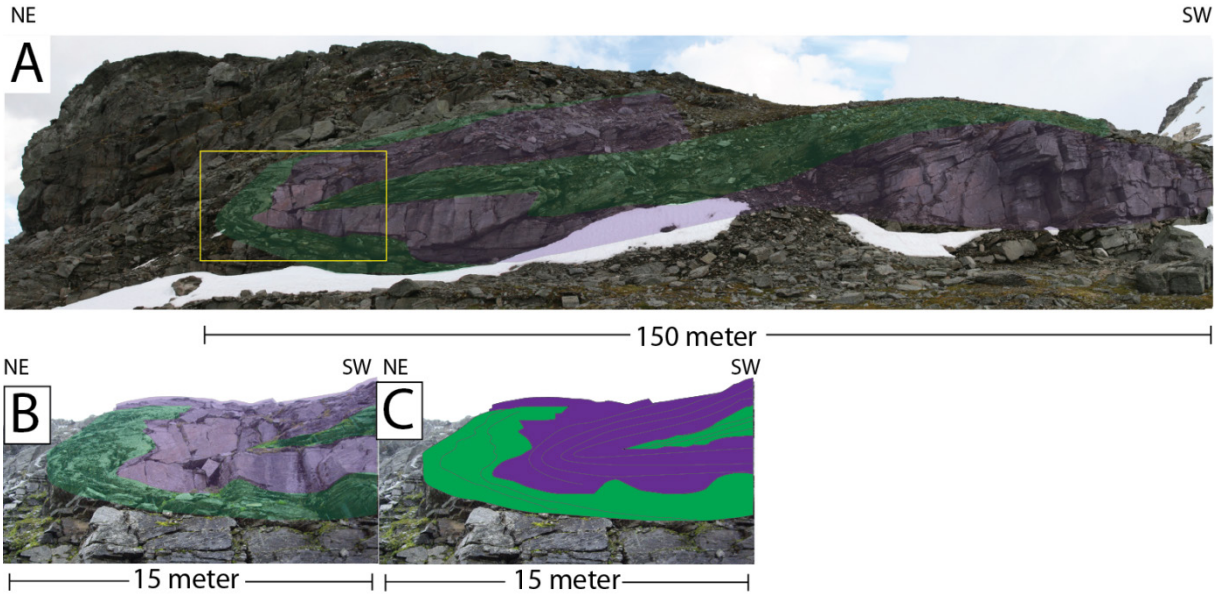

Fig. 48. ***Locality 8.*** *A: Recumbent fold where Lower nappe folds around a thin "layer" of Phyllite, which wedges out and stops close to the fold hinge. Fold axis is 300°-120 (NW-SE) °.B & C: Are close up illustration of the yellow square in A. The background picture below (same for both) is provided by Fernando Corfu.*

Locality 9

This locality is located east of Middalen glacier (Appendix 1). The cliff is approx. 150 meter long and approx. 2- 5 meter high. The closed in Phyllite incorporated in between the Lower nappe could also be recognized at this locality. But here the fold hinge is not visible, just the Phyllite unit that wedges out, and suddenly stops (Fig. 49). By comparing Fig. 48 with Fig. 49, the wedging out Phyllite in the middle appears as the same. Al though the fold hinge is not directly observed, it is likely that the fold-axis could be trending NW-SE(^{ca}), because the geometry is quite similar to Fig. 48, and not least the orienation of both vertical sections are the same (NE-SW).

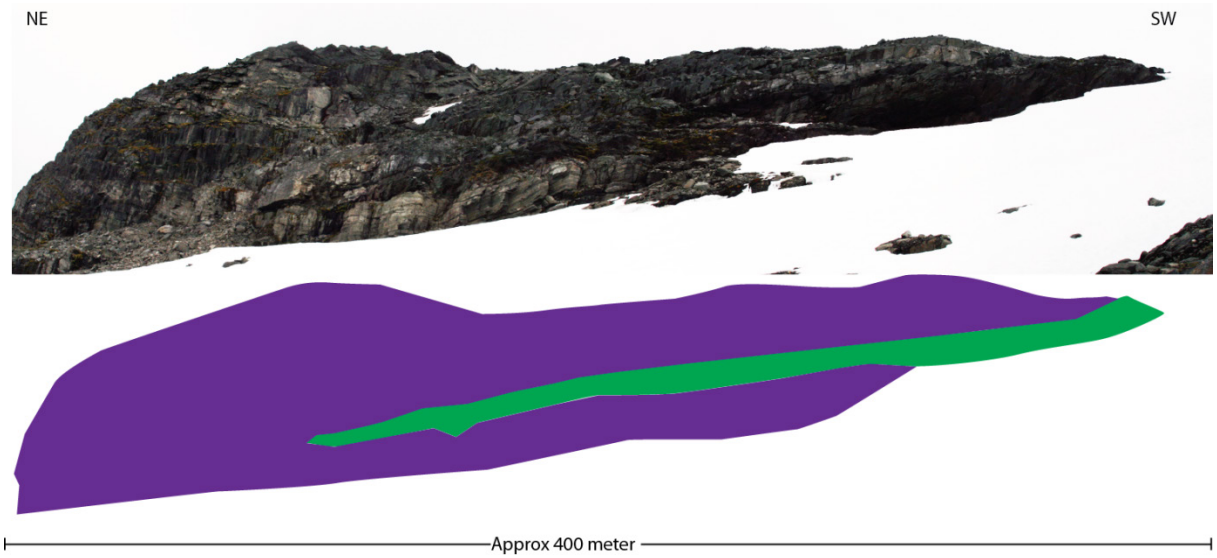

Fig. 49. ***Locality 9.*** *A thin Phyllite "layer", at most 1 meter thick, wedges out and stops. Lower nappe surrounding the Phyllite layer.*

Locality 10

This locality is located north-west of Middalen glacier (Appendix 1). The cliff is approx. 15 meter long and. 1 meter high. A *recumbent* fold is observed here, but in this case it is only the Lower nappe unit present. This outcrop represents some of the different rock type in the Lower nappe unit, as shown in Table 7, chapter 3.2.3.1. The darker area is a carbonate layer (Fig. 50 below). The foliation plane changes from almost vertical on the left side, to horizontal where the fold has become *recumbent* on the right side (Fig. 50). This fold– axis is oriented 130° - 310° (NW-SE).

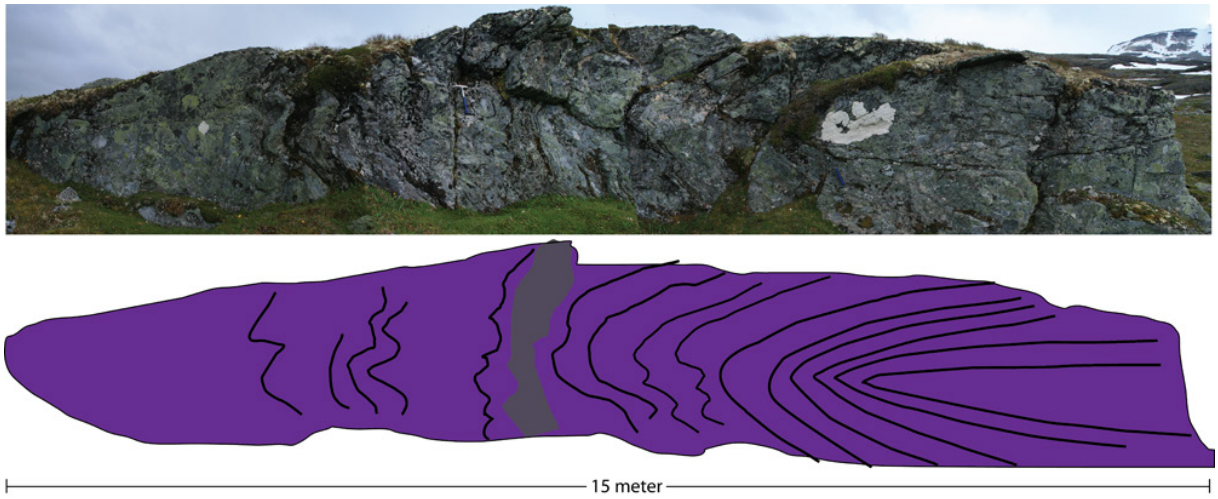

Fig. 50. ***Locality 10****. Recumbent Lower nappe unit. The structure gradually becomes steeper and eventually isoclinal and recumbent. The darker black field marks a carbonate layer, so this Lower nappe outcrop consists of several different rock type part of the unit (Table 7). Fold axis are 130° - 310° (NW-SE).*

Locality 11

This locality is located north-west of Middalen glacier, east of Locality 10 (Appendix 1). The cliff with the important structure is only approx. 5 meter wide and 4 meter high. Lower nappe is observed to be directly on top of the basement.

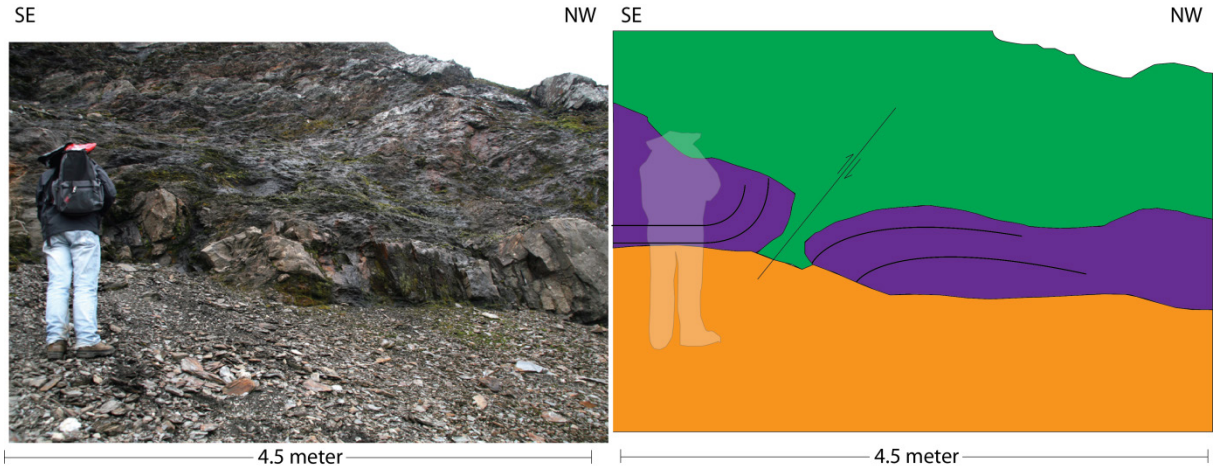

Fig. 51. ***Locality 11****.Lower nappe unit that are directly on top off the basement. This unit appears more in the shape of lenses than as a complete stratigraphic unit. A small thrust fault has slightly thrust the left lens above the right lens, and the right lens underneath the left lens.*

The person in the picture (Fig. 51) is standing on the basement. Above the basement is a small, approx. 1 meter thick Lower nappe unit. But this Lower nappe appears to consist of broken lenses displaced and separated relative to each other by a small scale reverse fault. The left lens is buckling up and almost over the right lenses, which is buckling under the left lens. The Phyllite unit above doesn't seem to be affected by this fault due to the much lower competence. The fault and fold –axis appears to be the same orientation, NE-SE (^{ca}).

3.3.3 Fold structures

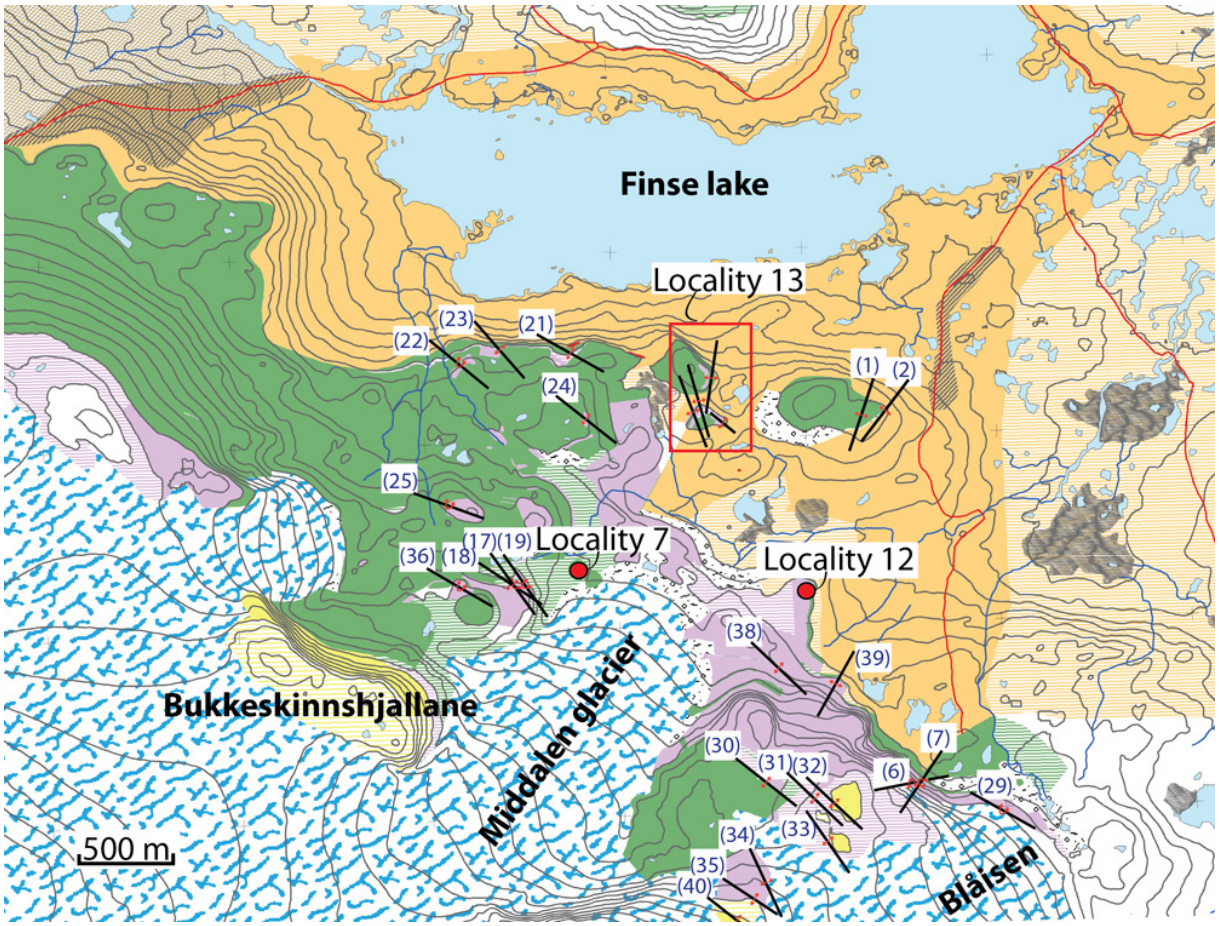

Fig. 52. All fold axes that have been measured are marked on the map. The fold axis orientation changes between 70° – 120 °. The areas marked either in a red circle or red square, are further described below. The blue numbers in brackets are fold-axis number listed in Appendix 2. Green color is Phyllite and Purple is Lower nappe. For complete color coding, see the map.

Based on the measurement from the field there are two fold-axes orientations, the prominent NE-SW direction and NW-SE direction. Not only is the study area shape from two different stress regime, but at some localities one of these ordinations have superimposed on the other. At **Locality 7, 12 & 13,** the fold axis rotates over a small area (100 m). Fig. 52 is an overview map that illustrates all fold axes at the study area, and with position of these three localities.

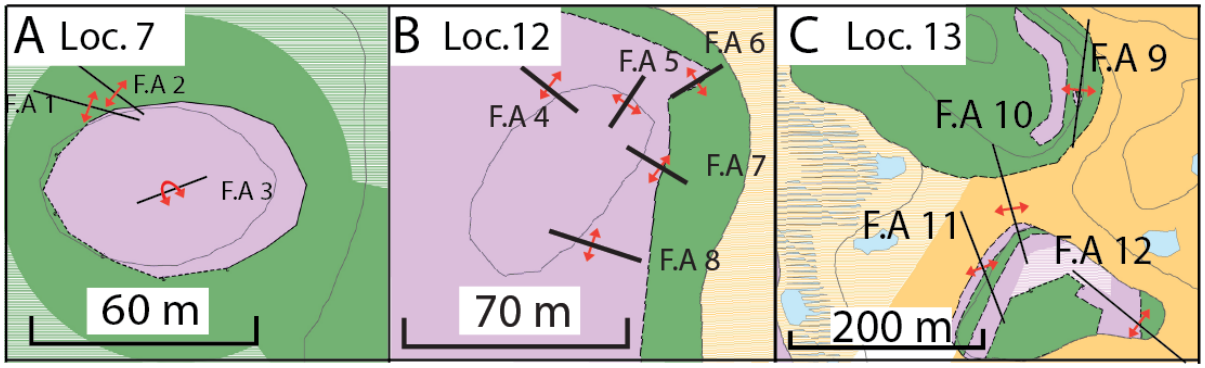

*Fig. 53. The different localities that shows a fold axis rotation. A: **Locality 7**. Phyllite and Lower nappe have quite different fold axis orientation, also the fold axis for Phyllite changes. B: **Locality 12**. The fold axes for Lower nappe changes over a small area. C: **Locality 13**. Fold axis measurements for both Lower nappe and Phyllite, and changes over a slightly larger area (relative to loc. 12 & 13. Green color is Phyllite and Purple is Lower nappe. For complete color coding, see the map.*

Fold axis nr.	Fold axis nr. Appendix 2.	Azimuth (both direction)
Locality 7		
F.A 1	26	290° - 110°
F.A 2	27	310° - 130°
F.A 3	28	250° - 70°
Locality 12		
F.A 4	15	310° - 130°
F.A 5	9	215° - 35°
F.A 6	8	240° - 60°
F.A 7	12	305° - 125°
F.A 8	14	290 - 110°
Locality 13		
F.A.9	37	190° - 37°
F.A.10	4	355° - 165°
F.A 11	5	340° - 160°
F.A 12	3	310° - 130°

Table 9. Fold axes data for the folds in Fig. 53. To correlate with the complete fold-axis dataset find the corresponding number in appendix 2.

.

4 Geochronology

4.1 Introduction

Four samples were collected from the basement. For a map over all the sample locations, see **Appendix 1,** blue text.

Sample C-11-5 is a Granodiorite.

Sample C-08-4 is granite

Sample C-11-8 a pegmatite

Sample C-08-5 is a gabbro

4.2 Granodiorite

The zircons in sample C-11-5 were divided into 3 groups, plus a titanite group. While there are abundant amounts of zircons in this sample, a lot of them were either affected by radiation damage, or they had developed cores. But the clear well-developed zircons were almost perfectly euhedral in shape.

Group 1 consists of euhedral, elongated zircons, with angular corners.
Group 2 consist of anhedral zircons with rounded corners.
Group 3 Zircons, prism, elongated.

The first group was subdivided into '**J**' and '**K'** (Fig. 54), which respectively contained 9 and 16 zircons. After abrasion these were some of the best quality zircons. Very clear, little to no inclusion, elongated with an almost perfect shape. During spiking and weighing, the zircons in the 'J' group were further subdivided into two groups. This gives a total 3 samples to be analyzed of group 1. Three zircons were selected from the second group, and categorized with the letter '**F**' (Fig. 55). The last group were given the 'I' letter, and contained 5 zircons taken from third group (Fig. 57).

For the titanite, it was subdivided into two groups, '**C**' and '**D**' (Fig. 56). Group C contained one large titanite, while group D contained four smaller titanite grains.

In total the Granodiorite (C-11-5) contained 5 samples, with 25 zircons and 3 grains of titanite.

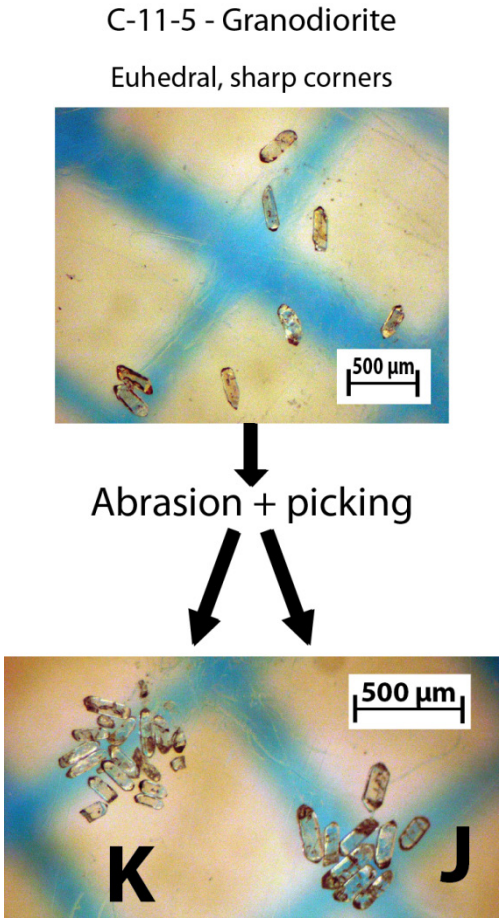

Fig. 54. Zircons - Sample C-11-5: Granodiorite. These samples contained a lot of zircons, but just some of them appeared to be in a very good condition. The picture above shows the zircons before abrasion. Below: After abrasion two sub-groups group, J and K, were selected after abrasion. The zircons in the J group were further sub-divided into 2 new groups during weighing and spiking.

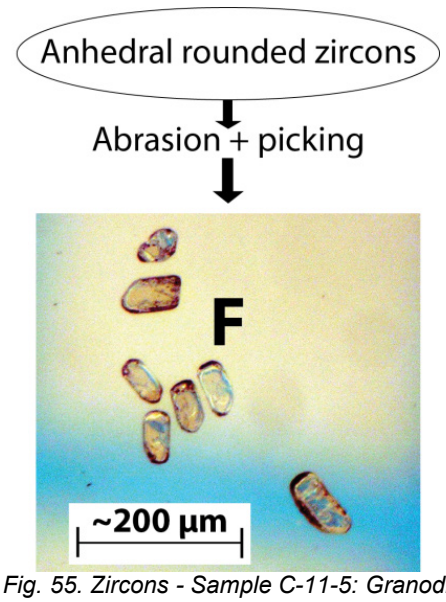

Fig. 55. Zircons - Sample C-11-5: Granodiorite. From anhedral rounded zircons, one sub-group with 7 zircons was selected after the abrasion, and categorized as group F.

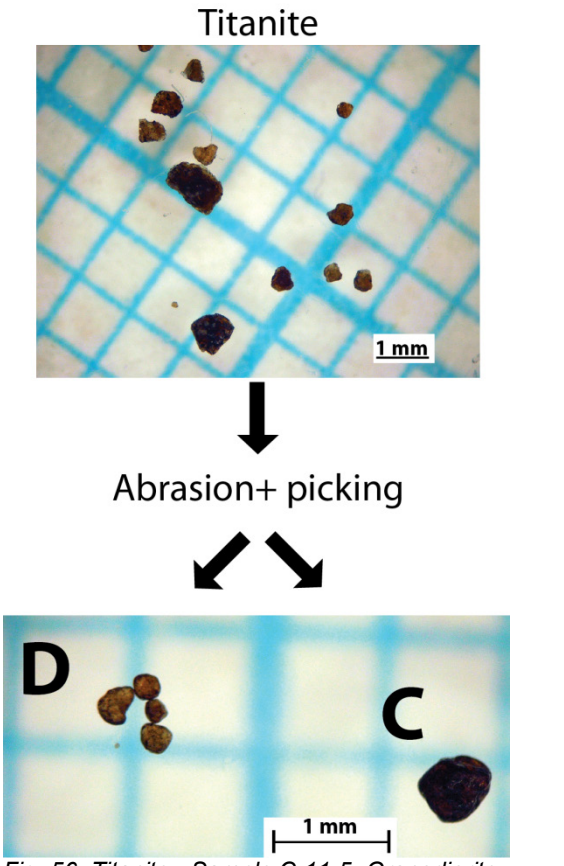

Fig. 56. Titanite - Sample C-11-5: Granodiorite. Some of the titanite in this sample had an unusually large size. The picture above shows the presorted titanite before the abrasion. Two sub-groups were picked after abrasion. Group C contained 1 large titanite and group D contained 4 titanite grains.

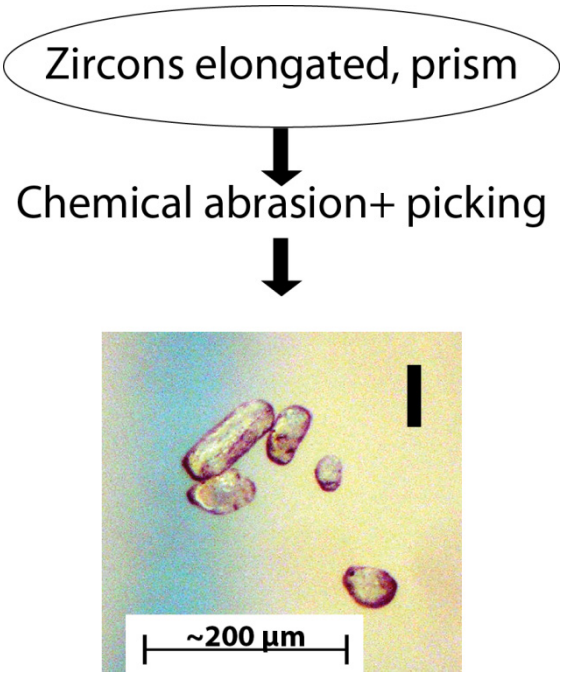

Fig. 57. Zircons - Sample C-11-5: Granodiorite. From nearly euhedral zircons with prismatic shape, one sub- group with 5 zircons were picked after the abrasion. This group was categorized as group I.

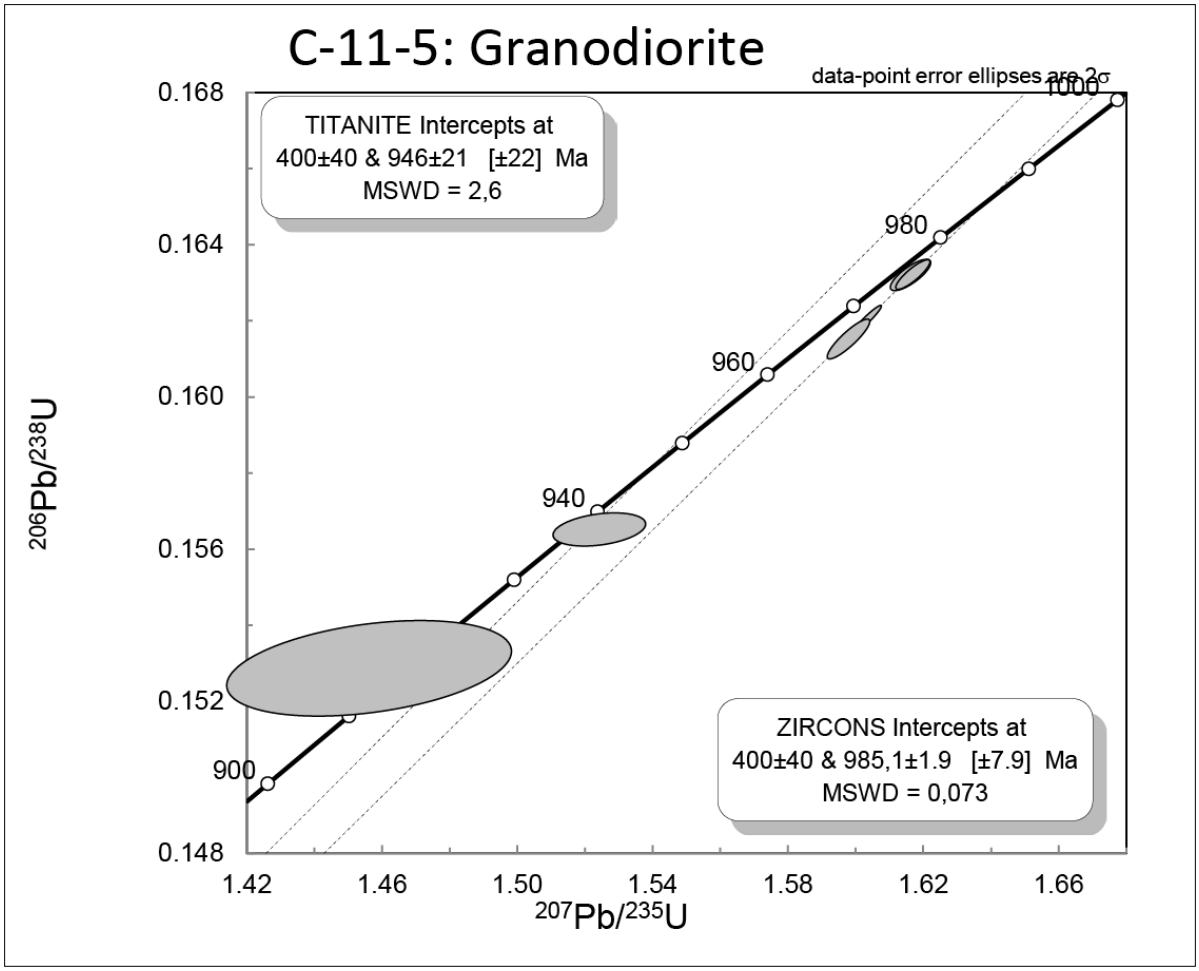

Fig. 58. Concordia diagram of sample C-11-5 Granodiorite. The zircons intercept at 989 ± 10 Ma when anchored to Caledonian orogeny at 400 Ma. Two titanite values with an age of 912.4 Ma and 940.1 Ma are interception at 946 ±21 Ma when also anchored to Caledonian orogeny.

Fig. 58 represents the analytical concordia diagram for the granite. These zircons are quite discordant, but they are perfectly placed along the discordia line. The upper point is 985.1±1.9 Ma, and lower point is anchored to the Caledonian orogeny. The age of the titanite is 937.7 ±2.2 Ma and 916.9 ±5.8 Ma with interception age at 946 ±21 Ma.

4.3 Granite

In this sample there were many zircons, but most of them where orange and affected by high amount of uranium. After a chemical abrasion, two sub-groups were selected from the pre-selected group, depending on their sizes. First one, '**G**', contained 3 larger zircons, and second one '**H**' contained 13 smaller zircons (Fig. 59).

In total there were 2 samples and 16 zircons in C-08-4.

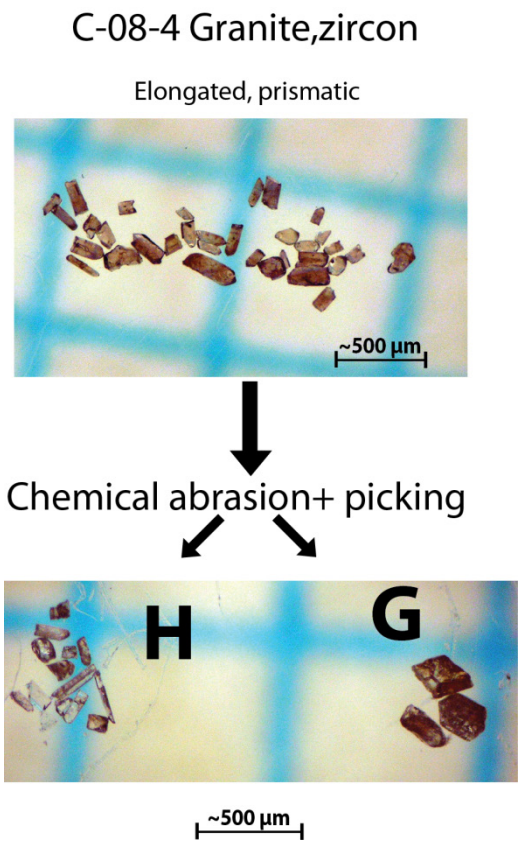

Fig. 59. . ***Zircon. Sample C-08-4: Granite.*** *The majority of the zircons had a high uranium content, which gives the orange color. Above: A pre-selected group that contained the best quality zircons in this sample. Below: Two sub-groups were selected after a chemical abrasion, depending on the sizes. The small zircons were defined as 'H', while the larger one were defined as 'G'.*

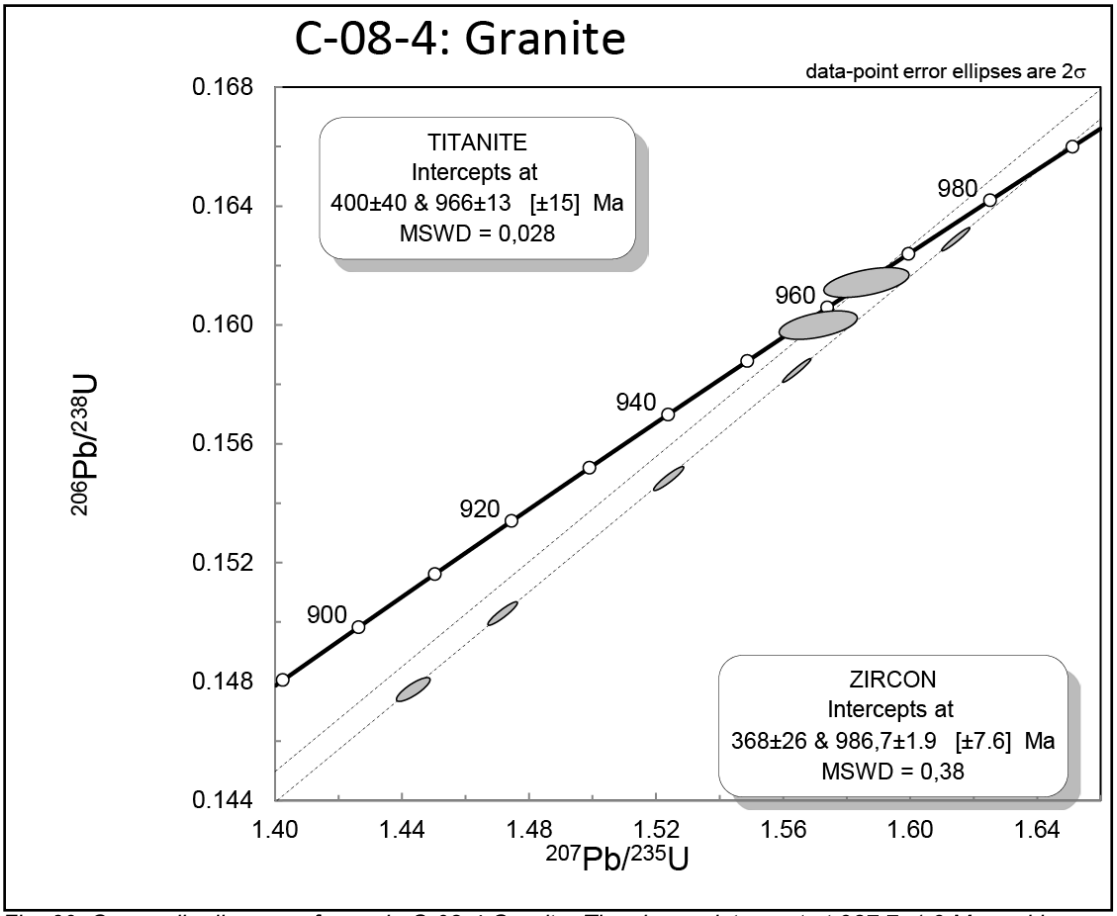

Fig. 60. Concordia diagram of sample C-08-4 Granite. The zircons intercept at 987.7±1.9 Ma and lower point intercepts at 368±26 M and could be related to Caledonian orogeny. Two titanite values with an age of 957.0±2.4 Ma and 964.8±2.5 Ma are interception 966 ± 13 Ma when anchored to Caledonian orogeny.

Fig. 60 represents the analytical concordia diagram for the granite. All zircons are almost perfectly fitting along the discordia line, where upper intercept age is 987.7±1.9 Ma and the lower point are 368±26 Ma. The latter are likely to be related to lead loss during Caledonian orogeny. The titanite has an age of 957.0 ±2.4 Ma and 964.8 ±2.5 Ma with an interception point at 966±13 Ma.

4.4 Pegmatite

The C-11-8 sample, pegmatite, had very little zircons and titanite. Because of this there was eventually only one group with 3 zircons that was pre-selected as the best one. After abrasion, two of the zircons were selected for further analysis. The last selection before spiking and weighing, only one zircon that was selected (Fig. 61). This grain was very small and only approx.55 µm. The age is based on this single small zircon grain, and no titanite.

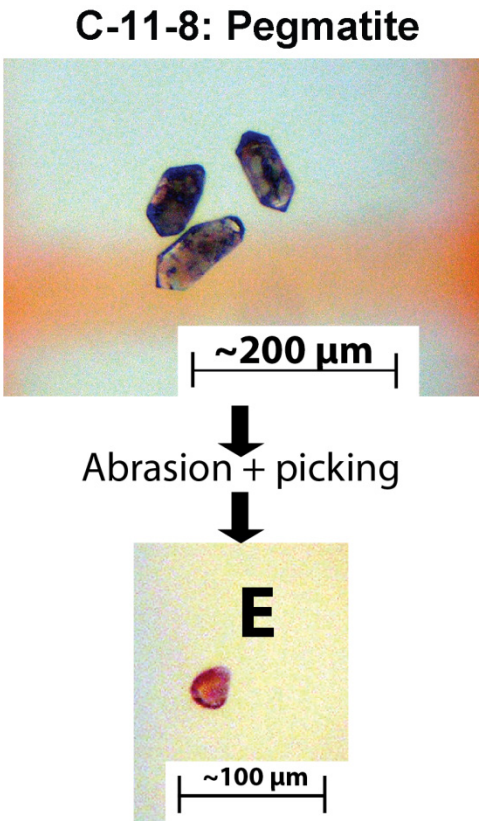

Fig. 61 Zircon. Sample C-11-8: Pegmatite. This sample contained very little zircons. The picture above shows the three pre-selected zircons picked out before abrasion. Only two zircons were eventually picked out after the abrasion. For the last selection only one zircon was suitable to use, and quite small in size ((approx. 50 µm).

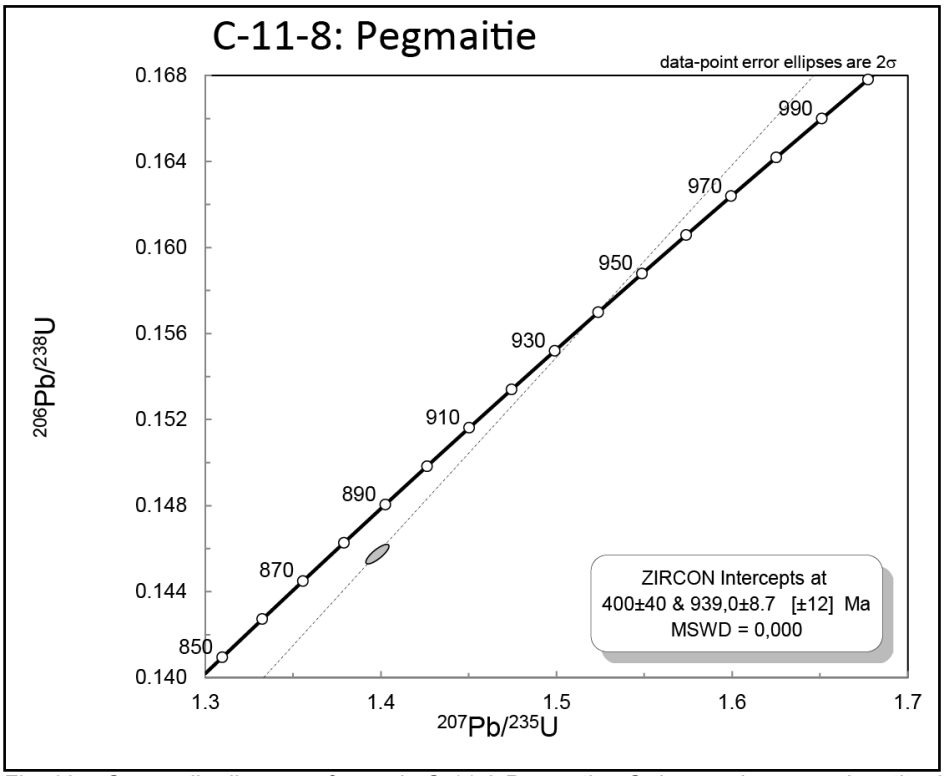

Fig. 62. . Concordia diagram of sample C-11-8 Pegmatite. Only one zircons and no titanite were analyzed. When anchored to Caledonian orogeny, 400 Ma, the zircon gives an interception age of 939.0 ±8.7 Ma.

The mass spectrometer gave a discordant value, and with only one data this had to be manually anchored to fix the interception point. Caledonian orogeny is likely to cause lead loss due to the increase heat from the thrusting, and this 420 Ma event was used as an anchor point. Fig. 62 shows the concordia diagram for the C-11-8 pegmatite sample, with an interception age of 939.0±8.7 Ma.

4.5 Gabbro

The zircons in the gabbro were both euhedral angular and rounded, an also anhedral shaped. The best quality zircons picked out, where the one that were rounded (before abrasion) and "large and fragmented".

After the abrasion the rounded zircons where further dived into two groups. The first group, which was given the letter '**L**', had 2 zircons that were slightly larger in size compare to '**M**', which consisted of 11 zircons (Fig. 63).
Two groups of titanite were sorted out. The difference between two of them were the color, one of them were more pail, while the other had a darker red/brown color. Another picking after abrasion ended using 3 grains of titanite from each group. The paler grains of titanite were defined as '**A**', while the other was given the letter '**B**' (Fig. 65).
The last group for this sample contained 2 zircons abraded from large fragmented zircons. These were categorized as '**N**' (Fig. 64).
In total for the C-08-5 gabbro, there were 6 samples, 14 zircons and 6 grains of titanite.

.

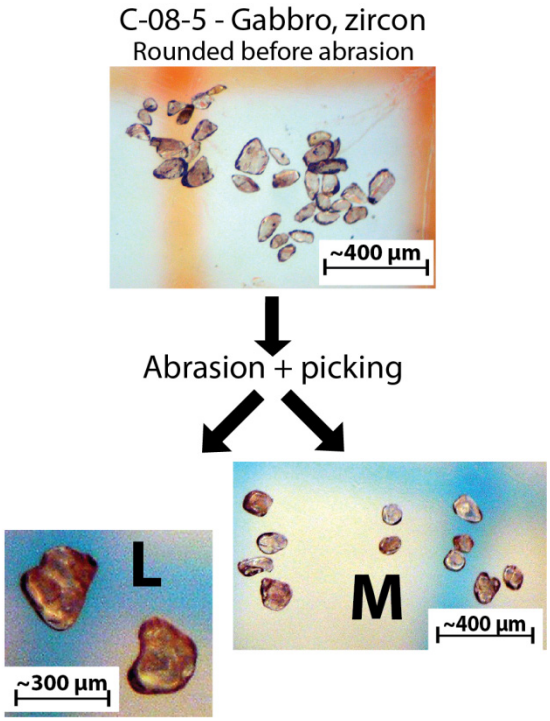

Fig. 63. ***Zircon. Sample C-08-5: Gabbro****. The shape of the zircons in this sample appeared to be a little different. Some were rounded and other was angular. But for a gabbro, there were many zircons in this sample. The picture above shows the un-abraded zircons, while the picture below show sorted and abraded. Two group depending on their sizes were selected, L and M.*

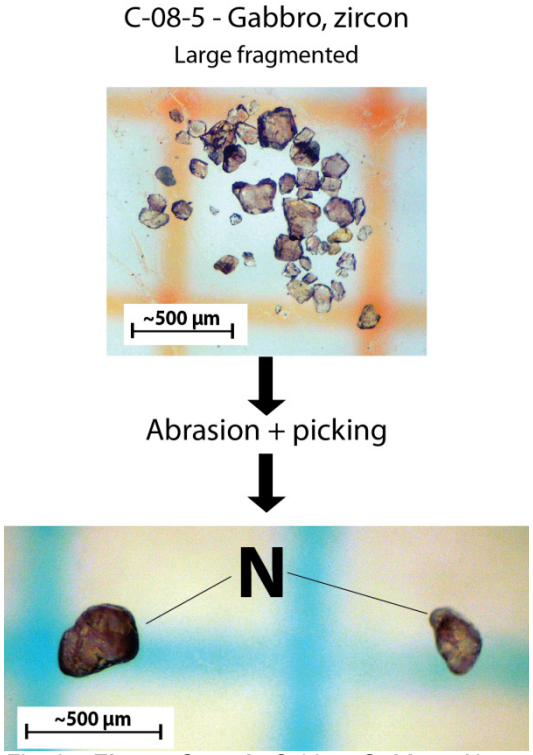

Fig. 64. ***Zircon. Sample C-08-5: Gabbro****. Above: Before abrasion, pre-selected zircons. Below: After the abrasion two larger fragmented zircons were placed into the sub-group N.*

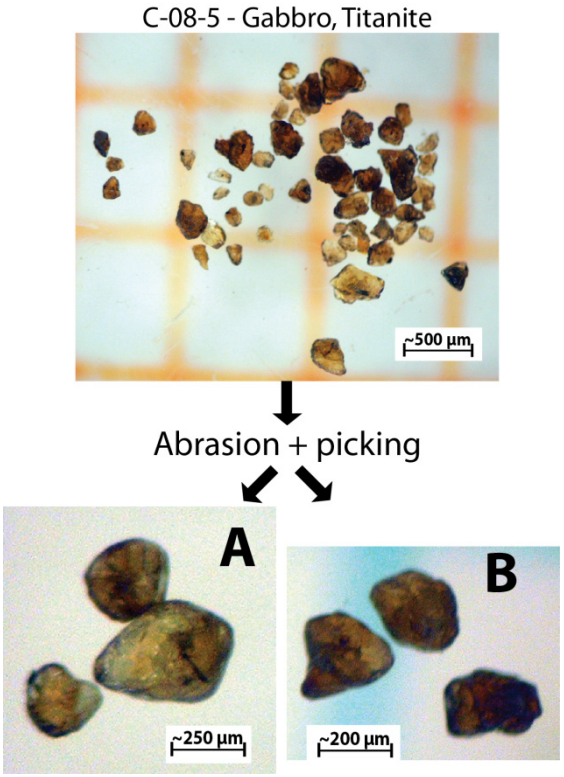

Fig. 65. ***Titanite. Sample C-08-5: Gabbro.*** *The titanite were separated based on their color, one group (A) with slightly paler and the other with slightly darker color (B). The picture above shows the un-abraded titanite, while the two pictures below there they are abraded and selected in to these sub-groups.*

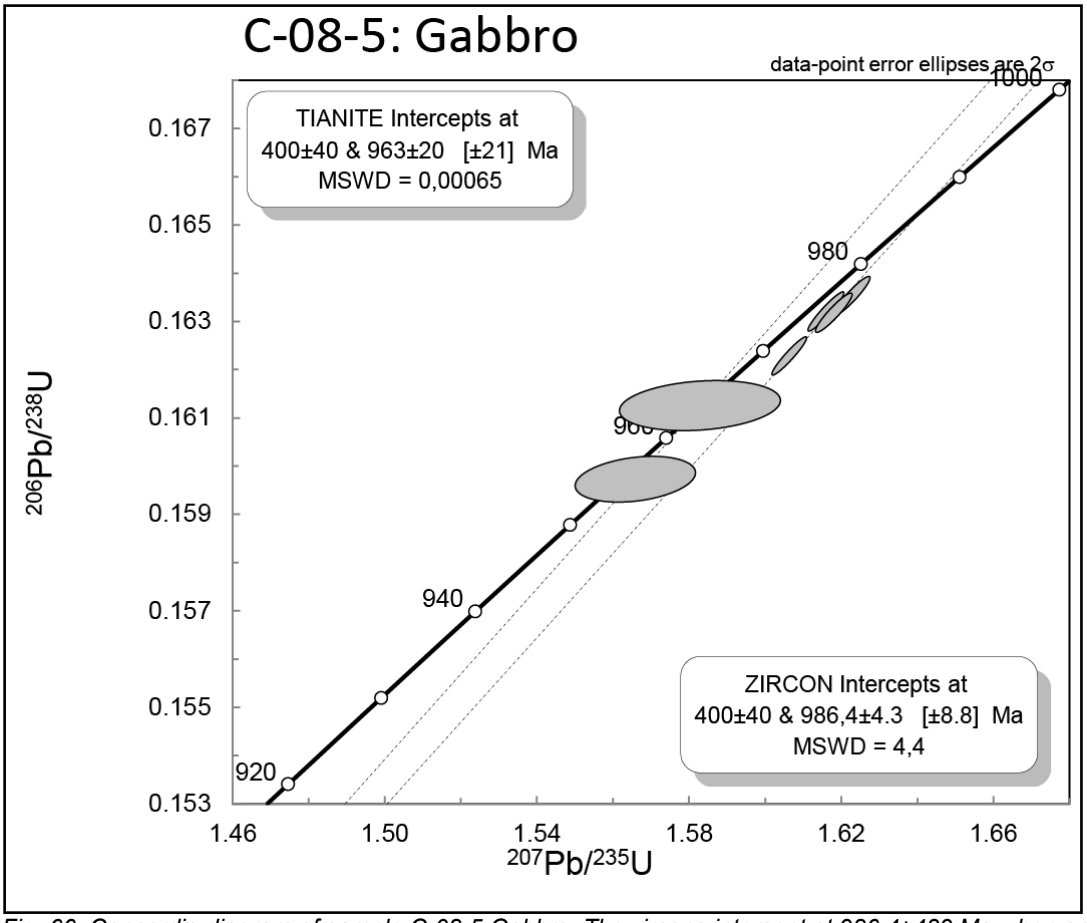

Fig. 66. Concordia diagram of sample C-08-5 Gabbro. The zircons intercept at 986.4±439 Ma when anchored to Caledonian orogeny at 400 Ma. Two titanite values have an age of 955.2 ±2.3 Ma and 963.8 ± 2.5 Ma, which intercept at 963±20 Ma when anchored to Caledonian orogeny, 400 Ma.

Fig. 66 represents the analytical measurements for the gabbro. The four zircons are discordant and had to be anchored to the 420Ma Caledonian orogeny event due likely lead to loss, else they displayed a high margin of error. The corrected interception displays an age of 986.4± 4.3 Ma. The two titanite in sample, were one of them were quite concordant and the other was bit more discordant. The age of the two grains were 955.5 ±2.3 Ma and 963.8±2.5 Ma, which intercept at 963±20 Ma when anchored to Caledonian orogeny, 400 Ma.

4.6 Datasheet Mass spectrometer

Fraction Analyzed	Weight [ug]	Pbt] [ppm]	U [ppm]	Th/U	Pbc [ppm]	Pbcom [pg]	206/204	207/235	2 sigma [abs]	206/238	2 sigma [abs]	rho	207/206	2 sigma [abs]	206/238	2 sigma [abs]	207/235	2 sigma [abs]	207/206	2 sigma [abs]	Disc. [%]
GRANITE																					
ZIRCONS																					
C-08-4 360/9	41	74	446	0.47	0.15	8.3	21828	1.56427	0.00366	0.15848	0.00033	0.96	0.07159	0.00005	948.3	1.8	956.2	1.5	974.2	1.3	2.9
C-08-4 360/10	13	69	392	0.60	0.00	1.5	35079	1.61438	0.00364	0.16290	0.00032	0.96	0.07188	0.00005	972.9	1.8	975.8	1.4	982.4	1.3	1.0
C-08-4 285/15	14	80	505	0.48	2.63	39.8	1661	1.44336	0.00435	0.14775	0.00033	0.83	0.07085	0.00012	888.3	1.8	906.3	1.8	950.4	3.5	7.0
C-08-4 285/54	4	124	695	0.86	1.12	6.6	4088	1.52389	0.00389	0.15485	0.00033	0.93	0.07138	0.00007	928.1	1.8	939.2	1.6	965.4	2.0	4.2
C-08-4 285/19	7	71	426	0.69	0.80	7.8	3633	1.47154	0.00383	0.15030	0.00032	0.92	0.07101	0.00007	902.7	1.8	918.0	1.6	954.9	2.1	5.9
TIANITE																					
C-08-4 285/S.3	45	48	157	3.19	3.26	152.7	481	1.57077	0.01007	0.16001	0.00039	0.50	0.07120	0.00040	956.8	2.2	957.9	4.0	960.4	11.4	0.4
C-08-4 285/S.2	69	49	171	2.68	3.59	256.0	484	1.58595	0.01099	0.16144	0.00041	0.51	0.07125	0.00043	964.8	2.3	963.9	4.3	961.8	12.2	-0.3
GRANODIORITE																					
ZIRCONS																					
C-11-5 360/1	5	24	125	0.98	0.18	3.0	2184	1.61630	0.00490	0.16322	0.00034	0.79	0.07182	0.00014	974.6	1.9	976.6	1.9	980.8	3.9	0.7
C-11-5 360/2	21	35	190	0.83	0.02	2.4	16683	1.60322	0.00365	0.16203	0.00032	0.95	0.07176	0.00005	968.1	1.8	971.5	1.4	979.2	1.4	1.2
C-11-5 360/12	2	92	502	0.77	0.00	1.9	5467	1.61698	0.00415	0.16323	0.00032	0.86	0.07185	0.00009	974.7	1.8	976.8	1.6	981.6	2.7	0.8
C-11-5 360/4	1	109	589	0.85	0.00	0.9	6724	1.59795	0.00515	0.16154	0.00043	0.88	0.07174	0.00011	965.3	2.4	969.4	2.0	978.7	3.1	1.5
C-11-5 360/3	12	27	149	0.85	0.01	2.1	8392	1.55028	0.00378	0.15669	0.00032	0.93	0.07176	0.00007	938.3	1.8	950.6	1.5	979.1	1.9	4.5
TIANITE																					
C-11-5 360/S.89	34	36	124	2.88	3.43	122.3	356	1.52403	0.01118	0.15652	0.00036	0.33	0.07062	0.00049	937.4	2.0	940.1	4.5	946.4	14.1	1.0
C-11-5 360/S.80	200	41	123	2.90	8.67	1788.6	148	1.45604	0.03435	0.15287	0.00103	0.36	0.06908	0.00153	917.0	5.9	912.4	14.2	901.1	44.9	-1.9
GABBRO																					
ZIRCONS																					
C-08-5 360/6	19	34	183	0.83	0.12	4.3	8286	1.61604	0.00388	0.16322	0.00033	0.95	0.07181	0.00006	974.6	1.8	976.5	1.5	980.6	1.6	0.7
C-08-5 360/7	23	31	163	0.91	0.09	4.1	9370	1.60639	0.00375	0.16230	0.00032	0.95	0.07179	0.00006	969.5	1.8	972.7	1.5	979.9	1.6	1.1
C-08-5 360/8	11	50	260	0.90	0.11	3.3	8932	1.62288	0.00391	0.16354	0.00033	0.93	0.07197	0.00007	976.4	1.8	979.1	1.5	985.1	1.8	1.0
C-08-5 360/11	27	48	258	0.74	0.63	19.7	3643	1.61811	0.00395	0.16319	0.00033	0.93	0.07191	0.00007	974.5	1.9	977.3	1.5	983.5	1.9	1.0
TIANITE																					
C-08-5 360/S.83	49	36	114	3.06	3.85	196.5	303	1.56586	0.01294	0.15974	0.00039	0.28	0.07110	0.00056	955.3	2.2	956.8	5.2	960.2	16.1	0.5
C-08-5 360/S.86	16	40	119	3.28	5.41	91.1	227	1.58287	0.01731	0.16126	0.00042	0.20	0.07119	0.00076	963.8	2.4	963.5	6.9	962.8	21.7	-0.1
PEGMAITITE																					
ZIRCONS																					
C-11-8 360/5	1	42	277	0.45	0.00	0.9	2916	1.39760	0.00540	0.14576	0.00037	0.81	0.06955	0.00016	877.1	2.1	887.9	2.3	914.9	4.8	4.4

Table 10. Data sheet containing all values acquired from the mass spectrometer

5 Discussion

The geological history of Finse is defined by at least two primary events occurring during the Precambrian and the Silurian. The dataset collected in the field and described in chapter 3, is used to discuss the deformation sequence. Evolution of the Precambrian basement is discussed first. The important part is to understand why Phyllite sometimes is appearing stratigraphically above Lower nappe, and also why it is often incorporated into the Lower nappe folding. Comparing the structural observation with the acquired ages, could give a reasonable explanation how this complex and complicated system developed.

5.1 Development of the Basement

According to Bingen et al. (2008b), one of the early phases of the Sveconorwegian orogeny started at 1190 Ma, with an extensional regime, as possibly developed in response to the collapsing mid oceanic ridge. This led to continental bimodal magmatism during 1190 – 1130 Ma, followed by sedimentary basins in the Telemarkia terrane. This terrane collided with Idefjorden Terrane between 1140 – 1080 Ma, as the first phase of the Sveconorwegian orogeny. After this phase, at 1035 Ma, Telemarkian terrane went into a period of crustal thickening, associated with new period with metamorphism. The response to this metamorphism was syn - collisional granitic plutonism.

Bimodal magmatism was a common feature which generated both felsic and mafic lithology from one magma chamber (Bingen et al., 2008b, Brewer et al., 2004). Brewer et al. (2004) suggested that bimodal magmatism in south-Norway developed in response to an extensional setting. Intially a mafic magma would remelt the pre-existing 1.5 Ga – 1.9 Ga felsic crust, and would subsequemtly give both felsic and mafic volcanism.
However this feature might be valid, but this magmatism my not necessarily have developed in response to an extensional setting, at least not documented. When implementing all the data for the granite, granodiorite and the gabbro (Fig. 67), they all fit quite nice along the discordia line, except one measurement. The overall age fits a magmatic bimodal episode occurring at 988.1 ±3.1 Ma, which would be part of the Agder Phase and is defined as the main Sveconorwegian event (Bingen et al., 2008b). However the bimodal time frame discussed by Bingen et al. (2008b) (1190 – 1130 Ma), was older and would have been part of another event.

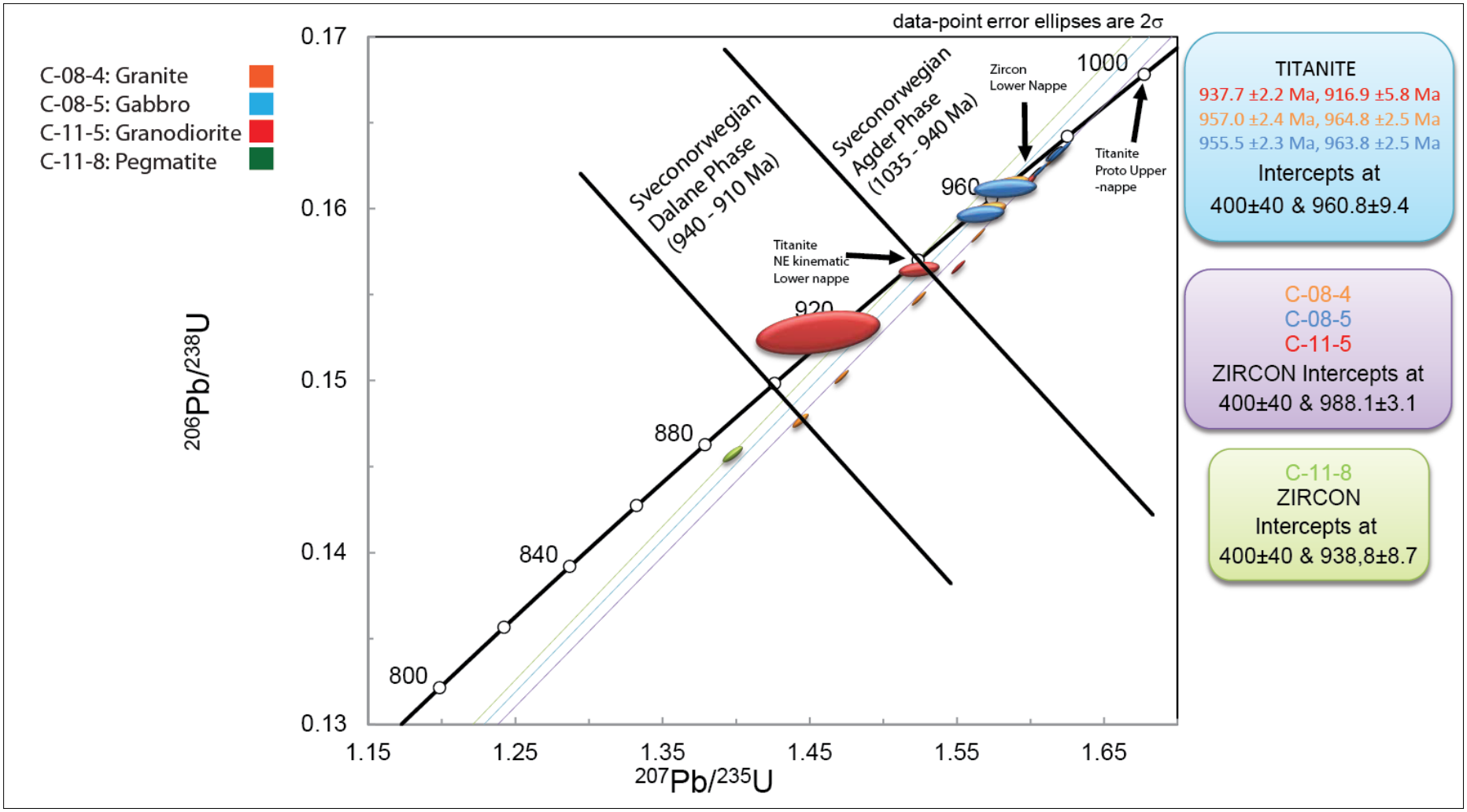

Fig. 67. All values placed into the same concordia diagram. Orange represents: C-08-4 Granite, Darker blue: C-08-5 Gabbro, Red: C-11-5 Granodiorite and Green: C-11-8 Pegmatite. Discordia line for titanite is light blue, all zircons (C-08-4, C-08-5, C11-5) except C-11-8 are light purple and for C-11-8 it is light green. The Sveconorwegian time frame with its different phase are from Bingen et al. (2008b). Lower nappe (volcanic tuff) and Upper nappe ages are from Roffeis and Corfu (2012).

By considering the different lithologies occurring in the basement, very coarse grained and fine grained granodiorite, and the megacrystic granite with feldspar phenocryst, these lithologies has been exposed to different cooling times. Therefore the study area is likely eroded down and exposed the more inner part of a pluton that fed magmatism (Fig. 68). This inner part of the pluton would have had slower cooling and therefore larger mineral sizes, and the border zone would have smaller grain sizes due faster cooling.

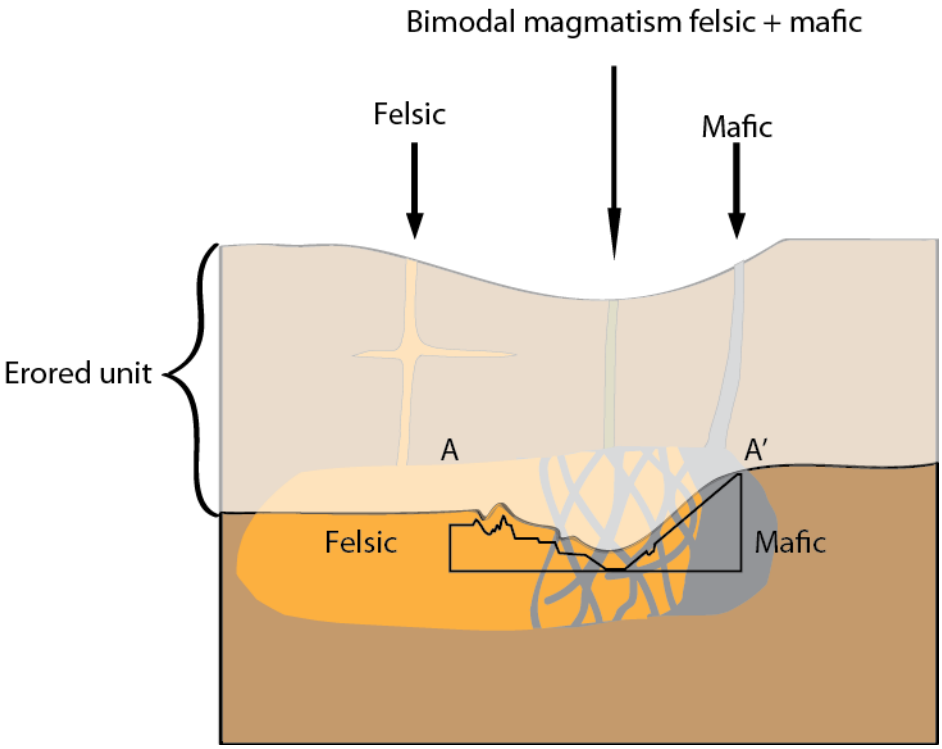

Fig. 68. Bimodal magmatism suggested by Bingen et al. (2008b). The study area has been subjected to erosion for 500 My, which eventually has reveal the more inner part of a pluton from the Sveconorwegian orogeny. But this magma chamber in this pluton has a felsic and mafic part, bimodal, which would correlate to the mafic and felsic dominated area. The intervening area would be the bimodal magmatism which fed both felsic and mafia. The tiny cross section in middle A- A' (Fig. 24) is placed to fit this model with the lithology in the basement. The age for both felsic and mafic lithologies (except dikes) is 988 Ma.

The mafic dominated area containing gabbro, north of Hardangerjøkulen would correlate to mafic magmatism in this model. While the felsic dominated area are correlated to felsic magmatism, the area in middle would both be felsic and mafic as bimodal, which is often observed as intermixing structure.

Titanite acquired from the granite and granodiorite displays two later events occurring at approx. 960 Ma and 920 Ma. The discordia line for all titanite values (Fig. 67) fits a reheating episode at 960.8 ±9.4 Ma when anchored to Caledonian orogeny. Taking into consideration this Sveconorwegian time frame were dominated by magmatism, it is therefore quite likely

the basement (988.1 ±3.1 Ma, both felsic and mafic) have been affected by some later heating in response from magmatism. When considering the thin section it was observed secondary titanite growth around biotite, which means the different titanite ages would correlate to either the primary titanite or the secondary titanite growth. But however there is little evidence to support the exact cause of the 960 Ma and 920 Ma events.

According to Bingen et al. (2008b), post collision magmatism was a common feature developed due to the thinning of the crust, which would reflect the formation of the 940 Ma pegmatite (Fig. 62 and Fig. 67)). This is not the same pegmatite as Fig. 21, but still it is likely this fit with the same time frame. The Dalane extension phase initiates during this 940 Ma time (Bingen et al., 2008b) and might be the reason for the brittle response in the 988.1 ±3.1 Ma basement.

There are at least three generations of intrusion, among them two generations of dikes with preferred orientation where one of the are the 940 Ma pegmatite. Since the mafic and felsic part of the basement both have a 988.1 ±3.1 Ma age, and both lithologies have similar trending structures, it is reasonable to assume that the dikes with same orientation are developed in response to the same event/time (Fig. 69).

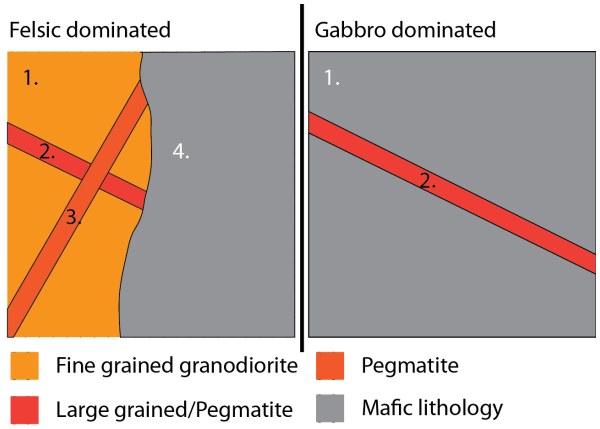

Fig. 69. The different generations of dikes and intrusion. Left pictures represent the felsic dominated part of the study area, north-east at Hardangerjøkulen which would be the primary field area. Including the bedrock, this area represents four different generation of magmatism. The "fine grained" granodiorite (1.) was later intruded by a "coarse grained" dikes oriented NW-SE (2). Later pegmatite cutting the previous structures oriented NE-SW orientation (3). Youngest structure would be the mafic intrusion that cuts all previous structures (4).The right picture represent the mafic dominated area, north side of Hardangerjøkulen. The gabbro (1) is cut by pegmatite (2) oriented NW-SE.

The development of the felsic areas in the basement:

1. The felsic basement was developed at 988.1 ±3.1 Ma with isolated areas that contains mafic lithology.
2. The coarser grained granite, and locally pegmatite intrudes the fine grained granite with a NW-SE orientation.

3. Another episode of coarse grained granite and/or pegmatite intrudes both the fine grained, and cut the older NE-SW oriented dikes.
4. Mafic magmatism intrudes the older structures as the final development observed.

The development of mafic basement (north of Hardangerjøkulen):

1. The mafic dominated basement developed at 988.1 ±3.1 Ma
2. Pegmatite intrudes the gabbro with a NW-SE orientation.

It is not certain which of these generations the pegmatite with a 940 Ma age is part of. But since it is collected north of Hardangerjøkulen it is likely the first generation dike trending NW-SE, as the dominant observed orientation.
There are several places (Fig. 29) were the dikes have been subjected to a later stress component and either folded or broken off and shared. By analyzing the pictures, it seems to be a nearly north - south stress component that has reshaped the dikes. Dikes folded during the Sveconorwegian orogeny is a possibility, but as the pegmatite is 940 Ma and might represent the oldest generation it is likely that these dikes were still warm enough to respond ductile when the crust get further thinned. A constrictional strain with both extension and contraction, similar to Fig. 70 is another possibility.

The time frame between 940 Ma and the Caledonian orogeny involves mostly erosion and weathering of the 988.1 ±3.1 Ma basement. The orogen will eventually be eroded down to a relative flat peneplain and subsequently weathered due to arid climate. This weathering feature gives the rusty red surface as observed repeatedly in the study area.
The titanite for the different samples displays a reheating episode long before the Caledonian orogeny. Besides causing some lead loss in both zircons and titanite (Appendix 6) there has been minimal heat changes in response to Caledonian orogeny, which means it likely this event have caused little deformation to the basement. At the north side of Hardangerjøkulen, Locality 1 is the only proof that the basement actually has been deformed. Since this fold appears to have a NW kinematic direction, its most likely part of the same system developing NE-SW trending fold-axes in the Lower nappe, discussed in chapter (5.2.6).
Faults and the fluctuating topography in the basement are further discussed in chapter 5.3.

5.2 Development of the allochthonous nappes and infolded Phyllite

5.2.1 Proto Upper nappe

The zircon and titanite age for the Upper nappe unit are respectively 1674 ± 17 Ma and 1021 ± 49 Ma (Roffeis and Corfu, 2012) . According to Bingen et al. (2008a), the first formation age would correlate to the Transcandinavian Igneous Belt (TIB) that developed from 1.86 Ga to 1.66 Ga. The 1021 Ma metamorphic age correlates to the Sveconorwegian overprint.

5.2.2 Proto Lower nappe

The different terranes developed during either Gothian or Telemarkia accretion are characterized by pre-sveconorwegian magmatism and interlayer clastic sediments. Also sedimentary basin have been discussed to exist during the Arendal phase (1140 – 1080 Ma) and Agder phase (1050 Ma) (Bingen et al., 2008b).

The Lower nappe consists of carbonate, mica rich layers and volcanic tuff, among other (See chapter 3.2.3.1). The different lithologies could be evidence that this is derived from a proto-sedimentary basin. But the sedimentary basin Bingen et al. (2008b) discussed, is far older than the 997.3 ± 3 Ma volcanic tuff, (Roffeis and Corfu, 2012).The volcanic tuff evidence means it must have deposited in either a basin or on the basement with preexisting sediments (Bingen et al., 2008b). The carbonate in this lithology supports the theory that this is either part of the clastic sediments or derived from a proto basin. Based on the existence of basin and the magmatic activity during the Sveconorwegian orogeny, it is likely that the Lower nappe is a meta sedimentary rock derived from a proto basin. But however, should not disregard that some rock type in the stratigraphy might be igneous due to the ongoing magmatism. So there also a chance the Lower nappe are a combination between meta-sedimentary and meta volcanic rock. As Sveconorwegian orogeny involved magmatism in form of plutons (Bingen et al., 2008b), these would affect the basin by adding volcanic tuff. The age of the volcanic tuff fits with a time frame during the Agder Phase (1050 Ma – 980 Ma) (Bingen et al., 2008b).Since this volcanic tuff and the granite (988.1 ±3.1 Ma) are almost the same age, it is unlikely that the basin with the volcanic tuff accumulated on this particular basement, but more likely later, and was then thrusted on top.

5.2.3 Proto-Upper nappe collision

Phyllite as very often incorporated into the fold structure (Fig. 48), has to be at least as old as the titanite age, 940 Ma for the Lower nappe (Roffeis and Corfu, 2012). This contradicts the general knowledge that this phyllite is Paleozoic and acted as a Paleozoic décollement zone to the Caledonian orogeny (Andresen and Færseth, 1982, Möller et al., 2007, and more). Therefore, two generations of phyllite have to exist in the study area, one deformed during 940 Ma (Phy1), and the other during the Caledonian orogeny, 420 Ma (*Phy2*). If this is the case, proto Upper nappe was thrusted on top of proto- Lower nappe with overlaying *phy2*, long before the Caledonian orogeny. The titanite age 1021 ± 49 Ma (Roffeis and Corfu, 2012) in the Upper nappe, reflects that this was deformed during the Sveconorwegian orogeny. However this is an older deformation age than the formation of the zircon in the volcanic tuff, which means it contradicts this "thrusting proto Upper nappe" model. But since the margin of error is quite large (± 49 Ma), it is still possible that the thrusting of proto Upper nappe is part of the collisional Agder Phase (1050 – 980 Ma), and occurred short after development of the proto Lower nappe unit. Since the Falkenberg phase (980 – 970 Ma) is primarily recorded in Eastern segment high pressure metamorphism it would not be related to this thrusting (Bingen et al., 2008b).

5.2.4 Sveconorwegian Extensional phase

The 940 Ma titanite age of the volcanic tuff lithology (Roffeis and Corfu, 2012) fits the time-frame during the extensional Dalane phase (970 Ma to 900Ma) (Bingen et al., 2008b). It is therefore likely that this phase has developed the structures in the Lower nappe as roughly seen today. The age was acquired from a NE verging (NW-SE trending fold-axes) Lower nappe unit. Bingen et al. (2008b) has discussed similar trending features in the Eastern segment and Idefjorden Terrane (Fig. 1). Structures at Idefjorden that are trending N-S to NW-SE are dated to 1046 ±6 Ma and 1026 ±5 Ma (Söderlund et al., 2008, as cited in Bingen et al., 2008b), this reflects an event that is slightly older than the study area. On the other hand the Eastern segment is also characterized by E-W to WNW-ESE trending folds, the zircon age of the latter direction are 976 ±7 Ma (Möller et al., 2007). These would be developed earlier than the volcanic tuff zircons in the study area. However, Möller

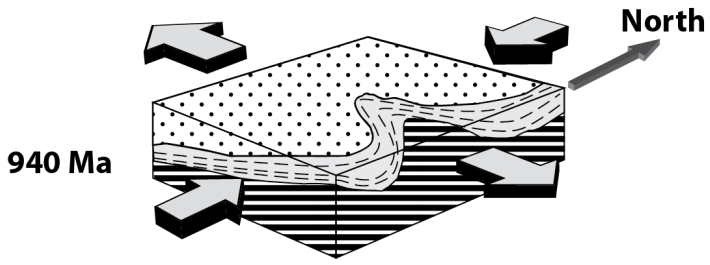

Fig. 70. Constrictional strain. N-S shortening and E-W extension (modfied from Chauvet and Séranne, 1994)

et al. (2007) discussed the possibility that these structures developed due to N-S shortening and E-W extension (constrictional strain) (Fig. 70).

Eastern segment reflects to some degree a different geological setting than Telemarkia terrane. But both are discussed to involve exhumation and doming of gneiss structure (Bingen et al., 2008b, Möller et al., 2007). During the thrusting of proto Upper nappe, it is likely that the proto Lower nappe unit was to some degree folded in response to the collision. The later 970- 940 Ma, Dalane phase involves exhumation that subsequently led to extension and gravitational collapse (Bingen et al., 2008b, Bingen et al., 2006). Structures, like folds developed during this phase, superimposed on the pre-existing folds developed in the proto-Lower nappe, and would gradually changes the fold towards a *gently inclined* geometry. As the stereonet representation illustrates (Fig. 36), and also observed in the field, the majority of folds are *gently inclined* with nearly horizontal axial surface. Some of these could also be characterized as *recumbent*. Any pre-existing sediments will get involved in this event and get incorporated into these folds as the meta-sedimentary phyllite. Bingen et al. (2008b) suggests an N-S to NE-SW directed extension (orogen parallel) in response to the first stage of the doming between 970 Ma and 940 Ma in the Telemarkia terrane. This fits with the NE kinematic directions in the study area. Although Möller et al. (2007) has discussed constrictional strain as a possibility for slightly similar trending fold-axes, it is still quite uncertain what the cause for developing these folds. Harris et al. (2002) discussed development of folds in an extensional setting, and suggested that recumbent folding developed during regional extension in the deep crust. Taking into consideration that Lower nappe (and also Upper nappe) has mylonitic fabric developed due to a ductile deformation, it would therefore (per definition) have been developed at 10 – 15 km depth and between 250°c - 350°C (Twiss and Moores, 2007). So the assumption from Harris et al. (2002) could be correct and the Lower nappe are likely to be developed in deep crust (10 -15 Km).

The developments of the folds in the study area could be illustrated in a model (Fig. 71).

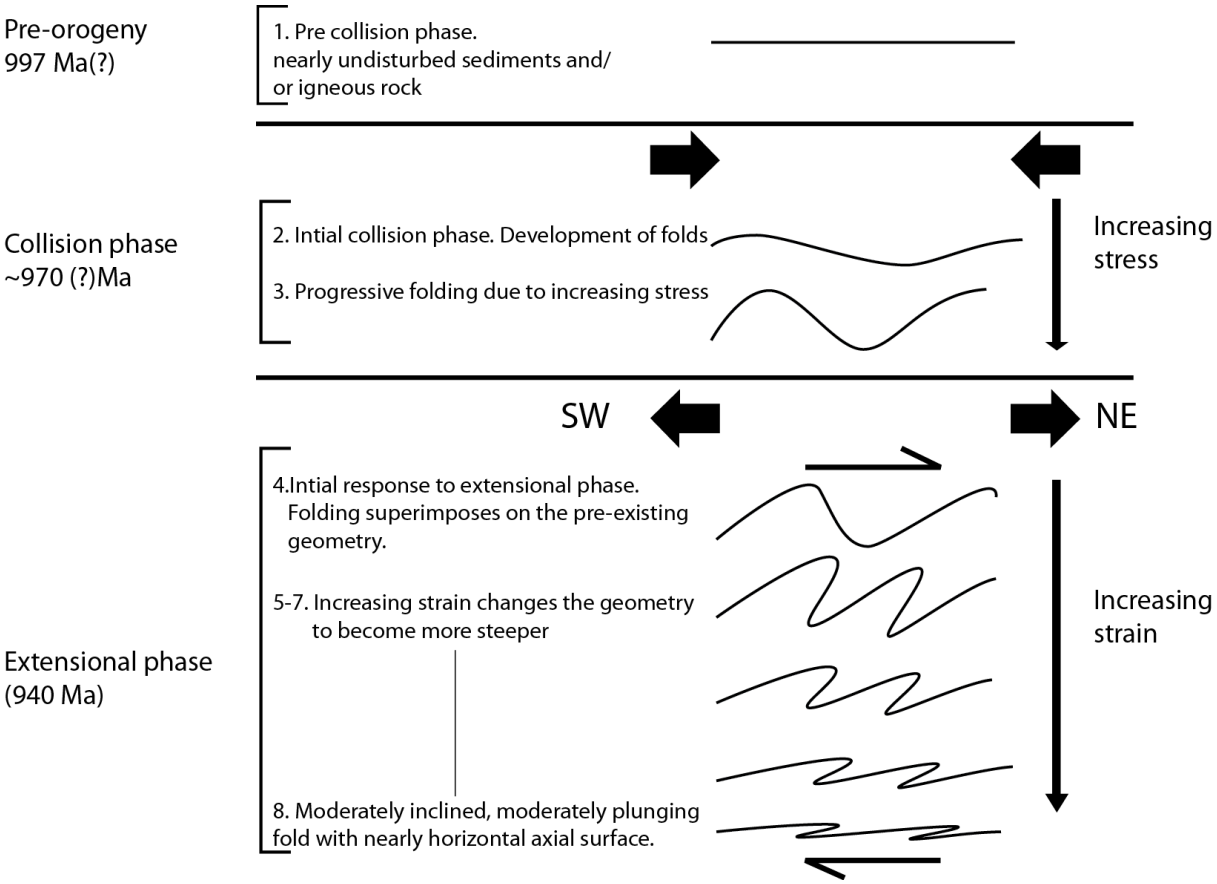

Fig. 71. The extensional model explains the development of the recumbent structure in the study area. The collisional phase, approx. 1000 Ma involves the thrusting of proto Upper nappe on proto Lower nappe unit. Fold structures in Lower nappe are likely to have developed in response to the collision. The later extensional phase 940 Ma (Bingen et al., 2008b), would develop new fold geometry that superimposes on the pre-existing folds, and changes gradually towards a recumbent geometry possibly due to increasing constrictional strain.(The Sveconorwegian time frame are based on Bingen et al. (2008b). The 997 Ma pre-orogeny time, are based on the volcanic tuff age acquired from Roffeis and Corfu (2012). Illustration is based on Harris et al. (2002, Fig 10)).

The **first** phase, could be given the notation ***D1***, and would be part of the thrusting of the Upper nappe unit on top the pre- Lower nappe unit, approx. 1000 Ma. **Second** and **third** phase, the geometry of fold would be the response to the increasing stress. **Fourth** phase would be given the notation ***D2***, and is the initial phase of the extension, approx. 940 Ma. A new stress direction superimposes on the pre-existing folds, and changes the geometry. With progressive increasing strain, the folds become steeper and eventually *gently inclined* or *recumbent* at the last **(eight)** phase.

The geometry of the folds in this model (Fig. 71) can be compared with the folds in the field.

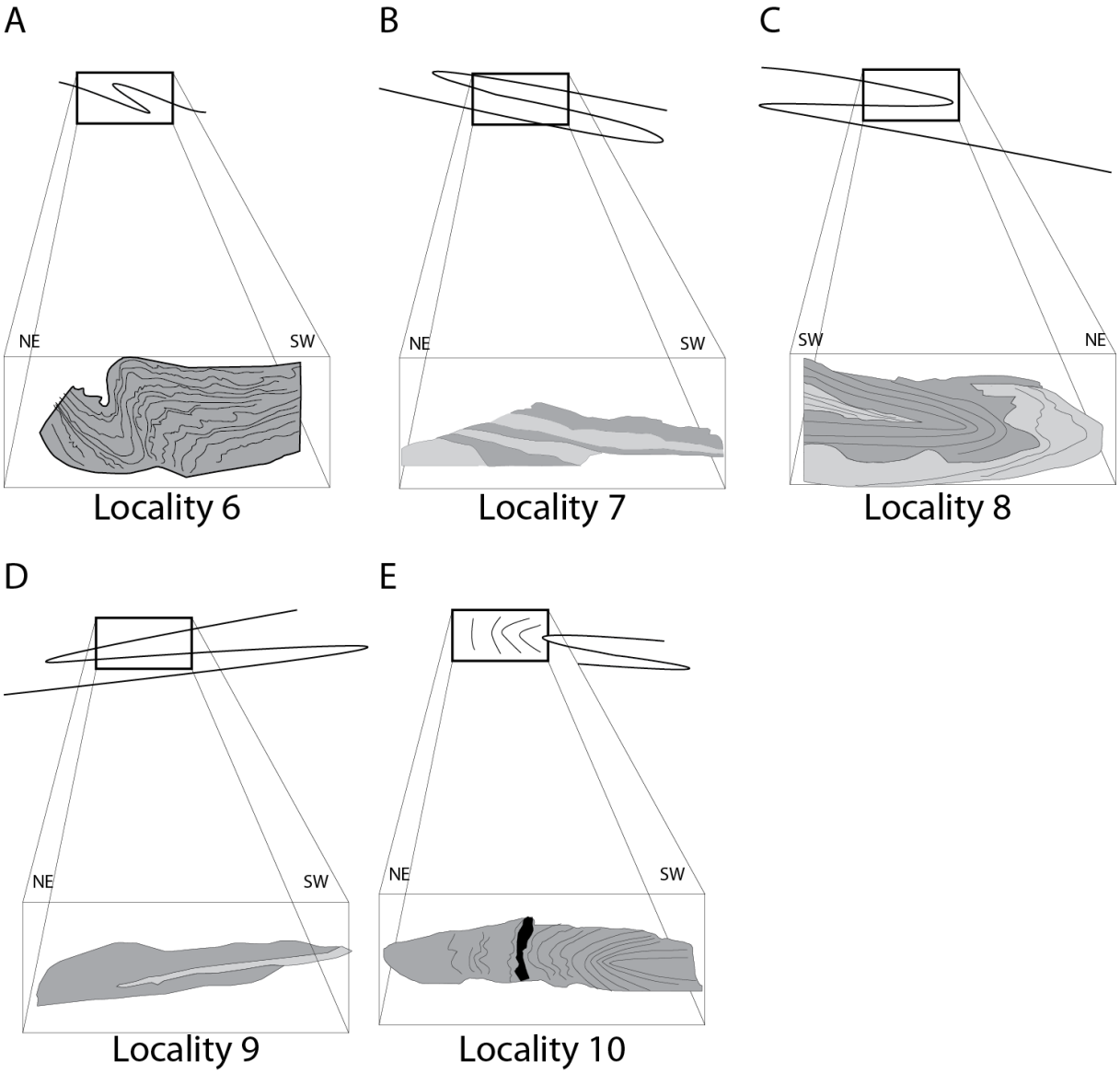

Fig. 72. Illustration is a projection of the different folds observed in the study area to the black square in behind, and compared with the model (Fig. 71). The projected line represents Lower nappe, and would be the darker part that represents folds in the study area. The lighter part would be Phyllite. ***A****. Fold at locality 6 correlates to phase 6* ***B.*** *Structure at locality 7 correlates to phase 8.* ***C****. Fold at locality 8 correlates to phase. 8* ***C****. Structure at locality 9 correlates phase 8.* ***D****. Structure at locality 10 correlates to phase 8.* ***E.*** *Fold at locality 10 correlates to phase 8.*

At **locality 6**, (Fig. 72 A) the fold geometry represents number 6 of the model (Fig. 71 phase 6). **Locality 7**, (Fig. 72 B) there were observed three "layers" of Lower nappe, and two "layers" of Phyllite. These "layers" are part of *gently inclined* fold, and represents the last step of the model (Fig. 71 phase 8). The outcrop exposes the central part where the Lower nappe has folded two times, and three limbs are exposed. Incorporated Phyllite in the folding structure gives the impression that there are three "layers" of Lower nappe, and two "layers" of Phyllite.

Locality 8, (Fig. 72 C) is also part of the last phase (Fig. 71 phase 8) of the model. But at this outcrop, only the fold hinge of the fold is exposed.

Locality 9, (Fig. 72 D) shows only two limbs of the folding and no axial surface. Incorporated Phyllite would appear to wedge out, as the axial surface would be quite near. This would also correlate to the last *recumbent* phase (Fig. 71 phase 8).
Locality 10, (Fig. 72 E) is the front part of the *recumbent* folding, where the steep dipping parts of the Lower nappe foliation is gradually becoming more horizontal towards the axial surface. This would also correlate to the last phase with *recumbent* geometry (Fig. 71 phase 8).

The Lower nappe appears at different topographical altitudes with almost 200 meters differences from highest to lowest point. This means the folding is not fixed to an absolute altitude. The cross sections (Appendix 4 & 5) show exactly this. The fold structure would propagate from SW at higher altitude and gradually decrease towards NE and eventually touch the basement and break up into lenses. This feature is seen in Locality 11, where the Lower nappe is broken up and into smaller lenses and in contact with the basement. This means the propagation of the Lower nappe is therefore "dipping" downwards towards the kinematic direction, NE.

5.2.5 Lithological mirror image

The east and the west side of Middalen glacier display almost a perfect lithological mirror image. As the west side there abundant amount of Lower nappe with layering of Phyllite, the east site are quite opposite. The two cross-sections, Appendix 4 & 5 show exactly this difference. On east side the Lower nappe fold appearing just as a thin layer, in a Phyllite dominated area, while the West side the Lower nappe are a lot thicker and dominates the lithology. The cross-section at Append 6 is and interpretation of this phenomena. This NW-SE direction is parallel to the (NE-SW) fold-axes in the field. So folding and also faulting is not taken into consideration in this cross section. The two areas where all lithologies are stippled are the two glaciers and extrapolated area.
In the cross section this mirror image is interpreted as a wedging out effect, as moving from SE towards NW the Lower nappe thins out, but simultaneously the Phyllite increases in thickness. This effect also occurring opposite, when looking in the NW to SE direction the Lower nappe increase in thickness and Phyllite thins out.
What the exact cause of this wedging out effect is not known. But at least, it is most likely developed during the Sveconorwegian time frame, probably during Dalane phase when the NW-SE trending fold axes were developed.

5.2.6 Multiple kinematic directions

The fold vergence observed in the study area has two primary kinematic directions, towards NE with fold axes trending NW-SE and towards NW with fold-axes oriented NE-SW. The third direction is towards SW ([ca]) and with fold axes oriented NW-SE, and analyzed in the Upper nappe. Since data related to the Upper nappe are very limited, it is very difficult to know if the SW verging folds are local (parasitic) features or more wide spread or appearing in whole stratigraphic unit. Taking into consideration that locality 3 (Bukkaskinnshjallane) which is also Upper nappe, appears to have NE ([ca]) verging folds, this last direction is not taken into consideration. By creating an illustration based on all fold-axes and beta-axes for both Phyllite (Table 6 and Fig. 32) and Lower nappe (Table 8 and Fig. 35), it is possible to compare the behavior of the two lithologies relative to the area.

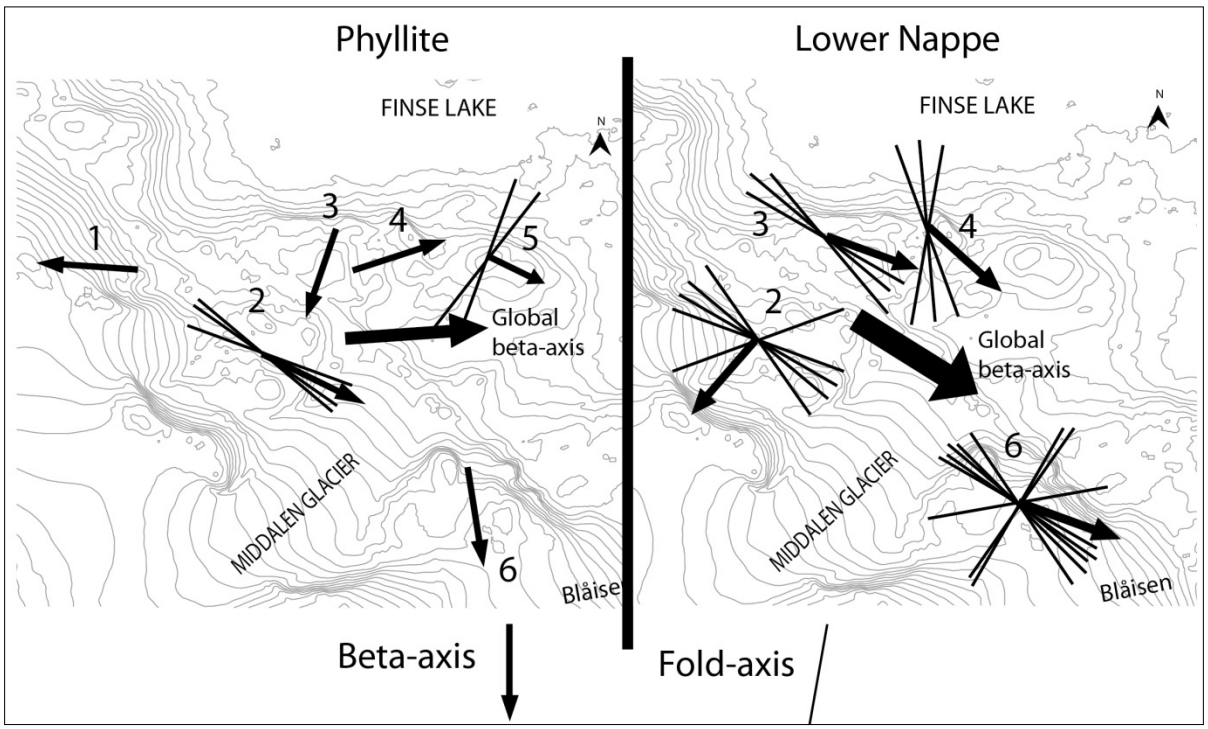

Fig. 73. Beta-axes and fold –axes orientations for Lower nappe and Phyllite. The beta-axes are calculated by stereonet software, while the fold axes are from field measurements. Note the fold-axes don't have any arrow because it is measured in two directions, while the beta-axes are pointing towards the plunge, and not the kinematic directions. Left: Lower nappe fold-axes measurements are compared with beta-axes calculations. Right: Phyllite fold-axes measurements compared with beta-axes measurements.

The Phyllite (Fig. 73, left) has been affected by a super imposed stress regime that changes it towards the global beta-axis orientation, 086/04 (east). But the system doesn't change homogeneously towards this direction since there are many inconsistencies. Number 1 and the global beta-axis are opposite from each other, and number 3 has a totally different beat-axis compare to nr.2 & 4. Number 5 the beta –axis is totally different to the fold-axes. The impression is a counterclockwise rotation from number: 1 - 2 - 6 and then global axis. While number 4 nearly does fit the global axis, number 5 is slightly more different and number 3 is

totally different. However, with a counterclockwise rotation number 3 would match the global axis, but this rotation is more difficult to fit at number 5. By comparing beta-axes and fold-axes for both Phyllite and Lower nappe (Fig. 73 left and right), there are a lot of inconsistencies. The Phyllite beta-axis calculations for number 3 and 4 don't match any of orientations of either fold-axis or beta-axis. At number 2 for Phyllite, both beta-axis and fold-axes are trending in same directions, which are also the case for Lower nappe, number 2 were the majority fold-axes are the same as Phyllite, expect the beta axis. The single Phyllite beta-axis orientation, number 6 is the same for few of the Lower nappe fold-axes orientations for the same number. It is very obvious that most of these areas have been subjected to a secondary folding, due to the rotating fold-axes and inconsistency between beta-axes and fold-axes. The Lower nappe (Fig. 73, left) displays a more consistency between fold-axis and beta-axis calculations. The majority of fold-axis are trending NW-SE, and as illustrated the calculated beta values are mostly trending towards SE, except at number 2 (Lower Nappe). Taking into consideration that there are fewer measurements for Phyllite, and this unit does not display the same consistency which means the Lower nappe is a stronger unit and did not respond so easy to deformation.

The two kinematic directions and the knowledge about the changing fold-axes, it appears to be a "border" between the NE and NW direction. This border would represent a contact zone between the two kinematic directions, and would follow from locality 12, locality 7 to locality 13, which roughly equals number 6, 2 and 4 (Fig. 32 and Fig. 35). This kinematic contact zone is interpreted in Fig. 74. Regardless that there are few NW oriented lithologies in a basement dominated area it still appears to be a consistency. At the north-east side of the kinematic contact zone are dominated by lithology oriented to NW, and vice versa further to the South West, West of the contact zone would represent lithology oriented towards NE.

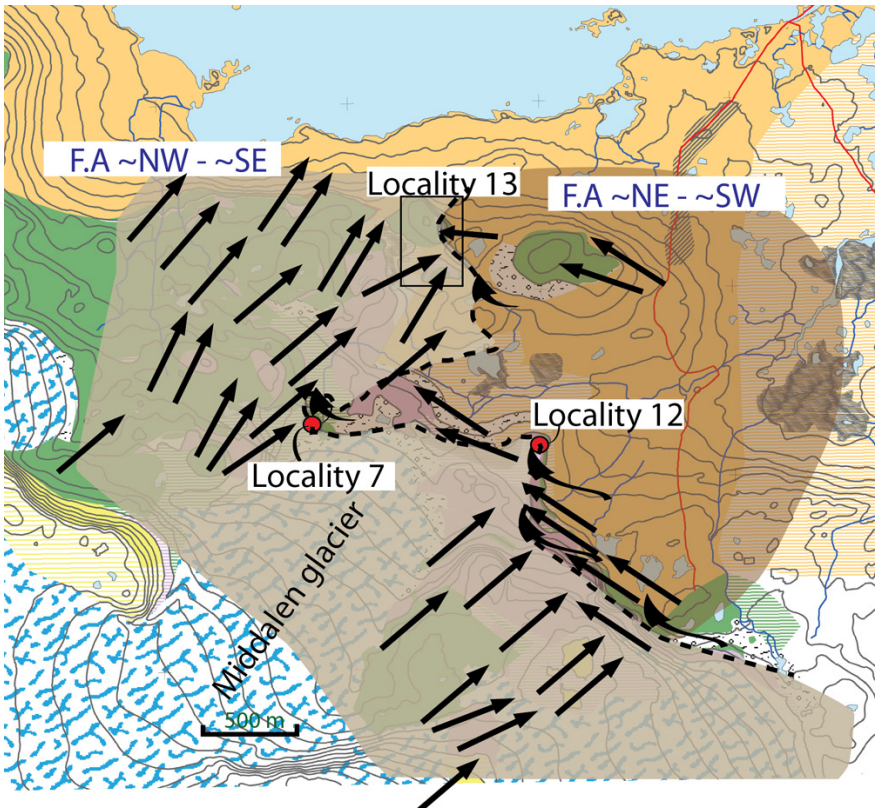

Fig. 74. The two kinematic directions as observed in the field. The majority has NW-SE trending fold axes (F.A) which are verging towards NE, and the other is NE-SW and verging towards NW. The kinematic contact zone, stippled line goes through locality 12, locality 7 and locality 13.

At **locality 7** is very obvious that the NE-SW trending folds have been superimposed on the older NW-SE trending folds. The "layering" represents part of *gently inclined* (Fig. 71) fold now being folded again, perpendicular to the older NW-SE trending folds. The fold axis are 35° - 215° (NE-SW), and the kinematic direction is towards NW.

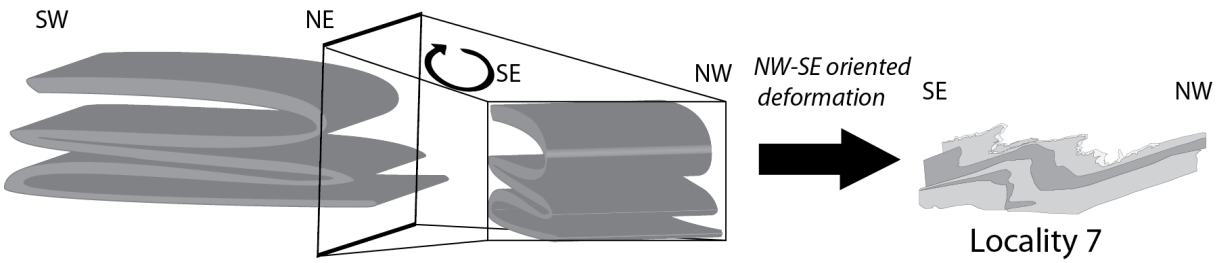

*Fig. 75. **Locality 7**. This locality displays secondary superimposed deformation on the older gently inclined folding. The older NW - SE fold-axes are being subjected to an earlier deformation that deforms the fold-hinges and developed a new fold-axis trending NE-SW with vergence towards NW. The illustration shows first the gently inclined folding as regularly observed in the study area. Perpendicular to the fold, looking almost parallel to the fold-axis would represent the outcrop not subjected to the secondary deformation, which later deforms it as the final stage.*

Fig. 75 illustrates just this development. First the folding with NW-SE fold axes is affected by a secondary and later deformation perpendicular to the previous fold system, and superimposes NE-SW trending fold axes. This new fold generation has a different geometry and defined as *gently inclined*.

The NW kinematic direction represents a different stress regime, it could either be still part of 940 Ma extensional phase or it could be part of the 410 Ma Devonian extension, since the NW kinematic direction is the same as the direction discussed by Fossen (1992).
Whether it is part of the 940 Ma or the 410 Ma event, in both cases there are some dilemmas to support either time frames:

- By assuming that the NW kinematic direction (NE-SW folds-axis) was developed in response to the post- Sveconorwegian orogeny, there would be little structurally evidence from the extensional phase (D4) in the study area. Fossen (1992) has discussed the existence of the S-C structures as a proof of the superimposed Devonian extension. These structures with some uncertainty might have been observed, but not measured. But however the superimposed extensional phase (D4), brings little evidence of its existence, and would therefore only be observed down to centimeter scale in form of these S-C structures.
- By assuming the NW kinematic direction (NE-SW folds-axis) are developed during the 410 Ma Devonian extensional phase. Two deformation events nearly 500 My apart interacts with a relative sharp contact. This would either be some sort of an unconformity or this extension underwent in an inhomogeneous fashion and left several areas unaltered.

5.2.7 Caledonian orogeny

At 420 Ma the Caledonian orogeny initiated as the final thrusting. During this phase the whole Upper nappe/Lower nappe unit got thrusted on top of the 988.1 ±3.1 Ma basement with overlaying Paleozoic sediments. Based on the 940 Ma titanite age in the Lower nappe unit and the ~1000 Ma titanite age for the Upper nappe (Roffeis and Corfu, 2012), the Caledonian orogeny did little internal deformation to these units.
During the Devonian,410 Ma, the Caledonian orogeny entered a extensional phase due to gravitational collapse (Koenemann, 1993, Fossen, 1992). Taking in to consideration, that there is no documented oblique Sveconorwegian extension that subsequently would rotate from NE to NW, and regardless of the NW directed features that Fossen (1992) observed were part of the Western gneiss region, it is still well documented how the structures responded to Caledonian extension. Since the secondary kinematic system has a NW direction, it is reasonable to assume this is also part of the Devonian extensional system. In

that case it is likely that Devonian extensional overprint has left several units and lithologies more or less unaffected since the majority kinematic direction is towards NE.
However, it is also likely that the two kinematic directions are hidden to each other since they are perpendicular. Therefore each outcrop that displays folding would be parallel to the other trending fold-axes. So a secondary overprint cannot be observed in the NE-SW oriented outcrops. Al though the east side displays a primarily Sveconorwegian extension in form of NW-SE trending fold-axes, it therefore still possible that it has been affected by some degree by the Devonian extension.

A graphical model that illustrates the different deformation events through time could be seen in Fig. 77.

5.3 Younger faults

The faults cutting both the basement (Fig. 27) and the overlaying units are located between "Blåisen" and Middalen glacier, and some are observed to have different and opposite displacement relative to the other. It appears that the cliff represent a small scale graben structure (Fig. 76) where normal faults displaces basement and overlaying unit downwards towards both SE and NW. In the middle would be an interpreted horst structures.
Nevertheless the general orientation of the faults would co-exist a NW-SE extension, it superimposes on the lithologies with fold axes trending NE-SW which means it has to be younger than Devonian. In this case it is not certain what time frame and event that has caused these faults.

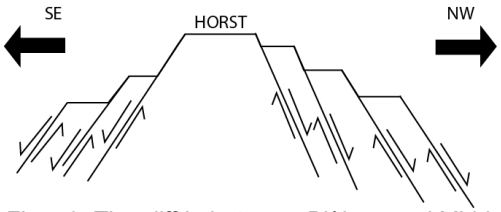

Fig. 76. The cliff in between Blåisen and Middalen glacier (Fig. 27) represent faults with different displacements, and could represent a small scale graben structures. From each side of the interpreted horst structure the blocks a displaced downwards, as observed in field.

Taking into consideration that the basement was folded with a NW kinematic direction, it is reasonable to assume that the same Devonian extension has affected both the basement and the Lower nappe. However, it is not certain if these apparently younger faults have developed the fluctuation in the basement, or it is developed in response to the Devonian extension.

5.4 Map and Cross section

Appendix 4 & 5 represents a cross section for, respectively, the east and west side of Middalen glacier. As illustrated, Lower nappe is folding with a kinematic direction towards NE, and with geometry as *gently inclined*, almost *recumbently*. The incorporated Precambrian Phyllite is very distinct in these illustrations, but it is not known where the contact between the Paleozoic and the Precambrian phyllite is.

The cross section is based on the *gently inclined* fold geometry observed in the field. This geometry is extrapolated for every fold on the cross-section. At **Locality 11**, the Lower nappe folding touches the basement, and is also a feature used when extrapolating the folds limbs at the NE side.

The map is constructed based on observations and measurements. Besides the stippled colors, which represent extrapolated areas, there isn't any extrapolation among the solid colors. This map represents a lot of small scale feature, as Lower nappe or Phyllite tends to be exposed on a very small area. These features are mostly lost when printing the map with a higher resolution. The contacts between the different lithologies were often obscured by glacial debris, and this is the reason why the majority of the contacts are stippled.

5.5 Graphical model

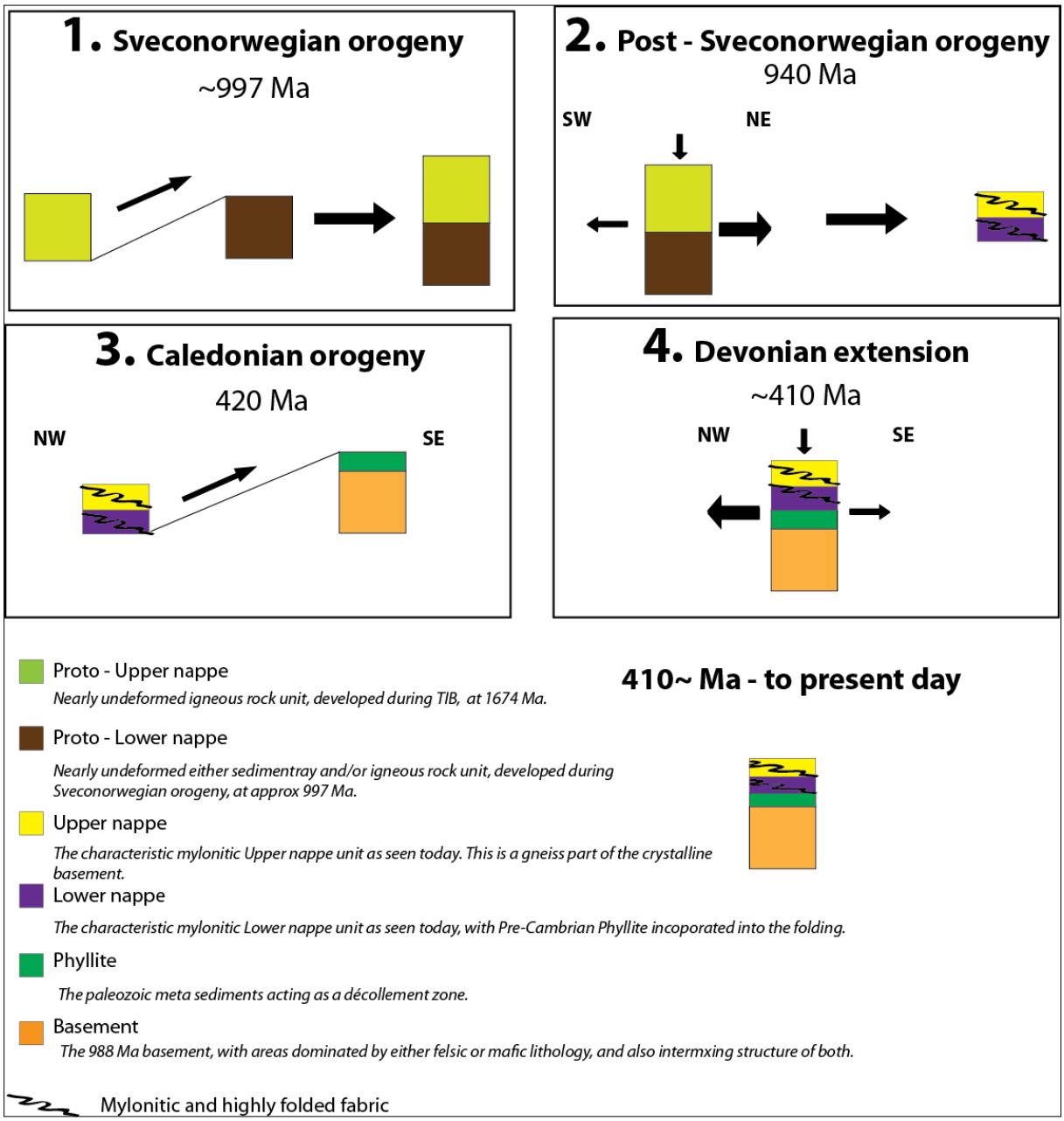

Fig. 77. A simplified graphical model showing the different deformation stages from pre-sveconorwegian to post Caledonian orogeny. Proto upper & -Lower nappe represents the undeformed rock type, as igneous or sedimentary rock. This model represents only the development of the allochthonous nappe, and not the basement. ***First*** *stage, approx. 997 Ma is the thrusting of proto- Upper nappe on proto-Lower nappe.* ***Second*** *stage is the 940 Ma extensional phase, Dalane involving gravitational collapse. This phase develops folds with nearly horizontal dip of the fold-axes plane.* ***Third*** *phase is the Caledonian orogeny, where the Upper nappe/Lower nappe unit gets thrusted on top of the 988 Ma basement.* ***Fourth*** *phase is Devonian extension which superimposes a NW kinematic direction on the older Sveconorwegian folds. Except massive erosion and weathering there would be little difference between the rock units at 410 Ma and today. (Sveconorwegian time frame and its phase are from Bingen et al. (2008b). The proto Upper and -Lower nappe ages are from Roffeis and Corfu (2012). Caledonian extensional phase are based on Fossen (1992)).*

6 Conclusion

Basement

The study area is dominated by two lithologies, mafic and felsic types which were developed at 988.1 ±3.1 Ma during Sveconorwegian orogeny. The felsic lithologies are granite with phenocryst of feldspar, and coarse and fine grained granodiorite. The mafic lithology is either amphibolite or gabbro. Intrusion of pegmatite at 940 Ma develops dikes often with preferred orientation, NE-SW or NW-SE. Superimposed constrictional strain sometimes deformers the folds either in a ductile or brittle manner. Intrusion also occurs as a random mixing feature that don't display any preferred orientations.

Allochthonous nappes and Phyllite

Two informal names are introduced, "Lower nappe" and "Upper nappe" which respectively are part of lower and upper middle allochthon. Lower nappe which is a unit which containing meta-volcanic tuff and carbonate rich and mica rich rock types. Upper nappe would be the crystalline basement. Both have a mylonitic fabric and are very folded, but the Upper nappe has larger grain size and is a gneiss. Lower nappe folds are usually appearing as *"recumbent*" to *gently inclined* with Phyllite in-folded into the structure. This Phyllite has to be the same age or older than the deformation age for the Lower nappe structure.

The east and west sides of Middalen glacier display a lithological mirror image of Lower nappe and Phyllite. The east side is dominated by Lower nappe with "layers" of Phyllite, while the west side is dominated by Phyllite with "layers" of Lower nappe

The majority of fold-axes are trending NW-SE with vergence towards NE, and the secondary orientation trends NE-SW with vergence towards NW. There is a transitional kinematic zone between the two fold-axes orientations were the folds displays a rotation from NW-SE to NE-SW.

Development stages for the basement

1. Bimodal magmatism occurred at 988.1 ±3.1 Ma as part of the Sveconorwegian orogeny
2. Pegmatitic dikes intrude the basement during the Dalane extensional phase.

Deformation stages for the nappes

D1 – Sveconorwegian orogeny

D2 – Dalane extension develops folds with a NE kinematic direction and with incorporation of Phyllite.

D3 – Caledonian orogeny pushes upper/Lower nappe on top of the 988.1 ±3.1Ma basement.

D4 – Devonian extension superimposes a NW kinematic direction in some part of the nappes.

7 References

ALLABY, A. & ALLABY, M. 2003. *A Dictionary of earth sciences,* Oxford, Oxford University Press.

ALLMENDINGER'S, R. 2012. *Stereonet 7* [Online]. Available: ***http://www.geo.cornell.edu/geology/faculty/RWA/programs/stereonet-7-for-windows.html***.

ANDERSSON, M., LIE, J. & HUSEBYE, E. 1996. Tectonic setting of post-orogenic granites within SW Fennoscandia based on deep seismic and gravity data. *Terra Nova,* 8**,** 558-566.

ANDRESEN, A. & FÆRSETH, R. 1982. An evolutionary model for the southwest Norwegian Caledonides. *American Journal of Science,* 282**,** 756.

BERGSTRÖM, J. & GEE, D. G. 1985. The Cambrian in Scandinavia. *In:* GEE, D. G. & STURT, B. A. (eds.) *The Caledonide orogen: Scandinavia and related areas.* Chichester: Wiley.

BEST, M. G. 2009. *Igneous and Metamorphic Petrology*, Wiley.

BINGEN, B., ANDERSSON, J., SÖDERLUND, U. & MÖLLER, C. 2008a. The Mesoproterozoic in the Nordic countries. *Episodes,* 31**,** 29-34.

BINGEN, B., NORDGULEN, O. & VIOLA, G. 2008b. A four-phase model for the Sveconorwegian orogeny, SW Scandinavia. *Norsk geologisk tidsskrift,* 88**,** 43.

BINGEN, B., STEIN, H. J., BOGAERTS, M., BOLLE, O. & MANSFELD, J. 2006. Molybdenite Re-Os dating constrains gravitational collapse of the Sveconorwegian orogen, SW Scandinavia. *Lithos,* 87**,** 328-346.

BRANDER, L. 2011. *The Mesoproterozoic Hallandian event-a region-scale orogenic event in the Fennoscandian Shield*, Department of Earth Sciences; Institutionen för geovetenskaper.

BREWER, T., ÅHÄLL, K. I., MENUGE, J., STOREY, C. & PARRISH, R. 2004. Mesoproterozoic bimodal volcanism in SW Norway, evidence for recurring pre-Sveconorwegian continental margin tectonism. *Precambrian Research,* 134**,** 249-273.

BRUTON, D. L., LIMDSTRÖM, M. & OWEN, A. W. 1985. The Ordovician of Scandinavia. *In:* GEE, D. G. & STURT, B. A. (eds.) *The Caledonide orogen: Scandinavia and related areas.* Chichester: Wiley.

BRYHNI, I. & STURT, B. A. 1985. Caledonides of Southwestern Norway. *In:* GEE, D. G. & STURT, B. A. (eds.) *The Caledonide orogen: Scandinavia and related areas.* Chichester: Wiley.

CAMERON, A. E., SMITH, D. H. & WALKER, R. L. 1969. Mass spectrometry of nanogram-size samples of lead. *Analytical Chemistry,* 41**,** 525-526.

CHAUVET, A. & SÉRANNE, M. 1994. Extension-parallel folding in the Scandinavian Caledonides: implications for late-orogenic processes. *Tectonophysics,* 238**,** 31-54.

CORFU, F. 2004. U–Pb age, setting and tectonic significance of the anorthosite–mangerite–charnockite–granite suite, Lofoten–Vesterålen, Norway. *Journal of Petrology,* 45**,** 1799-1819.

CORFU, F. & GRUNSKY, E. C. 1987. Igneous and tectonic evolution of the Batchawana greenstone belt, Superior Province: a U-Pb zircon and titanite study. *The Journal of Geology***,** 87-105.

CORFU, F., HANCHAR, J. M., HOSKIN, P. W. O. & KINNY, P. 2003. Atlas of zircon textures. *Reviews in Mineralogy and Geochemistry,* 53**,** 469.

DAVIS, D. W., KROGH, T. E. & WILLIAMS, I. S. 2003. Historical development of zircon geochronology. *Reviews in Mineralogy and Geochemistry,* 53**,** 145.

DAVIS, G. H. & REYNOLDS, S. J. 1996. *Structural geology of rocks and regions,* New York, Wiley.

DEMPSTER, T., JENKIN, G. & ROGERS, G. 1994. The origin of rapakivi texture. *Journal of Petrology,* 35**,** 963-981.

DICKIN, A. P. 2005. *Radiogenic isotope geology,* Cambridge, University Press.

DOWNTHEYELLOWCAKEROAD. 2012. *Decay Chains* [Online]. Available: ***http://www.downtheyellowcakeroad.org/html/sciencebasics.html*** [Accessed 04.05 2012].

ESRI.CARTOGRAPHY.TEAM. 2010. *Geologic Mapping Template* [Online]. ESRI. Available: ***http://resources.arcgis.com/gallery/file/map-templates/details?entryID=6AA281F3-1422-2418-8825-C44631AFA8EE*** [Accessed 11.01 2012].

FGDC. 2006. *Final Draft -- FGDC (The Federal Geographic Data Committee) Digital Cartographic Standard for Geologic Map Symbolization* [Online]. Available: ***http://www.fgdc.gov/standards/projects/FGDC-standards-projects/geo-symbol/FGDC-GeolSymFinalDraft.pdf*** [Accessed 14.09 2012].

FOSSEN, H. 1992. The role of extensional tectonics in the Caledonides of south Norway. *Journal of Structural Geology,* 14**,** 1033-1046.
FOSSEN, H. 2010. Extensional tectonics in the North Atlantic Caledonides: a regional view. *Geological Society, London, Special Publications,* 335**,** 767-793.
FOSSEN, H. & RYKKELID, E. 1992. The interaction between oblique and layer-parallel shear in high-strain zones: observations and experiments. *Tectonophysics,* 207**,** 331-343.
GAAL, G. & GORBATSCHEV, R. 1987. An outline of the Precambrian evolution of the Baltic Shield. *Precambrian Research,* 35**,** 15-52.
GARMIN 2012. Garmin Mapsource.
GOOGLE. 2012. *Google Earth* [Online]. Available: ***http://www.google.com/earth/index.html*** [Accessed 15.04 2012].
GORBATSCHEV, R. & BOGDANOVA, S. 1993. Frontiers in the Baltic shield. *Precambrian Research,* 64**,** 3-21.
HAAPALA, I., RÄMÖ, O. T. & FRINDT, S. 2005. Comparison of Proterozoic and Phanerozoic rift-related basaltic-granitic magmatism. *Lithos,* 80**,** 1-32.
HALLIDAY, A. N. 1997. Radioactivity, the discovery of time and the earliest history of the Earth. *Contemporary Physics,* 38**,** 103-114.
HARRIS, L. B., KOYI, H. A. & FOSSEN, H. 2002. Mechanisms for folding of high-grade rocks in extensional tectonic settings. *Earth-Science Reviews,* 59**,** 163-210.
HOSSACK, J. & COOPER, M. 1986. Collision tectonics in the Scandinavian Caledonides. *Geological Society, London, Special Publications,* 19**,** 285-304.
KLEIN, C., HURLBUT, C. S. & DANA, J. D. 2002. *Manual of mineral science,* New York, Wiley.
KOBER, B. 1986. Whole-grain evaporation for 207Pb/206Pb-age-investigations on single zircons using a double-filament thermal ion source. *Contributions to Mineralogy and Petrology,* 93**,** 482-490.
KOENEMANN, F. 1993. Tectonics of the Scandian orogeny and the Western Gneiss Region in southern Norway. *Geologische Rundschau,* 82**,** 696-717.
KROGH, T. 1973. A low-contamination method for hydrothermal decomposition of zircon and extraction of U and Pb for isotopic age determinations. *Geochimica et cosmochimica acta,* 37**,** 485-494.
MATHEZ, E. A. 2004. A Birthstone for Earth. *Natural History,* 113.
MEERT, J. G. & TORSVIK, T. H. 2003. The making and unmaking of a supercontinent: Rodinia revisited. *Tectonophysics,* 375**,** 261-288.
MILNES, A., WENNBERG, O., SKÅR, Ø. & KOESTLER, A. 1997. Contraction, extension and timing in the South Norwegian Caledonides: the Sognefjord transect. *Geological Society, London, Special Publications,* 121**,** 123-148.
MÖLLER, C., ANDERSSON, J., LUNDQVIST, I. & HELLSTRÖM, F. 2007. Linking deformation, migmatite formation and zircon U–Pb geochronology in polymetamorphic orthogneisses, Sveconorwegian Province, Sweden. *Journal of Metamorphic Geology,* 25**,** 727-750.
NIRONEN, M. 1997. The Svecofennian Orogen: a tectonic model. *Precambrian Research,* 86**,** 21-44.
POWELL, C. M. A., LI, Z., MCELHINNY, M., MEERT, J. & PARK, J. 1993. Paleomagnetic constraints on timing of the Neoproterozoic breakup of Rodinia and the Cambrian formation of Gondwana. *Geology,* 21**,** 889-892.
PRESS, F., SIEVER, R., GROTZINGER, J. & JORDAN, T. H. 2003. *Understanding earth,* New York, W.H. Freeman.
PUBLISHING, B. E. & RAFFERTY, J. P. 2010. *Geochronology, Dating, and Precambrian Time: The Beginning of the World as We Know It*, Encyclopaedia Britannica.
RAMBERG, I. B., BRYHNI, I., NØTTVEDT, A., SOLLI, A. & NORDGULEN, Ø. 2006. *Landet blir til: Norges geologi,* Trondheim, Norsk geologisk forening.
ROBERTS, D. & GEE, D. G. 1985. An Introduction to the structure of the Scandinavian Caldedonides. *In:* GEE, D. G. & STURT, B. A. (eds.) *The Caledonide orogen: Scandinavia and related areas.* Chichester: Wiley.
ROFFEIS, C. & CORFU, F. 2012. Correlation of Caledonian crystalline nappes in SW-Norway by means of U-Pb geochronology: old problems and new data. *Unpublished*.

SILVER, L. T. & DEUTSCH, S. 1963. Uranium-lead isotopic variations in zircons: a case study. *The Journal of Geology*, 721-758.
STATENS.KARTVERK. 2012. *Norgeskart* [Online]. Available: ***http://www.norgeskart.no/*** [Accessed 11.01 2012].
STEIGER, R. & JÄGER, E. 1977. Subcommission on geochronology: convention on the use of decay constants in geo-and cosmochronology. *Earth and Planetary Science Letters,* 36**,** 359-362.
SÖDERLUND, U., ELMING, S. Å., ERNST, R. E. & SCHISSEL, D. 2006. The Central Scandinavian Dolerite Group—Protracted hotspot activity or back-arc magmatism? Constraints from U–Pb baddeleyite geochronology and Hf isotopic data. *Precambrian Research,* 150**,** 136-152.
SÖDERLUND, U., HELLSTRÖM, F. & KAMO, S. 2008. Geochronology of high-pressure mafic granulite dykes in SW Sweden: tracking the P–T–t path of metamorphism using Hf isotopes in zircon and baddeleyite. *Journal of Metamorphic Geology,* 26**,** 539-560.
TORSVIK, T., SMETHURST, M., MEERT, J., VAN DER VOO, R., MCKERROW, W., BRASIER, M., STURT, B. & WALDERHAUG, H. 1996. Continental break-up and collision in the Neoproterozoic and Palaeozoic--A tale of Baltica and Laurentia. *Earth-Science Reviews,* 40**,** 229-258.
TORSVIK, T. H. & STEINBERGER, B. 2006. From Continental Drift To Mantle Dynamics. *Geo,* 8**,** 24-39.
TWISS, R. J. & MOORES, E. M. 2007. *Structural geology,* New York, W.H. Freeman Co.
USGS. 2012. *Geochronology* [Online]. Available: ***http://geomaps.wr.usgs.gov/common/geochronology.html*** [Accessed 03.05 2012].
WETHERILL, G. W. 1956. Discordant uranium-lead ages, I. *Transations, American Geophysical union,* 37**,** 320-326.
WILSON, J. T. 1966. Did the Atlantic close and then re-open? *Nature,* 221**,** 676-681.
WINDLEY, B. F. 1993. Proterozoic anorogenic magmatism and its orogenic connections. *Journal of the Geological Society,* 150**,** 39-50.
ÅHÄLL, K. I., BREWER, T., CONNELLY, J. & LARSON, S. 1996. Temporal and spatial relationships between intra-cratonic magmatism and 1.70–1.55 Ga westward growth of the Baltic Shield. *GFF,* 118**,** 5-5.

Appendix 1: Fold axes

Fold Axis	Rock type/unit	Azimuth		GPS Long	GPS Lat	Altitude
1	Phyllite	200	20	417287	6717111	1380
2	Phyllite	218	38	415172	6716247	1371
3	Lower nappe	310	130	416560	6717081	1364
4	Lower nappe	355	165	416437	6717197	1355
5	Lower nappe	340	160	416406	6717141	1347
6	Lower nappe	260	80	417520	6715190	1401
7	Ln + Phyllite	215	35	417571	6715195	1389
8	Lower nappe	240	60	417019	6716210	1373
9	Lower nappe	215	35	416997	6716204	1337
10	Lower nappe	230	50	417005	6716198	1365
11	Lower nappe	240	60	417008	6716199	1364
12	Lower nappe	305	125	417007	6716183	1379
13	Lower nappe	305	135	417002	6716180	1380
14	Lower nappe	290	110	416985	6716160	1378
15	Lower nappe	310	130	416973	6716209	1367
16	Lower nappe	210	30	417182	6715067	1612
17	Lower nappe	325	145	415448	6716258	1467
18	Lower nappe	300	120	415443	6716259	1464
19	Lower nappe	325	145	415503	6716259	1465
20	Lower nappe	300	120	415797	6717481	1342
21	Lower nappe	300	120	415769	6717458	1350
22	Lower nappe	310	130	415203	6717403	1364
23	Lower nappe	320	140	415372	6717465	1352
24	Lower nappe	310	130	415845	6717111	1410
25	Lower nappe	290	110	415118	6716672	1462
26	Ln + Phyllite	290	110	415765	6716345	1410
27	Ln + Phyllite	310	130	415774	6716348	1408
28	Lower nappe	250	70	415788	6716319	1416
29	Lower nappe	300	120	417995	6715037	1416
30	Lower nappe	310	130	416760	6715205	1544
31	Lower nappe	315	135	417011	6715116	No data
32	Upper nappe	315	135	417113	6715088	1607
33	Upper nappe	326	146	417076	6714893	1597
34	Lower nappe	335	155	416748	6714686	1608
35	Lower nappe	305	125	416689	6714598	1623
36	Ln + Phyllite	300	120	415172	6716247	1504
37	Lower nappe	190	10	416504	6717318	1504
38	Lower nappe	315	135	416831	6715800	1390
39	Lower nappe	210	30	417130	6715711	1381
40	Upper nappe	230	130	416603	6714475	1643

Appendix 2

Information map

Locations for:

Different sections
Cross section: A-A', B-B', C-C' & D-D'
Localities
Samples

Section x: Enlarged view of current area in a seperate map
Cross sections: Thick line from X-X'
Localites: Red text. Lz = Locality Z
Sample: Blue text and is the sample number.

Legend

CrossSection

- CrossSection
- inset *Close up map of current area. Correlate section number with the proper map.*

Contour Line

- Contour Line *Equidistance: 20 meter*

Contacts

- Contact—Identity and existence certain, locationa ccurate
- Contact—Identity and existence certain, location approximate
- Contact—Identity or existence questionable, locaction inferred
- Glacial limit or terminus—Identity and existence certain, location approximate

Other

- Trail
- River
- Lake/water

Tectonostratigraphic units

Allochton

Upper Nappe	felsic gneiss, amphibolite, mylonitic gneiss
Upper Nappe (Interpreted)	Extrapolation of the Upper Nappe
Lower Nappe	fine grained, banded schist/gneisses, volcanic tuff, mica, carbonate
Lower Nappe (Interpreted)	Extrapolated Lower Nappe unit.

Meta-sediment

Phyllite	Rusty, mica and graphite rich, distinct sheen.
Phyllite (Interpreted)	Extrapolated Phyllite
Pieces of Lower Nappe	Smaller fragments of Lover Nappe incoporated into the Phyllite

Autochton

Regolith	Top most layer of the basement, red/rusty appearance
Granitic	Both large and fined grained granodiorite, and granite with megacryst
Granitic (Interpreted)	Extrapolated granitic composition. Both large and fined grained Granodiorite, and granite with megacryst
Mafic	Amphibolititie and Gabbro
Mafic (Interpreted)	Extrapolation of Amphibolititie and Gabbro

Glacial

Glacier	Glacial cover (the glacial extends are traced from a 2009 map)
Glacier feature	moraine, debris or other glacial deposit that covers the bedrock

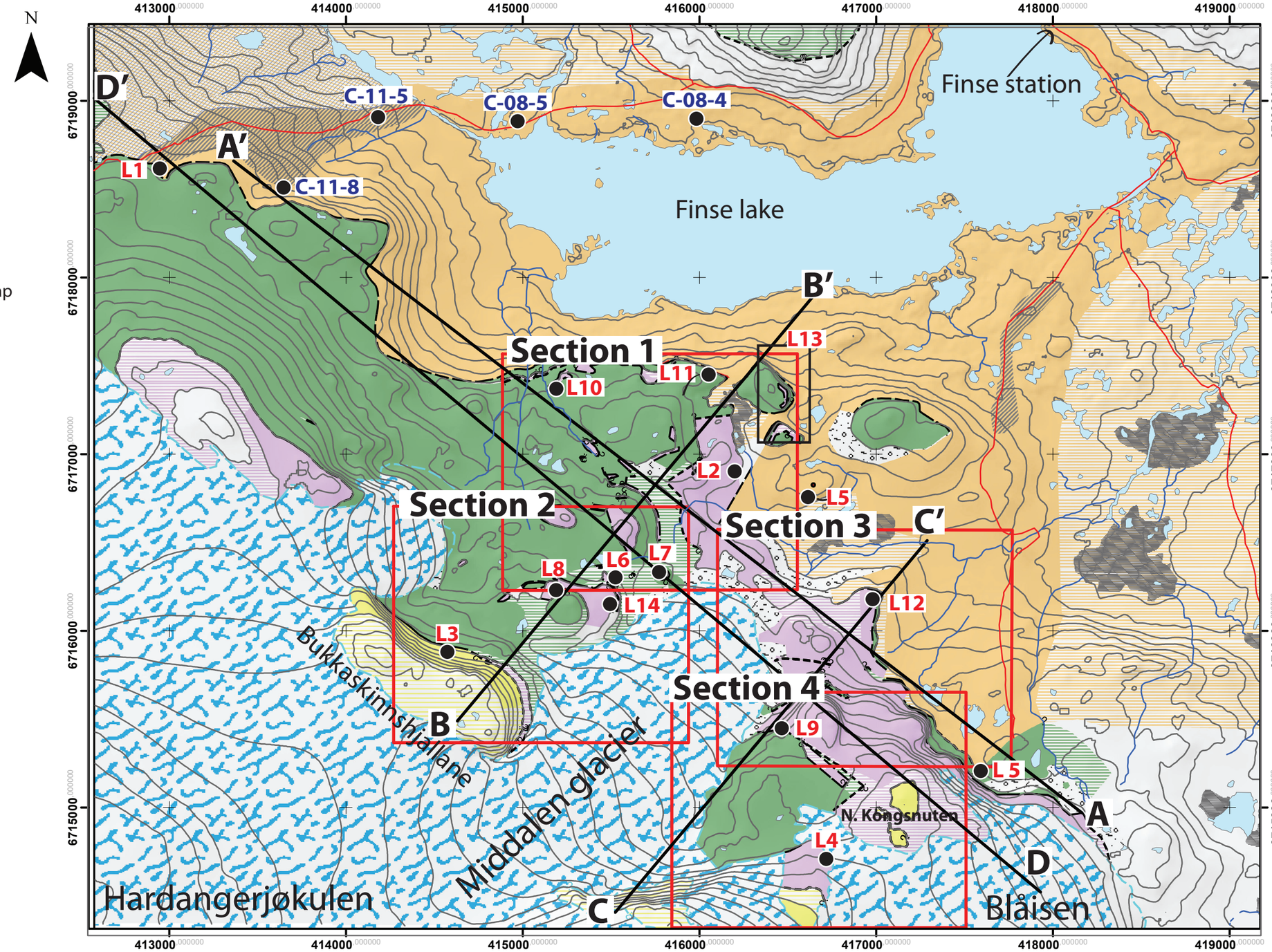

Appendix 3

Geological map of Finse

Mapped by Erik Jensen

Area: Overview

Coordinate System: WGS 1984 UTM Zone 32N
Datum: WGS 1984

1:24 000

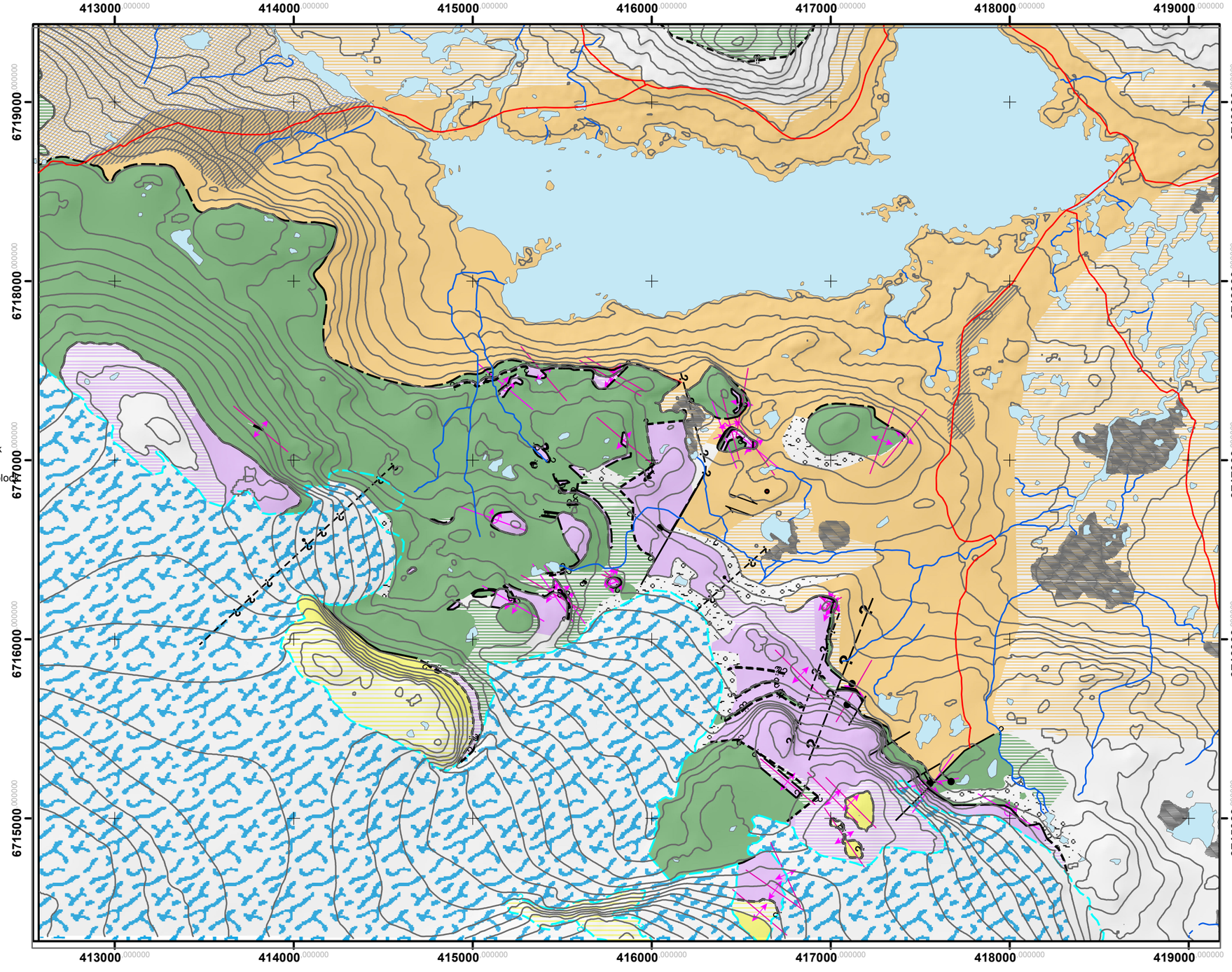

Legend

Contour Line

- Contour Line *Equidistance: 20 meter*

Contacts

- Contact—Identity and existence certain, locationa ccurate
- Contact—Identity and existence certain, location approximate
- Contact—Identity or existence questionable, locaction inferred
- Glacial limit or terminus—Identity and existence certain, location approximate

Faults

- Normal fault—Identity and existence certain, location accurate. Ball and bar on downthrown block
- Normal fault—Identity or existence questionable, location accurate. Ball and bar on downthrown block
- Normal fault—Identity or existence questionable, location approximate. Ball and bar on downthrown block
- Normal fault—Identity or existence questionable, location inferred. Ball and bar on downthrown block
- Fault showing local right-lateral strike-slip offset— Arrows show relative motion

Folds

- Anticline - Identity and existence certain, location accurate
- Overturned anticline - Identity and existence certain, location accurate.
- Syncline - Identity and existence certain, location accurate

Other

- Trail
- River
- Lake/water

Tectonostratigraphic units

Allochton

Upper Nappe	felsic gneiss, amphibolite, mylonitic gneiss
Upper Nappe (Interpreted)	Extrapolation of the Upper Nappe
Lower Nappe	fine grained, banded schist/gneisses, volcanic tuff, mica, carbonate
Lower Nappe (Interpreted)	Extrapolated Lower Nappe unit.

Meta-sediment

Phyllite	Rusty, mica and graphite rich, distinct sheen.
Phyllite (Interpreted)	Extrapolated Phyllite
Pieces of Lower Nappe	Smaller fragments of Lover Nappe incoporated into the Phyllite

Autochton

Regolith	Top most layer of the basement, red/rusty appearance
Granitic	Both large and fined grained granodiorite, and granite with megacryst
Granitic (Interpreted)	Extrapolated granitic composition. Both large and fined grained Granodiorite, and granite with megacryst
Mafic	Amphibolititie and Gabbro
Mafic (Interpreted)	Extrapolation of Amphibolititie and Gabbro

Glacial

Glacier	Glacial cover (the glacial extends are traced from a 2009 map)
Glacier feature	moraine, debris or other glacial deposit that covers the bedrock

0 270 540 1 080 1 620 2 160 Meters

Appendix 3

Geological map of Finse

Mapped by Erik Jensen

Area: Section 1

Coordinate System: WGS 1984 UTM Zone 32N
Datum: WGS 1984

1:6 272

Legend

Contour Line

Contour Line *Equidistance: 20 meter*

Foliation

Inclined metamorphic or tectonic foliation— Showing strike and dip

Lineation

Approximate plunge direction of inclined generic lineation or linear structure

Contacts

Contact—Identity and existence certain, locationa ccurate

Contact—Identity and existence certain, location approximate

Contact—Identity or existence questionable, locaction inferred

Glacial limit or terminus—Identity and existence certain, location approximate

Faults

Normal fault—Identity and existence certain, location accurate. Ball and bar on downthrown block

Normal fault—Identity or existence questionable, location accurate. Ball and bar on downthrown block

Normal fault—Identity or existence questionable, location approximate. Ball and bar on downthrown block

Normal fault—Identity or existence questionable, location inferred. Ball and bar on downthrown block

Fault showing local right-lateral strike-slip offset— Arrows show relative motion

Folds

Anticline - Identity and existence certain, location accurate

Overturned anticline - Identity and existence certain, location accurate.

Syncline - Identity and existence certain, location accurate

Other

Trail

River

Lake/water

Tectonostratigraphic units

Allochton

Upper Nappe	felsic gneiss, amphibolite, mylonitic gneiss
Upper Nappe (Interpreted)	Extrapolation of the Upper Nappe
Lower Nappe	fine grained, banded schist/gneisses, volcanic tuff, mica, carbonate
Lower Nappe (Interpreted)	Extrapolated Lower Nappe unit.

Meta-sediment

Phyllite	Rusty, mica and graphite rich, distinct sheen.
Phyllite (Interpreted)	Extrapolated Phyllite
Pieces of Lower Nappe	Smaller fragments of Lover Nappe incoporated into the Phyllite

Autochton

Regolith	Top most layer of the basement, red/rusty appearance
Granitic	Both large and fined grained granodiorite, and granite with megacryst
Granitic (Interpreted)	Extrapolated granitic composition. Both large and fined grained Granodiorite, and granite with megacryst
Mafic	Amphibolititie and Gabbro
Mafic (Interpreted)	Extrapolation of Amphibolititie and Gabbro

Glacial

Glacier	Glacial cover (the glacial extends are traced from a 2009 map)
Glacier feature	moraine, debris or other glacial deposit that covers the bedrock

N

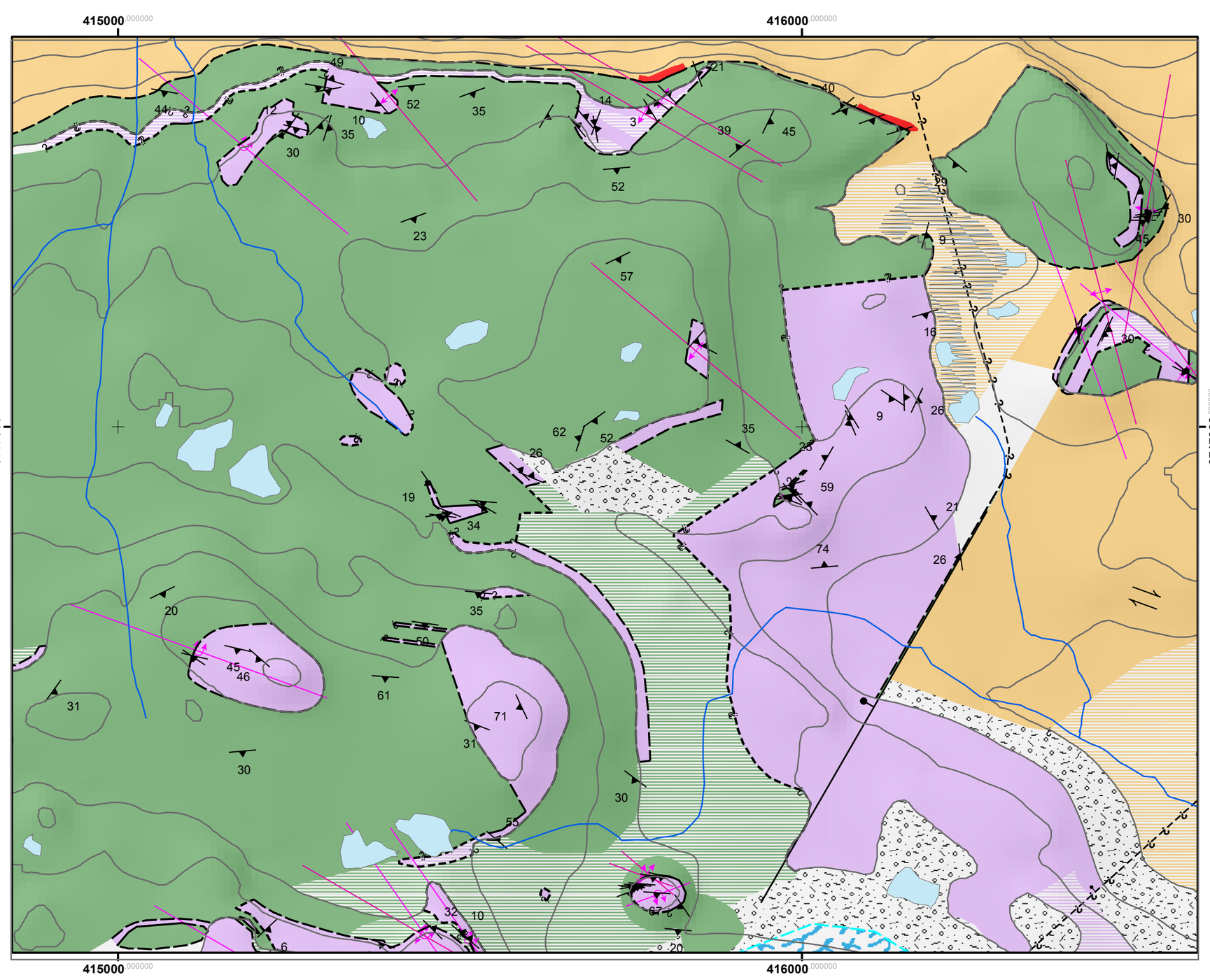

0 70 140 280 420 560 Meters

Appendix 3

Geological map of Finse

Mapped by Erik Jensen

Area: Section 2

Coordinate System: WGS 1984 UTM Zone 32N
Datum: WGS 1984

1:6 272

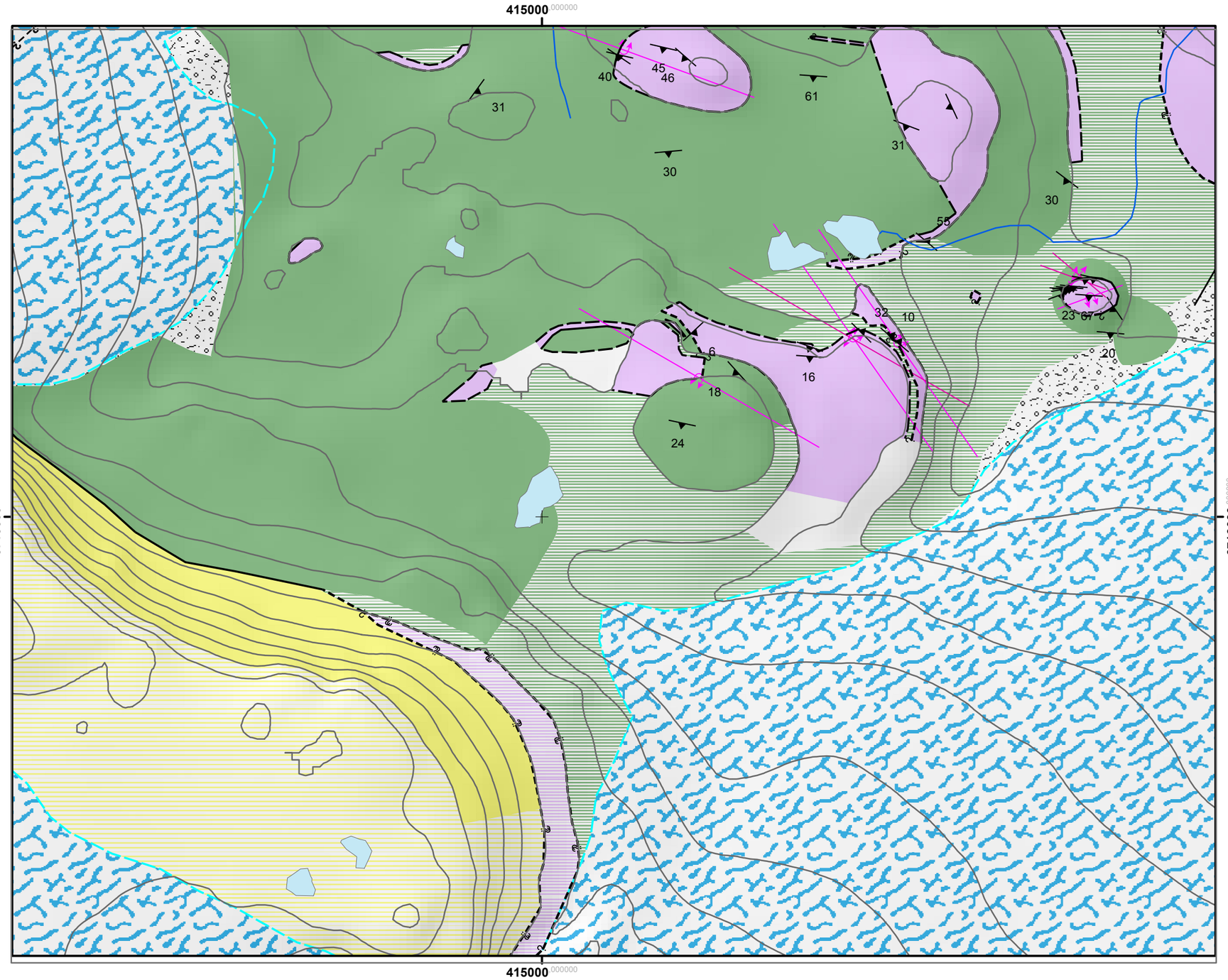

Legend

Contour Line

Contour Line *Equidistance: 20 meter*

Foliation

Inclined metamorphic or tectonic foliation— Showing strike and dip

Lineation

Approximate plunge direction of inclined generic lineation or linear structure

Contacts

Contact—Identity and existence certain, locationa ccurate

Contact—Identity and existence certain, location approximate

Contact—Identity or existence questionable, locaction inferred

Glacial limit or terminus—Identity and existence certain, location approximate

Faults

Normal fault—Identity and existence certain, location accurate. Ball and bar on downthrown block

Normal fault—Identity or existence questionable, location accurate. Ball and bar on downthrown block

Normal fault—Identity or existence questionable, location approximate. Ball and bar on downthrown block

Normal fault—Identity or existence questionable, location inferred. Ball and bar on downthrown block

Fault showing local right-lateral strike-slip offset— Arrows show relative motion

Folds

Anticline - Identity and existence certain, location accurate

Overturned anticline - Identity and existence certain, location accurate.

Syncline - Identity and existence certain, location accurate

Other

Trail

River

Lake/water

Tectonostratigraphic units

Allochton

Upper Nappe	felsic gneiss, amphibolite, mylonitic gneiss
Upper Nappe (Interpreted)	Extrapolation of the Upper Nappe
Lower Nappe	fine grained, banded schist/gneisses, volcanic tuff, mica, carbonate
Lower Nappe (Interpreted)	Extrapolated Lower Nappe unit.

Meta-sediment

Phyllite	Rusty, mica and graphite rich, distinct sheen.
Phyllite (Interpreted)	Extrapolated Phyllite
Pieces of Lower Nappe	Smaller fragments of Lover Nappe incoporated into the Phyllite

Autochton

Regolith	Top most layer of the basement, red/rusty appearance
Granitic	Both large and fined grained granodiorite, and granite with megacryst
Granitic (Interpreted)	Extrapolated granitic composition. Both large and fined grained Granodiorite, and granite with megacryst
Mafic	Amphibolititie and Gabbro
Mafic (Interpreted)	Extrapolation of Amphibolititie and Gabbro

Glacial

Glacier	Glacial cover (the glacial extends are traced from a 2009 map)
Glacier feature	moraine, debris or other glacial deposit that covers the bedrock

Appendix 3

Geological map of Finse

Mapped by Erik Jensen

Area: Section 3

Coordinate System: WGS 1984 UTM Zone 32N
Datum: WGS 1984

1:6 272

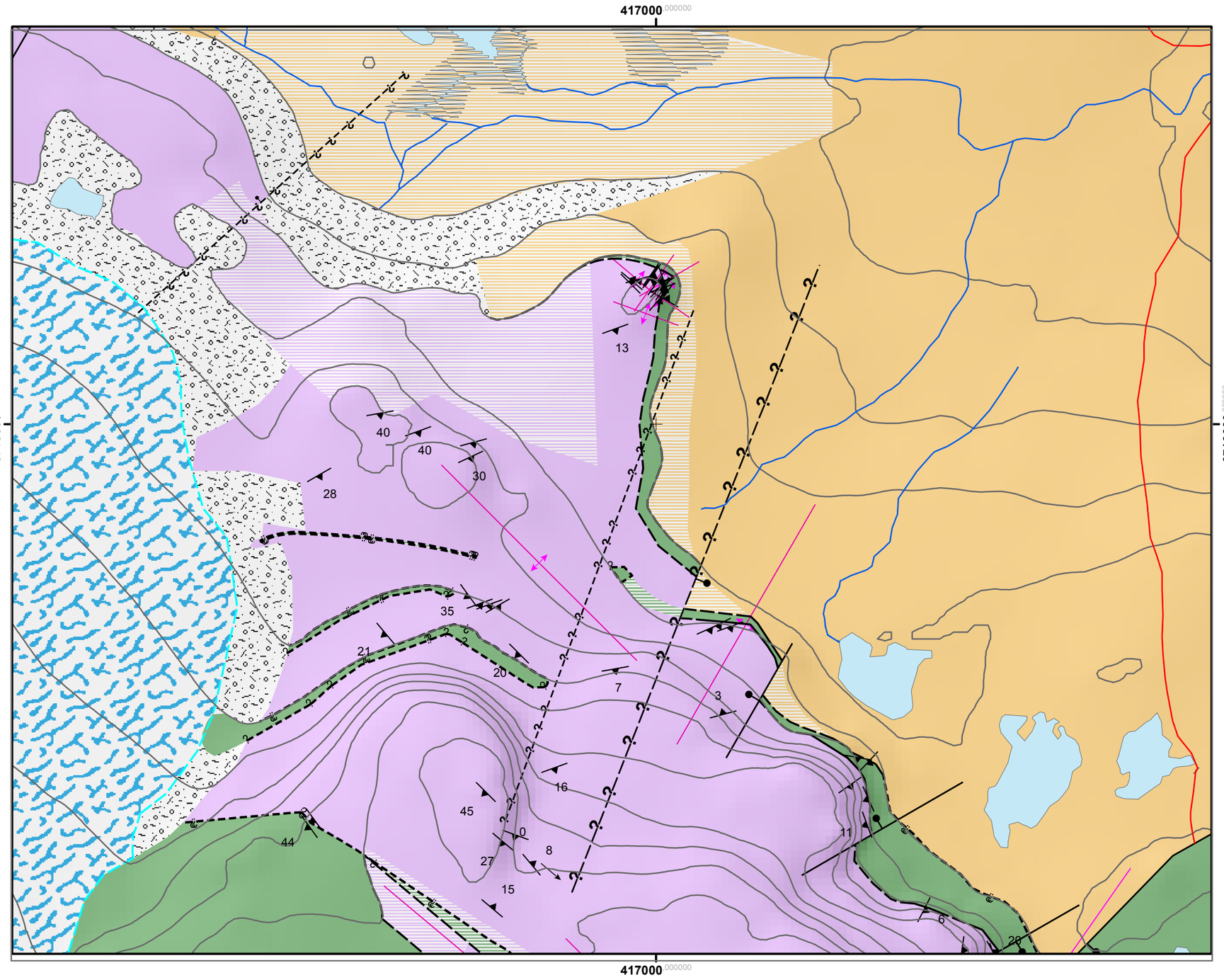

Legend

Contour Line

Contour Line *Equidistance: 20 meter*

Foliation

Inclined metamorphic or tectonic foliation— Showing strike and dip

Lineation

Approximate plunge direction of inclined generic lineation or linear structure

Contacts

Contact—Identity and existence certain, locationa ccurate

Contact—Identity and existence certain, location approximate

Contact—Identity or existence questionable, locaction inferred

Glacial limit or terminus—Identity and existence certain, location approximate

Faults

Normal fault—Identity and existence certain, location accurate. Ball and bar on downthrown block

Normal fault—Identity or existence questionable, location accurate. Ball and bar on downthrown block

Normal fault—Identity or existence questionable, location approximate. Ball and bar on downthrown block

Normal fault—Identity or existence questionable, location inferred. Ball and bar on downthrown block

Fault showing local right-lateral strike-slip offset— Arrows show relative motion

Folds

Anticline - Identity and existence certain, location accurate

Overturned anticline - Identity and existence certain, location accurate.

Syncline - Identity and existence certain, location accurate

Other

Trail

River

Lake/water

Tectonostratigraphic units

Allochton

Upper Nappe	felsic gneiss, amphibolite, mylonitic gneiss
Upper Nappe (Interpreted)	Extrapolation of the Upper Nappe
Lower Nappe	fine grained, banded schist/gneisses, volcanic tuff, mica, carbonate
Lower Nappe (Interpreted)	Extrapolated Lower Nappe unit.

Meta-sediment

Phyllite	Rusty, mica and graphite rich, distinct sheen.
Phyllite (Interpreted)	Extrapolated Phyllite
Pieces of Lower Nappe	Smaller fragments of Lover Nappe incoporated into the Phyllite

Autochton

Regolith	Top most layer of the basement, red/rusty appearance
Granitic	Both large and fined grained granodiorite, and granite with megacryst
Granitic (Interpreted)	Extrapolated granitic composition. Both large and fined grained Granodiorite, and granite with megacryst
Mafic	Amphibolititie and Gabbro
Mafic (Interpreted)	Extrapolation of Amphibolititie and Gabbro

Glacial

Glacier	Glacial cover (the glacial extends are traced from a 2009 map)
Glacier feature	moraine, debris or other glacial deposit that covers the bedrock

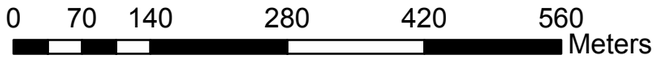

Appendix 3

Geological map of Finse

Mapped by Erik Jensen

Area: Section 4

Coordinate System: WGS 1984 UTM Zone 32N
Datum: WGS 1984

1:6 272

Legend

Contour Line

Contour Line *Equidistance: 20 meter*

Foliation

Inclined metamorphic or tectonic foliation— Showing strike and dip

Lineation

Approximate plunge direction of inclined generic lineation or linear structure

Contacts

Contact—Identity and existence certain, locationa ccurate

Contact—Identity and existence certain, location approximate

Contact—Identity or existence questionable, locaction inferred

Glacial limit or terminus—Identity and existence certain, location approximate

Faults

Normal fault—Identity and existence certain, location accurate. Ball and bar on downthrown block

Normal fault—Identity or existence questionable, location accurate. Ball and bar on downthrown block

Normal fault—Identity or existence questionable, location approximate. Ball and bar on downthrown block

Normal fault—Identity or existence questionable, location inferred. Ball and bar on downthrown block

Fault showing local right-lateral strike-slip offset— Arrows show relative motion

Folds

Anticline - Identity and existence certain, location accurate

Overturned anticline - Identity and existence certain, location accurate.

Syncline - Identity and existence certain, location accurate

Other

Trail

River

Lake/water

Tectonostratigraphic units

Allochton

Upper Nappe	felsic gneiss, amphibolite, mylonitic gneiss
Upper Nappe (Interpreted)	Extrapolation of the Upper Nappe
Lower Nappe	fine grained, banded schist/gneisses, volcanic tuff, mica, carbonate
Lower Nappe (Interpreted)	Extrapolated Lower Nappe unit.

Meta-sediment

Phyllite	Rusty, mica and graphite rich, distinct sheen.
Phyllite (Interpreted)	Extrapolated Phyllite
Pieces of Lower Nappe	Smaller fragments of Lover Nappe incoporated into the Phyllite

Autochton

Regolith	Top most layer of the basement, red/rusty appearance
Granitic	Both large and fined grained granodiorite, and granite with megacryst
Granitic (Interpreted)	Extrapolated granitic composition. Both large and fined grained Granodiorite, and granite with megacryst
Mafic	Amphibolititie and Gabbro
Mafic (Interpreted)	Extrapolation of Amphibolititie and Gabbro

Glacial

Glacier	Glacial cover (the glacial extends are traced from a 2009 map)
Glacier feature	moraine, debris or other glacial deposit that covers the bedrock

N

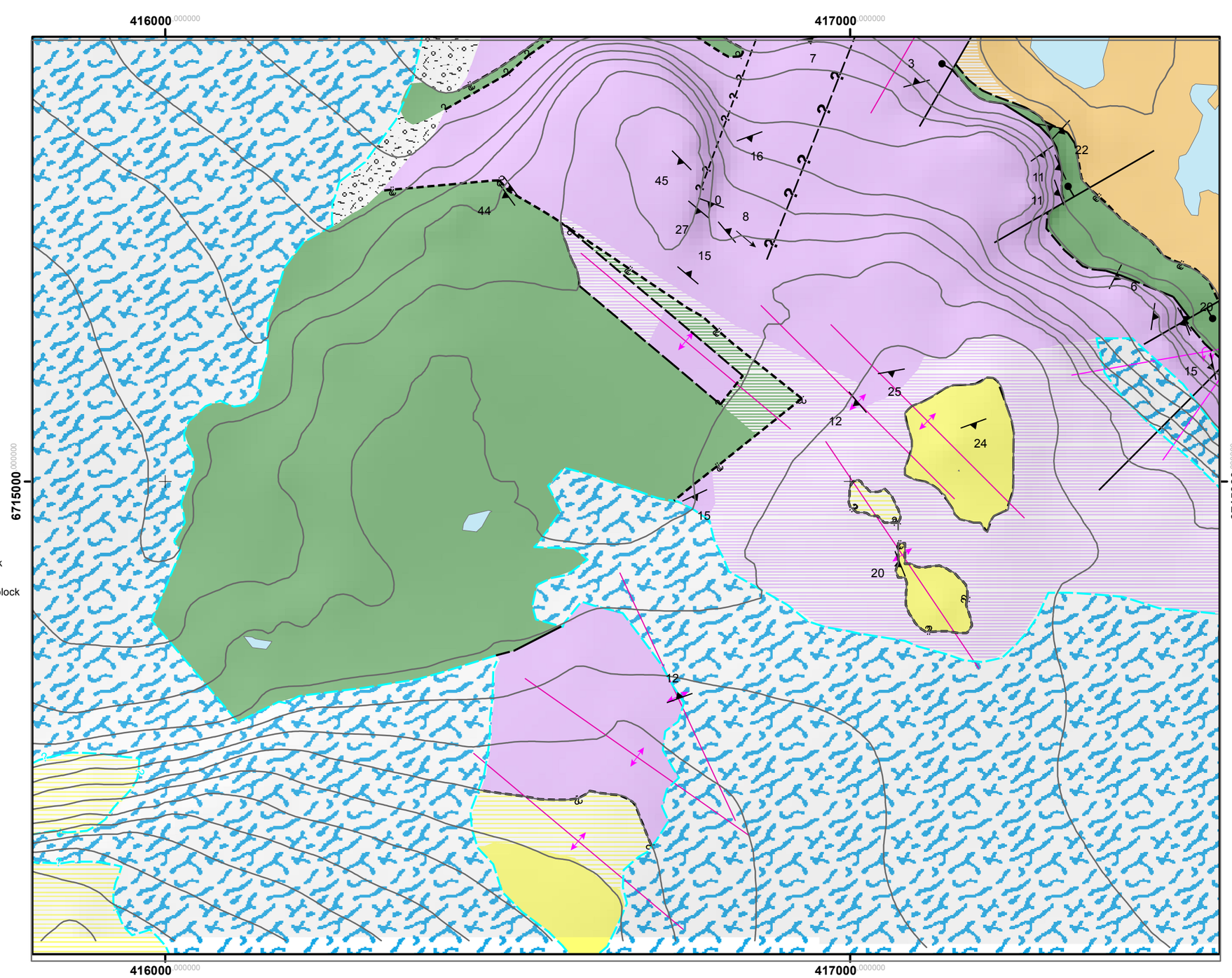

0 70 140 280 420 560 Meters

Appendix 4

Finse cross-section B - B'

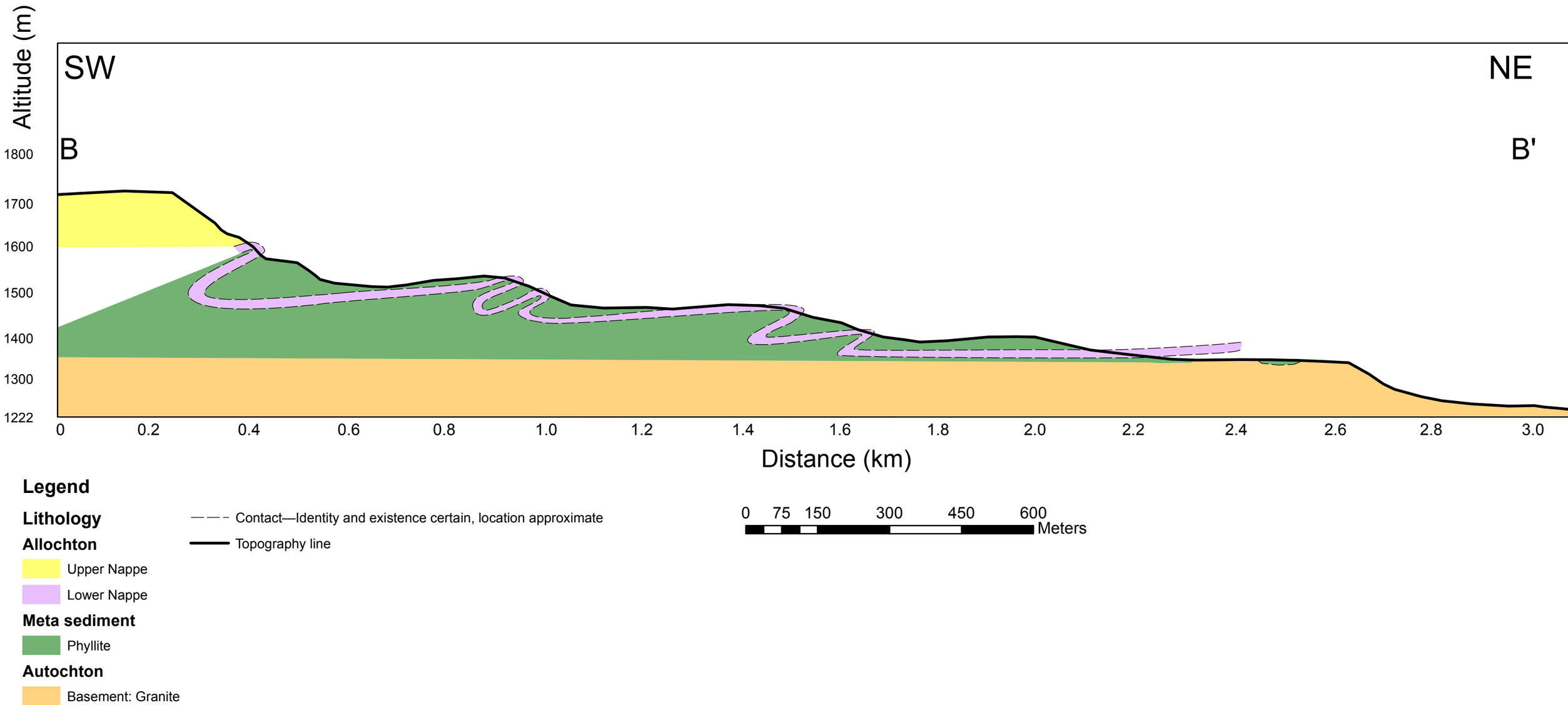

Legend

Lithology

Allochton

- Upper Nappe
- Lower Nappe

Meta sediment

- Phyllite

Autochton

- Basement: Granite

- Contact—Identity and existence certain, location approximate
- Topography line

0 75 150 300 450 600 Meters

Appendix 5

Finse cross-section C - C'

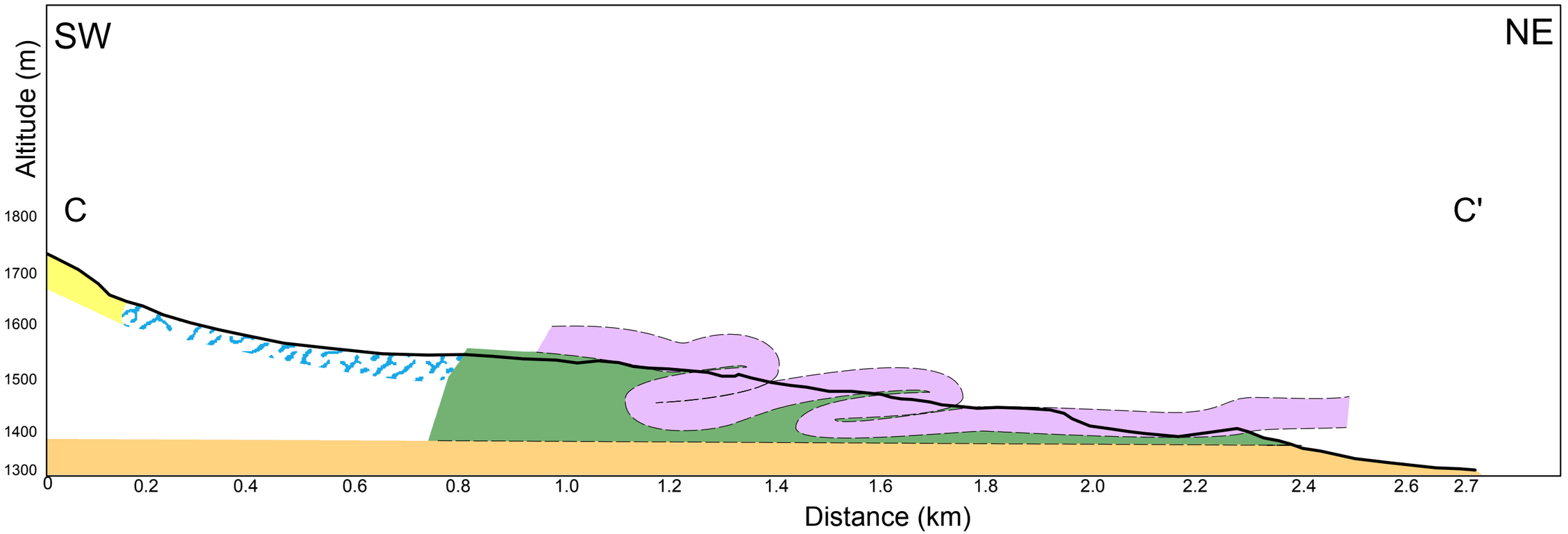

Legend

Lithology

Other

Glacier

Allochton

Upper Nappe

Lower Nappe

Meta sediment

Phyllite

Autochton

Basement: Granite

Contact—Identity and existence certain, location approximate

Topography line

0 115 230 460

Meters

Appendix 6

Finse cross-section D - D'

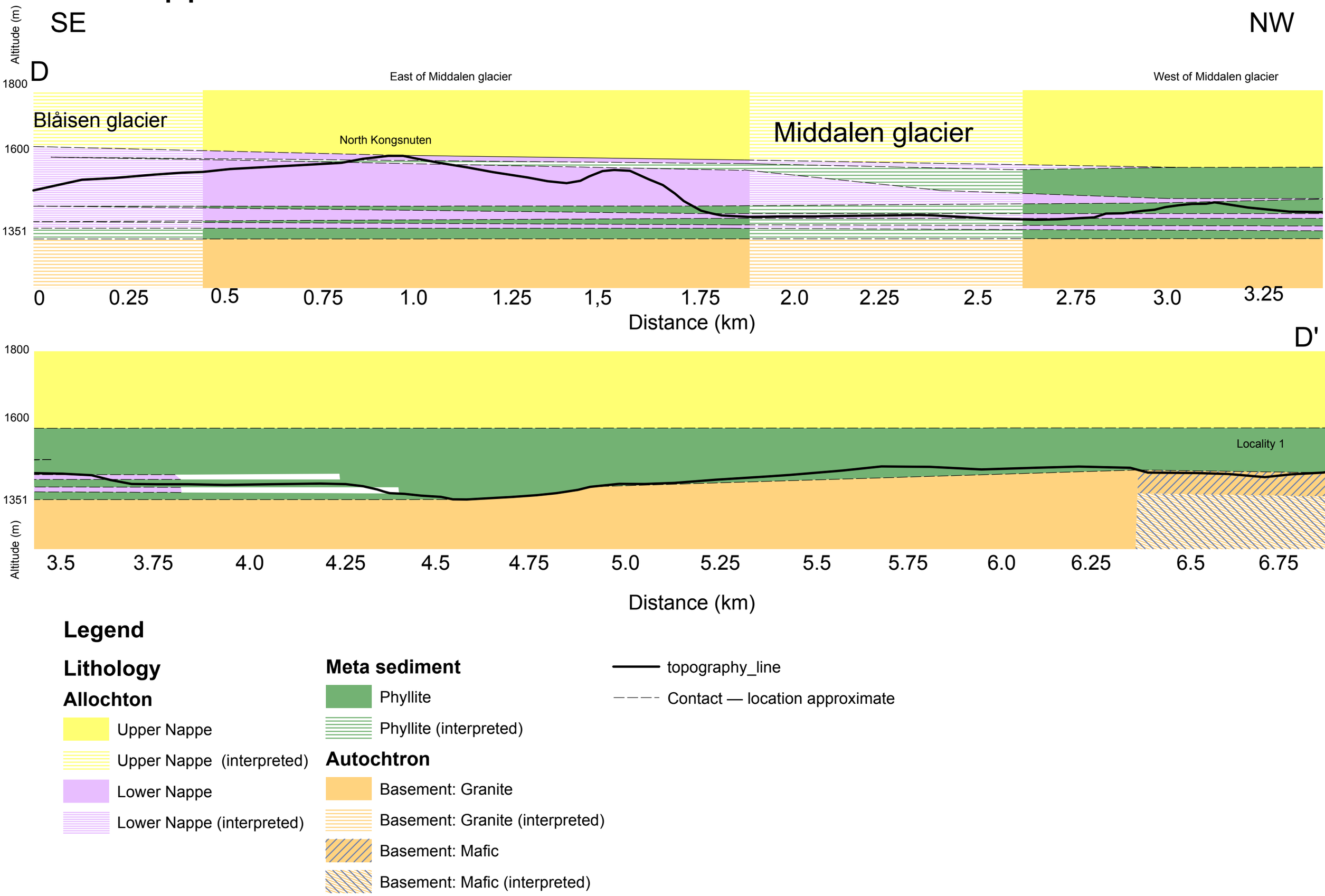

Legend

Lithology

Allochton

- Upper Nappe
- Upper Nappe (interpreted)
- Lower Nappe
- Lower Nappe (interpreted)

Meta sediment

- Phyllite
- Phyllite (interpreted)

Autochtron

- Basement: Granite
- Basement: Granite (interpreted)
- Basement: Mafic
- Basement: Mafic (interpreted)

- topography_line
- Contact — location approximate